
# Incorporating residual strength regarding clay resistance in dike safety assessment - a case study of the Ketelmeerdijk

Master thesis

**Author:**
Jildert de Jong (s1963260)

**Date:**
17-7-2024

**Faculty:**
Engineering Technology (ET) – Water Engineering and Management (WEM)

UNIVERSITY OF TWENTE.

WATERSCHAP ZUIDERZEELAND

Graduation committee:

| | | |
|---|---|---|
| prof. dr. S.J.M.H. (Suzanne) Hulscher | - | Chair (UT) |
| ir. N. (Niels) van der Vegt | - | Daily supervisor (UT) |
| dr. M. (Marijke) Visser | - | Supervisor (Waterschap Zuiderzeeland) |

The presented research in this thesis is carried out at Waterboard Zuiderzeeland, in close collaboration with the Water Engineering and Management (WEM) department, Civil Engineering and Management, University of Twente, the Netherlands.

# Preface

This master's thesis concludes my period at the University of Twente as a student. During the past 8 months, I made the attempt to make a small leap in the large knowledge gap that exists regarding residual strength. Residual strength is a concept intended to make the Dutch dike safety assessments sharper and more accurate. It is not taken into account yet, but should be done so, while it is a significant strength component of the dike and contributes to its overall stability. To achieve this goal I saw some challenges on my way, and while trying to find the answer to one question, I often came up with two or more questions. In this super interesting, but difficult field of study, I was in good hands with my supervisors. I would like to thank Niels van der Vegt dearly, my daily supervisor from the UT, who accompanied me along the search for integrating clay erosion as part of the Ketelmeerdijk safety assessment. Combined with work at HKV, starting up a PhD, and giving lessons at the same, Niels never failed to respond to my questions for help. I am super thankful for that. Further, from the UT, I would like to thank Geert Campmans, who spent the first two months as a temporary daily supervisor. Even though it is not your field of research, I learned a lot about the process, setting realistic targets and how to place boundaries, thank you for that! Also, I would like to thank Suzanne Hulscher, my head of chair, who helped to lift my research to a higher level and make it relevant.

Also, I would like to thank my supervisor at the waterboard Zuiderzeeland, Marijke Visser. Together, we had some great discussions, stood together on the Ketelmeerdijk, and were able to make a long trip from Enschede to Amersfoort actually really nice. Always when I had a question, there would be an answer from Marijke and that expertise, combined with a lot of enthusiasm, was more than I could ever ask for regarding my guidance in Lelystad, at the waterboard. I am grateful for their supervision and help where I needed that, but also their realistic view of the project, while pushing the brake sometimes a little bit when I desired to research more than I could. Further, from the waterboard Zuiderzeeland, I would sincerely thank all colleagues, who made me feel welcome from the very first day.

At last, I would like to thank all those who supported me throughout the full period in countless ways. I want to thank those with which I count endlessly debate and critically review on the topic. I want to thank those who told me it would all be fine in the late hours working behind the laptop. And of course, I would like to thank my parents for their unconditional support.

I thoroughly enjoyed researching this novel topic. Throughout the 8 months I spent researching the subject, I was waiting for that really large setback. As I type now my final words of this thesis, I am still waiting for that moment, which surely says a lot about the enthusiasm I maintained while researching the topic. The potential of residual strength is enormous, with so many dike trajectories failing the new safety standards, requiring millions of euros to improve and reinforce these. It is a big step in our ever-lasting search for improvement and rising efficiency, also in dike design. With this research, I hope to have contributed - albeit slightly - to bridging the gap between academia and the field of application, at the waterboard.

I hope you will enjoy reading this thesis.

With kind regards,

Jildert

Utrecht, June 2024

# Summary

The Netherlands is protected against the threat of flooding through an extensive network of flood defences. To ensure their stability, and thereby the safety of those living behind, these are constantly monitored, assessed, and when necessary reinforced. Every 12 years, all flood defences are subjected to a safety assessment, evaluating whether a range of failure mechanisms meet the legal norm set by the Dutch Government. Among these failure mechanisms, the stability of revetments on the outer slope of a dike is evaluated against the loading caused by wave impact. However, the erosion resistance of the clay layer and the core of the dike is not (yet) considered in these assessments, as the topic is too complex. For now, it is assumed that the dike fails once the revetments fail in theory.

This thesis aims to explore why the strength of the dike body is not part of the dike safety assessment, map the possibilities and uncertainties in trying to integrate the strength component and propose a methodology for integrating it in Dutch dike safety assessment. This way, the risk of breaching can be estimated more accurately, allowing for a more efficient dike (re-)design. This could lead to significant savings in future dike reinforcements.

The Ketelmeerdijk is used as a case for this research, to identify whether integrating clay erosion in the strength calculation could prove this point. This trajectory did not meet the safety norm in the latest assessment round, among others on the revetment layers, and is therefore scheduled for reinforcement.

To evaluate the strength of the clay layer beneath the cover layers, a model was set up, to determine the erosion volume, when loaded with normative hydraulic conditions, on a cross-sectional level. To derive this erosion volume, the model requires input through hydraulic loading (i.e. water levels, wave conditions), and dike properties (i.e. geometry, soil characteristics, current condition). The research examined the wave impact during a normative storm, which is expected to occur once every 10,000 years over a 35-hour storm event, using BOI-compliant software. This analysis identified specific moments in time when the revetment layers failed, for respectively basalt and Basalton below the berm, and grass cover above the berm. Consecutively, this leads to clay erosion, until the sandy core is reached.

Clay erosion was modelled through methodologies set up through large-scale modelling tests in Delta Flume. Klein Breteler et al. (2012), Mourik (2020), and Klein Breteler (2022) showed to be the best options to apply for the Ketelmeerdijk. The respective model performance was tested for each of these methods, which resulted in the latter two options being selected. From these analyses, the model was sensitive to hydraulic loading (through wave steepness and wave height), and the type of clay used. Gathering data on these two aspects is therefore also a crucial recommendation to the waterboard.

This research has shown that for a storm event with a failure probability of once in 10,000 years, the Ketelmeerdijk does not carry sufficient residual strength on the upper slope. After 15.2 hours, clay erosion was initiated, after the failure of both the turf layer and upper clay layer. The consecutive 4-hour peak load at constant water level would inflict an erosion depth ranging from 0.81 to 1.16 meters to the 1-meter thick clay layer, perpendicular to the upper slope. Conservatism is appropriate here, and therefore, it is concluded that the clay layer does not carry sufficient residual strength after initial failure.

Nonetheless, clay erosion clearly shows to estimate the risk of breaching more accurately. Adding the component of clay erosion to failure mechanisms related to dike erosion of the outer slope was shown to improve the strength through the probability of failure by more than 125 per cent. Also, sand erosion is a component to which strength – albeit a lot less than clay erosion – can be assigned. This makes residual strength a promising topic, and it could cause many future dike designs or reinforcement to be (partially) adjusted, enabling economic benefits, all while improving overall dike safety.



*Keywords: Flood protection, Dike safety assessment, Waterside slope failure, Residual strength, Erosion Resistance, Clay erosion*

# Table of contents


Preface 2

Summary 4

List of figures 6

1. Introduction 9

1.1. Context 9

1.2. Problem statement 11

1.3. Knowledge and research gap 12

1.4. Research goal and scope 12

1.4.1. Research questions 12

1.4.2. Research scope 13

1.4.3. Research approach and outline 14

1.4.4. Approach per research question 15

2. Theoretical background 16

2.1. Hydraulic conditions 16

2.1.1. Hydraulic parameters 16

2.1.2. Synthetic storm: evolution and duration 18

2.2. Dike cover layers 19

2.2.1. Flood defence safety assessment 19

2.2.2. Instability of cover layers 19

2.2.3. Typical cover layer design on Dutch dikes 20

2.3. Clay erosion 21

2.3.1. Erosion profile 21

2.3.2. Clay erosion formulas 22

2.4. Case study Ketelmeerdijk 23

2.4.1. Normative cross-section 24

2.4.2. Geometric characteristics 25

2.4.3. Clay properties 25

3. Methodology 26

3.1. Hydraulic conditions 27

3.1.1. Hydraulic parameters 27

3.1.2. Synthetic storm 27

3.2. Failure of dike cover layers 29

3.2.1. Failure of block revetment 30

3.2.2. Failure of grass cover 30

3.3. Clay erosion 33

3.3.1. Inventory clay erosion models 33

3.3.2. Time step selection 38

3.3.3. Sensitivity analyses 38

3.4. Progressive clay erosion model 39

3.4.1. Model set-up 39

3.4.2. Setting up geometric erosion profiles 40

3.4.3. Uncertainties 41

3.5. Application to case study Ketelmeerdijk 42
4. Results 43
4.1. Hydraulic conditions 43
4.1.1. Hydraulic parameters 43
4.1.2. Synthetic storm 44
4.1.3. Conclusion for the case study Ketelmeerdijk 45
4.2. Failure of dike cover layers 45
4.2.1. Instability of block revetment 45
4.2.2. Erosion of grass cover 47
4.2.3. Conclusion for the case study Ketelmeerdijk 49
4.3. Clay erosion 49
4.3.1. Timestep selection 50
4.3.2. Overview clay erosion models 51
4.3.3. Sensitivity analysis 52
4.3.4. Conclusion for the case study Ketelmeerdijk 54
4.4. Progressive clay erosion model 54
4.4.1. Clay erosion during peak at constant water level 54
4.4.2. Influence of clay type on erosion 58
4.4.3. The erosion process for different failure probabilities 58
4.4.4. Conclusions for the case study Ketelmeerdijk 61
5. Discussion 62
5.1. Validity of research 62
5.2. Discussing results 62
5.3. Limitations 62
5.4. Implications of research 64
5.5. Follow-up studies 64
6. Conclusion 65
7. Recommendations 67
8. General advice 68
9. References 69
Appendix 1 – Hydraulic conditions 71
Appendix 1.1 - Hydra-NL output 71
Appendix 1.2 – Angle of incidence 74
Appendix 2 - Cover layers 76
Appendix 2.1 - STEENTOETS input 76
Appendix 3 – Model set-up 78
Appendix 3.1 - Input case study 78
Appendix 4 – Sand erosion 79

# List of figures

Figure 1: Geographical location IJsselmeer, indicating relatively high ‘original’ lands, low-lying newly reclaimed land (polders), and dikes 9
Figure 2: Locations of the dike trajectories around the southern polder of Flevoland 10

Figure 3: Reporting of WBI2017 results for failure mechanisms of GEBU and ZST, showing where both mechanisms meet the standard (green), one meets the standard (orange), and neither meets the standard (red) 10
Figure 4: Simplified cross-sectional profile of the dike trajectory Ketelmeerdijk 11
Figure 5: The research approach per question and outline of the thesis 14
Figure 6: Frequency lines for both the IJssel- and Markermeer (Botterhuis, Waterman, & Geerse, 2017) 16
Figure 8: Hydraulic loadings schematized, with lake water levels, peak period, significant wave height, and wave steepness 17
Figure 7: Standard schematized water level evolution used in Dutch lake dike safety assessment (Ministry of I&W, 2007) 18
Figure 9: Schematical resemblance of deformation due to sliding and forming of an S-profile (Klein Breteler, Mourik, & Bosters, 2014) 20
Figure 10: Schematical resemblance of block revetment failure as a result of a pressure gradient (Klein Breteler M. , 2016) 20
Figure 11: Construction of artificial Basalton cover layer, with the geotextile, filter layer and clay layer visible 21
Figure 12: Composition of the cover layer and the required layers beneath in a schematized overview 21
Figure 13: Schematical representation of the typical erosion process occurring above hard revetment 21
Figure 14: Schematized development of the erosion profile (Mourik, 2020) 22
Figure 15: Cross-sectional profile of dike trajectory of Ketelmeerdijk (HM 13.4) 24
Figure 16: Outer slope of Ketelmeerdijk 24
Figure 17: Normative location with left the effective fetch displayed, on which wind can cause water levels set-up and wave development 25
Figure 18: Different steps in the erosion process and how these are calculated in this research 31
Figure 19: Definitions of geometry points for erosion formulas of Klein Breteler et al. (2012) 34
Figure 20: Geometry erosion profile for erosion formula of Mourik (2020) 35
Figure 21: Schematization of erosion profile with relevant definitions for erosion formula of Klein Breteler (2022) 37
Figure 24: Frequency curve for HR-location 30 (hm 13.4) 43
Figure 22: Difference between the two conversion methods of Q-variant and trapezoidal schematization 44
Figure 23: Storm evolutions of water levels and related wave characteristics for a storm with P = 10,000 years at Ketelmeerdijk HM 13.4 45
Figure 25: Graph with hydraulic loading for first basalt, then Basalton, and the time series which remains after block revetment failure 46
Figure 26: Strength duration graph for upper clay layer showing the time before failure occurs 48
Figure 27: Time step size analysis for application of Klein Breteler et al. (2012) computation 50
Figure 28: Time step size analysis for application of Mourik (2020) showing the impact of using different time steps in a computation 50
Figure 29: Time step size analysis for application of Klein Breteler (2022) showing the impact of using different time steps in a computation 50
Figure 30: Calculated erosion volume for the Ketelmeerdijk with normative hydraulic conditions, using different relevant clay erosion methodologies 51
*Figure 31: Sensitivity analysis for significant wave height* 52
Figure 32: Sensitivity analysis for slope steepness tan(α) 52
*Figure 33: Sensitivity analysis for wave steepness* 53
Figure 34: Cumulative erosion volume following the approach of Mourik (2020) 56
Figure 35: Erosion profile during peak of the storm (from T=15.5 to 19.5 hours) following approach of Mourik (2020) 56
Figure 36: Illustration of erosion volume development at Ketelmeerdijk for Klein Breteler (2022) 57
Figure 37: Erosion profile during peak of the storm (from T=15.5 to 19.5 hours) following approach of Klein Breteler (2022) 57
Figure 38: Probability curve for erosion volume with use of the erosion formulas of Mourik (2020) 59
Figure 39: Probability curve for the erosion depth with the erosion formulas of Mourik (2020) 59
Figure 41: Water level evolutions with different probabilities of occurrence, indicating points of failure for top layer (yellow), upper clay layer (orange), clay erosion with Mourik (2020) (red) and Klein Breteler (2022) (purple) 60
Figure 40: Probability curve for strength duration of different sublayers 61
Figure 42: Refraction of waves near the Ketelmeerdijk 74

# 1. Introduction

## 1.1. Context

The IJsselmeer, a freshwater lake located in the north of the Netherlands, is surrounded by flood defences, to protect Dutch precious land from flooding, see figure 1. The province of Flevoland is a low-lying polder, located directly within the IJsselmeer, and has for that reason an extensive dike network, see figure 2. In total, more than 100 kilometres of primary flood defences are protecting Flevoland against flooding from both the Markermeer and IJsselmeer. The Ketelmeerdijk is one of these trajectories, with a length of 9.2 kilometres, at the northern side of the Flevopolder. The Ketelmeerdijk is protecting the Flevopolder against the threat of flooding from the Ketelmeer, which is part of the IJsselmeer.

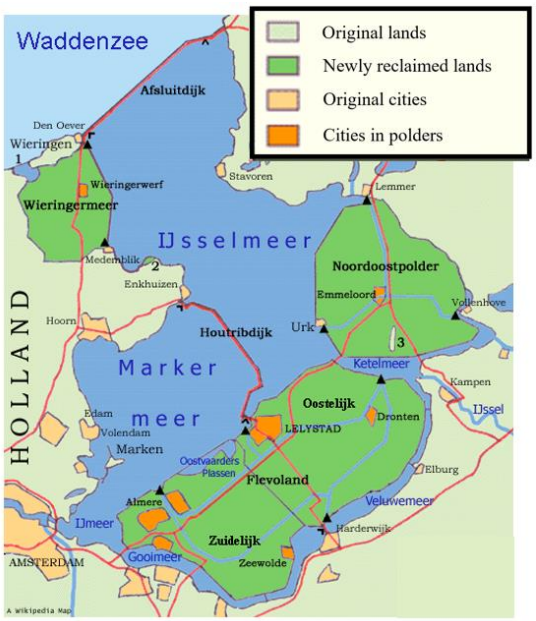


*Figure 1: Geographical location IJsselmeer, indicating relatively high 'original' lands, low-lying newly reclaimed land (polders), and dikes*

To guarantee high flood defence safety standards, the Dutch Government states in The Environmental and Planning Act (in Dutch: *Omgevingswet*) that water authorities should assess their existing flood defences on relevant failure mechanisms. To make this manageable, the primary flood defences are split up into dike trajectories. For delimiting the dike trajectories, it is identified which sections have the same quality and geometric properties, as well as the respective consequences in case of breach. For each dike trajectory, safety norms are separately given as prescribed by law. Through assessing a dike trajectory on all relevant failure mechanisms, on a cross-sectional level, conclusions on its safety are made. Once it turns out during an assessment that one or more failure mechanisms do not meet the legal norm, further steps are taken and possibly dike reinforcement is planned. The protocol that describes how this safety assessment should be concretely conducted is created by Rijkswaterstaat. As of 2023, this protocol is prescribed in the Assessment- and Design Protocol (in Dutch: *Beoordelings- en Ontwerp Instrumentarium* or *BOI*), and describes the guidelines to which water authorities should adhere in dike safety assessment. The latest protocol which has been finished and published by all water authorities is The Legal Assessment Protocol (in Dutch: *Wettelijk Beoordelings Instrumentarium*, or *WBI-2017*), and the results of this assessment round are documented in the First National Assessment Round (in Dutch: *Eerste Landelijke Beoordelingsronde*, or *LBO-1*). Following these guidelines, a target failure probability for a relevant failure mechanism (in Dutch: *doorsnede eis*) is determined for a dike section on a cross-sectional level. This is the tolerable probability of failure for this dike section.

The results of LBO-1 show that for the failure mechanism "instability of block revetment (ZST)", 12 per cent of the total Dutch primary flood defences do not meet the safety standard. On top of that, 5 per cent is near failing the safety standard and can expect reinforcements to the revetments in the next few years. For the failure mechanism of "grass cover erosion due to wave loading on the outer slope (GEBU)", 5 per cent does not meet the safety standard. For 20 per cent, the water authorities can expect dike improvements or indirect adjustments to reduce the impact of wave loading in the coming years. One of the trajectories that partially does not meet the safety standards for both ZST as well as GEBU, is the Ketelmeerdijk. As documented in LBO-1, the trajectory has over 10 kilometres of block revetment (ZST) which does not meet the legal standards (Ros & Vlaming, 2021). Also, more than 6 kilometres of the Ketelmeerdijk does not meet the norm regarding GEBU. Particularly the dike segments exposed to relatively intense wave loading fail to meet the safety standards of both mechanisms. Illustratively, figure 3 shows the Ketelmeerdijk and surrounding dikes, and indicates which sections do meet the safety norm (green) for both mechanisms GEBU and ZST, meet the safety norm for one of the two mechanisms (in orange), or fail for both mechanisms (in red). This caused a dike reinforcement program to be set up in 2024 for trajectory 8-4, of which the Ketelmeerdijk is a section.


*Figure 2: Locations of the dike trajectories around the southern polder of Flevoland*

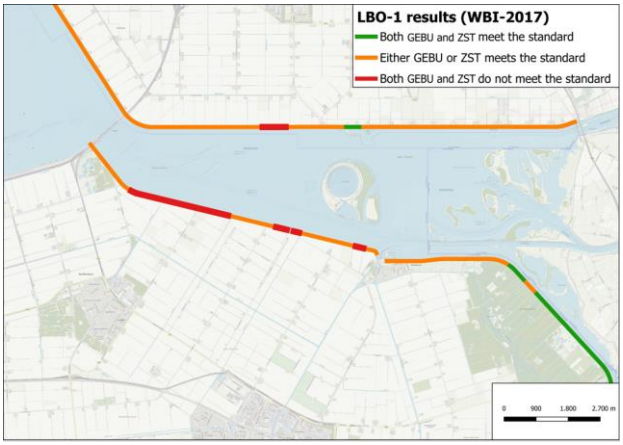


*Figure 3: Reporting of WBI2017 results for failure mechanisms of GEBU and ZST, showing where both mechanisms meet the standard (green), one meets the standard (orange), and neither meets the standard (red)*

When BOI is consulted to assess whether a flood defence (on cross-sectional) meets the safety standard with regard to the failure mechanisms related to dike erosion from the outer slope, only the cover layers (i.e. block revetment, asphalt layer, grass cover) are included in the assessment. The strength between failure of the revetment and full breach, provided by the dike body, is not taken into account in the latest dike safety assessments. This means that, in conventional dike safety assessment, the dike is considered to have failed as soon as revetment failure occurs. This causes the current methodology to give a conservative safety assessment. The question remains whether the dike should have enough erosion resistance left after initial failure to resist such a storm event, and be repaired in time for the next storm event. The remaining strength, provided by the clay layer and core of the dike, is called residual strength. It is dependent on the dike's geometry, soil properties and related hydraulic loading (Remmerswaal, Hicks, & Vardon, 2019). It is not included (yet) in the dike safety assessment due to a lack of research, and too much uncertainty related to that research which is available, focussed on progressive clay cover erosion. As a result, only components of the concept have been integrated into the BOI protocols so far. In practice, this could mean that the latest dike safety assessment results can be sharpened, while residual strength could form the decisive factor in meeting or failing a safety norm. Particularly for the Ketelmeerdijk, which is characterized by its relatively wide crest, due to the placement of a two-lane roadway and bicycle pathway on the 3-meter wide berm. In figure 4, a simplification of the cross section, and how it will be treated in the remainder of this research.

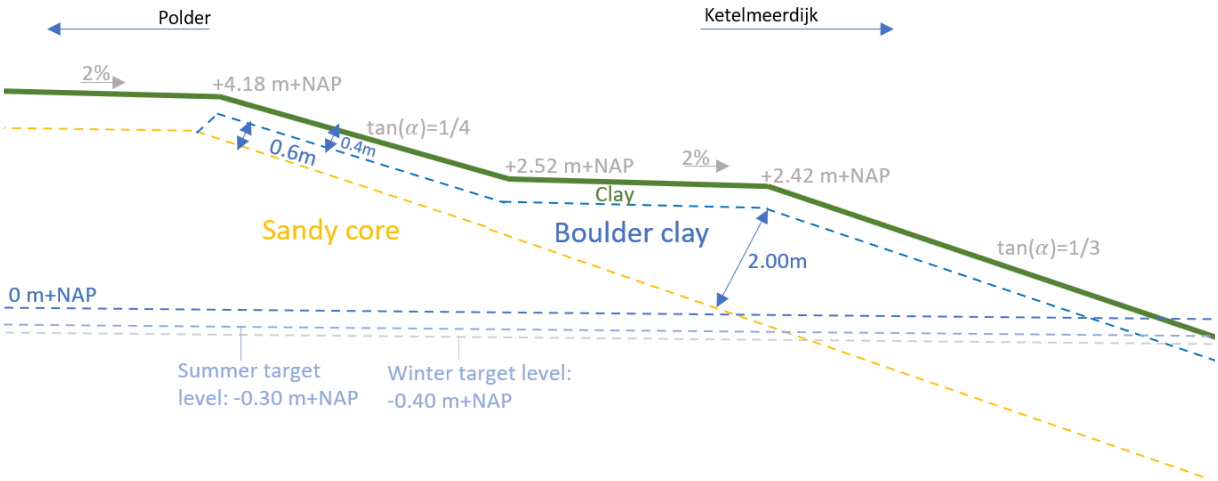


*Figure 4: Simplified cross-sectional profile of the dike trajectory Ketelmeerdijk*

The potential of residual strength is widely recognized and therefore thoroughly researched. The latest insights are constantly shared through new publications. To gain a better understanding of the topic, and reduce the uncertainties related to clay erosion, large-scale modelling tests have been carried out. One of these is the strength assessment of a clay cover on a slope loaded with wave impact in the Delta Flume, as part of the research program "*Sterkte en Belastingen Waterkeringen*" (Wolters & Klein Breteler, 2011). Also, Kaste & Klein Breteler (2015) have analysed the dike erosion of a practical sample in the Delta Flume and derived empirical equations between hydraulic conditions and dike erosion. The latest large-scale modelling research was published in 2022 by (Klein Breteler M. , 2022). The study describes progressive clay erosion on the upper slopes of the Wadden Sea dikes as a result of wave impact. Incentives have been set up, to integrate the results from the modelling tests in a dike safety assessment. Examples are the Bekledingsmodel ("Cover Layer model"), in a probabilistic way, and the DiKernel, in a deterministic manner, designed respectively by HKV (Rongen, 2020) and Deltares, describe erosion resistance models designed for revetments. These try to integrate the concept of residual strength of clay dikes in the dike safety assessment. Despite all these advancements, the concept still is not fully integrated into the BOI.

## 1.2. Problem statement

The probability of flooding caused by erosion of the outer slope is solely composed of instability of revetment or failure to grass cover. It does not take into account the residual strength of the dike body that remains after revetment failure. Therefore, the probability of failure is overestimated. This means the assessed flood defence gives conservative results from the safety assessment regarding dike erosion of the outer slope. It remains to be seen, however, how much and how long a dike body can resist hydraulic loading before a dike breach will occur, once revetment failure occurs, and with that, establish a new probability of failure which is more accurate.

As of now, several preliminary dike erosion modelling methods (both probabilistic and deterministic) have been set up, to take into account residual strength after revetment failure. Within the WBI-2017, these types of modelling methods could already be applied within a customized safety assessment of a flood defence, albeit including large conservative assumptions. Within the BOI, the responsibility is placed more on the user and the choice of modelling method per failure mechanism is allowed to be applied as long as it is properly substantiated. However, the concept of residual strength is complex and little validated scientific research is available. For that reason, Dutch water authorities are hesitant to use the few modelling methods available right now. This means that the latest LBO-1 results often do not include any form of residual strength as a stability component of the dike, which makes that a wide range of flood defences is required to be reinforced, while it is not fully known whether this is necessary.

## 1.3. Knowledge and research gap

The knowledge gap of residual strength originates from the presence of uncertainties on residual strength and the absence of a validated residual strength model. The concept is recognized in science and practice as a field of study with a lot of potential in gaining an understanding of the full stability of flood defences. This has led to propositions for the integration of the concept in future guidelines such as the BOI, the setting up of pilots for progressive clay erosion models, and a lot of large-scale modelling research to gain a better understanding of the process.

However, current models on residual strength are limited in both scope, possibilities and accuracy, they are difficult to validate, and the full extent of the related uncertainties is unclear. This means that in practice, water authorities and Rijkswaterstaat are prudent to include it in their dike trajectories' safety assessments. The translation from a broad theoretical base and tests from the DeltaFlume, towards the practical application such as in the BOI and the water authorities, has not been established. To bridge this gap, practical studies have attempted to provide insights into the dike erosion of block revetments, clay covers, and separately of sand erosion. However, a research gap remains with regard to the combination and interaction of the aforementioned erosion processes.

The Ketelmeerdijk is an outstanding example where the knowledge of residual strength is not applied. The dike fails on both ZST and GEBU, but the clay cover erosion is not taken into account in the strength assessment. This means that the dike now has to see reinforcements as a result of conservative calculations. In practice, the erosion resistance of the clay layer and maybe the sandy core can prove the dike meets the latest dike safety standards. The potential, however, has been recognized by the waterboard Zuiderzeeland (ZZL). It remains unclear which methodology is the best for quantifying the residual strength of the Ketelmeerdijk. This study aims to bridge this gap. Scientifically, the potential of residual strength will be analysed on a dike with the characteristics of the Ketelmeerdijk. Specifically, this study will apply the concept of residual strength to assess and quantify the effect of incorporating clay erosion as part of the dike stability assessment.

## 1.4. Research goal and scope

The main goal of this research is as follows:

*"To evaluate the possibilities and the influence of integrating residual strength, after the failure of the revetment on the outer slope, in a dike safety assessment applied to a dike with the characteristics of the Ketelmeerdijk"*

### 1.4.1. Research questions

To answer the research posed above, the main research question is formulated:

*"How can a progressive erosion model quantify the residual strength of a dike such as the Ketelmeerdijk, incorporating the processes of hydraulic loading, cover layer failure, and clay erosion?"*

To answer the main question, it is divided into sub-questions. By answering these questions, substantiated research is conducted and with the answers, the research goal is attempted to be met.

1. How can the evolution of a storm event at the IJsselmeer be schematized, and how does this result in the normative hydraulic loading for Ketelmeerdijk?
2. In what way are the hydraulic conditions determined for the failure of the grass cover and block revetment, based on the latest dike safety assessment methods, during a normative storm event at Ketelmeerdijk?
3. Which methods to model clay erosion on the outer slope of a dike with the characteristics of the Ketelmeerdijk are most suitable?
4. How can a progressive erosion model be set up, and applied to a dike with the characteristics of the Ketelmeerdijk?

### 1.4.2. Research scope

The concept of residual strength is relatively broad in interpretation and application. To make this study realistic and achievable within the timeframe, the focus will lie solely on progressive clay erosion. The steps of progressive dike erosion are treated as follows: (1) setting up hydraulic conditions, (2) failure of the cover layer, (3) erosion of clay cover. Another component of residual strength, which is the sandy core, is left out of the scope. The focus will solely lie on the erosion of the outer slope of a dike, and not on the inner slope.

Hydraulic conditions will be set up with the current methodologies used in the latest dike safety assessment. No future forecast scenarios will be taken into account. The scope is restricted to the specific case study of the Ketelmeerdijk. This dike is subjected to hydraulic loading from the Ketelmeer, which could see water level set-up from its connection to both the IJssel-Vecht delta and the IJsselmeer.

The revetment layers that are considered are block revetment (ZST) and grass cover (GEBU), and their moment of failure will be the initiation point of the clay erosion process. The instability of block revetment and grass cover failure are aspects that will be assessed using the models currently in use by ZZL and approved within the BOI.

The clay cover erosion process will be calculated through empirical formulas, all resulting from large-scale modelling tests from the Delta Flume. The failure criteria for residual strength in this research is set at failure of the clay cover. Once the clay cover fails, and the wave loading is subjected to the sandy core, the erosion process will be very rapid. For this reason, low confidence is placed in the erosion resistance of the sandy core, and it will not be taken into account for this research.

Also, the application of the model will be solely to the case study of the Ketelmeerdijk. It could then be applied to other dikes with similar characteristics as that of the Ketelmeerdijk. Be aware that the results from the model cannot be trusted fully before proper validation occurs.

### 1.4.3. Research approach and outline

The research approach is presented in figure 5. This study focuses on the implementation of clay erosion formulas to a typical dike that does not meet the safety standards following the latest WBI-2017. These clay erosion formulas can quantify erosion volume as a function of hydraulic loading, and show that residual strength can be the decisive factor so that a dike does not require reinforcement. To find the erosion volume, empirical clay erosion formulas are used. As input, these require the normative hydraulic loading and the dike's geometric and soil properties. The starting point at which clay erosion will be initiated is the point of failure for the revetment layers. This point is calculated in RQ2, through using the black-box model of STEENTOETS, and retrieving the formulas behind BM Gras Buitentalud. These two software programs are used by ZZL in the dike safety assessment and are prescribed in the BOI. Through the selection of the most adequate erosion formulas, a calculation model can be set up in which a preliminary assessment of the dike's residual strength is made. The model is used to apply the theoretical basis that has been set up through large-scale modelling tests in a practical context.

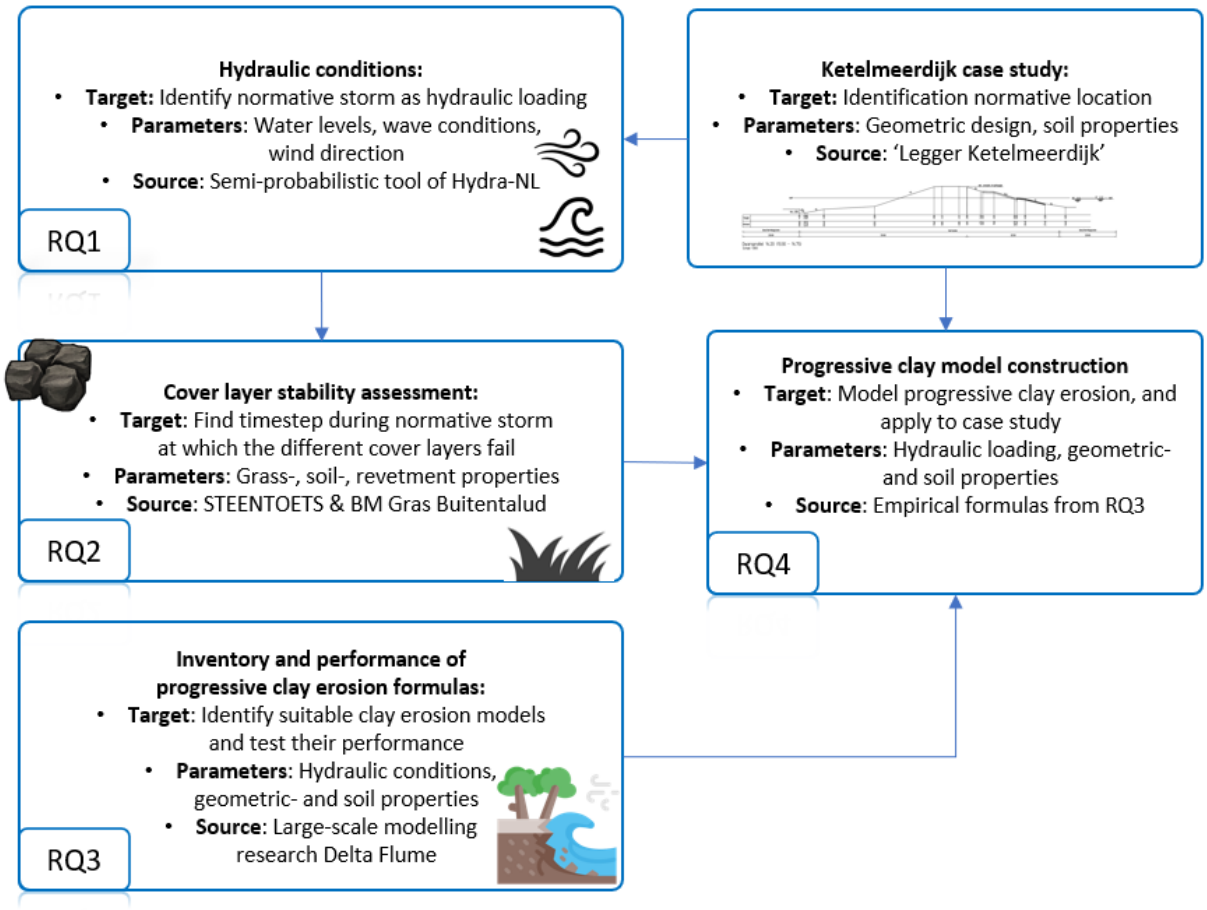


*Figure 5: The research approach per question and outline of the thesis*

Below, the research approach for each of the research questions is briefly posed.

### 1.4.4. Approach per research question

**RQ1** First, the different options with regard to synthetic storms are analysed. This involves both the storm duration, the water level evolution and the conversion from water levels towards wave conditions. The most suitable option is then selected for the application of a dike safety assessment for the Ketelmeerdijk. To identify the stationary hydraulic conditions, literature is consulted. To find the peak values, the semi-probabilistic tool of Hydra-NL will be consulted. The relevant hydraulic conditions for the Ketelmeerdijk, so at a cross-sectional level, and for the proper return times, will be documented.

**RQ2** The goal is to find the moment in time during a synthetic storm at which the cover layers fail. For that, STEENTOETS and BM Gras Buitentalud are consulted. These two software programs are prescribed in the latest WBI-2017 dike safety assessment round. By identifying the hydraulic loading at which the cover layers will fail, the point is identified at which clay erosion will be initiated. The relevant outcome for the Ketelmeerdijk will be documented.

**RQ3** An inventory of the relevant clay erosion formulas is collected, analysed through sensitivity studies and from these formulas, the most adequate method is selected which can then be applied to the Ketelmeerdijk. This analysis will prove vital for understanding how the formulas have been built up, on what principles these rest, and how they can be applied. Sensitivity analyses will be performed to identify the extent to which certain parameters impact the outcome, as well as to identify the influence of time step size. Based on the outcome, a substantiated choice can be made on the most adequate erosion formulas that can be used when applying it to the Ketelmeerdijk.

**RQ4** In this question, a progressive clay erosion model can be set up, with the use of the input from the previous questions. By calculating the erosion volume that occurs during hydraulic loading, and linking that to specific dike geometry points, an erosion profile is set up. By subjecting the dike geometry to a full normative storm, an answer can be given to the question of whether the dike will or will not contain sufficient residual strength after initial damage has occurred to the cover layer. After the model has been set up, frequency curves will be made, to show the behaviour of the erosion models to different failure probabilities. The model will be applied to the Ketelmeerdijk. After the cover layers have eroded, it is checked how the Ketelmeerdijk deals with the 4-hour peak loading at a constant water level.

# 2. Theoretical background

This chapter provides a theoretical base that is required as a first step in finding the normative hydraulic loading, gives the latest expertise on deriving a point of failure for the revetment layers, and subsequently, describes the newest modelling options for describing clay erosion. When these are combined, a framework is created in which a progressive clay erosion model is set up and applied to the Ketelmeerdijk.

## 2.1. Hydraulic conditions

The IJsselmeer functions as a freshwater buffer and its water levels are controlled by the Dutch water authorities. The water levels are kept artificially low in times of excessive precipitation and large discharges from the rivers IJssel and Vecht, by increasing spillage to the Wadden Sea. In times of summer and drought, the water levels are kept higher. This facilitates extra evaporation, and maintains the required basin, as potential drinking water and sudden need for fresh water for agriculture. The target lake's water levels are flexible, and controlled through policy regulations of the Dutch government. The levels range in the winter between -0.40 and -0.10 m+NAP (Rijkswaterstaat, 2018), and in the summer, between -0.30 and -0.10 m+NAP. The lake water levels are influenced by discharges from major rivers such as the Vecht and IJssel, smaller rivers and canals like the Zwarte Water, surface runoff from the land, precipitation and evaporation, and the operation of pumping stations (e.g. Vissering and Colijn pumping from the hinterland) as well as spillways (Kornwerderzand and Den Oever at the Afsluitdijk leading to the Wadden Sea).

During a storm surge, the wind could cause shear stress on the IJsselmeer resulting in wind setup. When a storm exerts its forces on the IJsselmeer, the water levels are tilted, leading to a water level increase at the Ketelmeerdijk. Also, a storm or extensive rainfall upstream of the rivers could result in higher water levels at the inlet of the IJsselmeer. When the water cannot be discharged in the Wadden Sea near the Afsluitdijk, due to increased water levels at the Wadden Sea, this could cause extremely high water levels at the dikes surrounding the IJsselmeer. The impact of the wind conditions on the respective water levels at a dike toe has a more decisive role than increased river discharges and surface run-off (Chbab, 2012). In the future, the water levels are expected to increase more, see figure 6. Precipitation is expected to occur more intensely and frequently, influencing the lake water levels (KNMI, 2023). In the summer, the water levels are already kept higher than the design water level to accommodate for extra evaporation and droughts. Also, a sea level rise at the Wadden Sea could cause fewer windows of opportunity to spill water under free decay at the spillways at the Afsluitdijk.

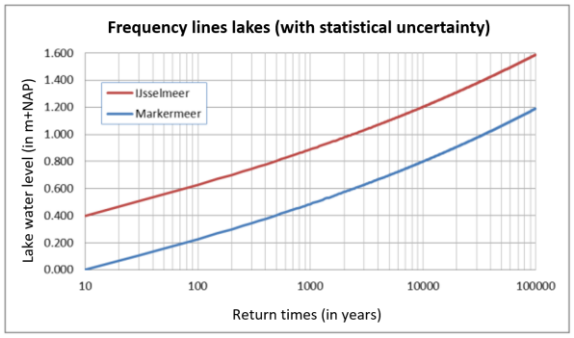


*Figure 6: Frequency lines for both the IJssel- and Markermeer (Botterhuis, Waterman, & Geerse, 2017)*

### 2.1.1. Hydraulic parameters

In order to safeguard sufficient strength, dikes are assessed periodically on their stability. These safety assessments keep on evolving, being fed by new research and new insights. Also, the input for the hydraulic loading keeps on developing and is slowly traversing from a deterministic to a probabilistic methodology. Each failure mechanism is sensitive to other (combinations of) critical hydraulic loading.

For instance, piping (backward sand erosion below a dike) is more responsive to prolonged high water levels. In contrast, dike erosion of the outer slope is more susceptible to intense wave impacts, typically associated with relatively brief storm events accompanied by a storm surge. The hydraulic system at the IJsselmeer is mainly wind-driven, which could result in tilting water levels and increased waves. During a storm, the set-up of water levels and waves is often relatively short, ranging from a few hours to a few days. So when assessing a dike on a specific failure mechanism, different combinations of hydraulic parameters are required.

The normative hydraulic loading parameters for a specific location are often calculated in a probabilistic way, through software programs such as Riskeer and Hydra-NL. For a specific location, these programs can compute a large number of combinations of both high water levels (caused by high river discharge, and/or discharge limitations at the spillways), extreme wind set-up (leading to lake level set-up and waves) or a combination of both (Ministry I&W, 2017). These lake water levels and wind conditions (possibly in combination with river discharges), are then translated to wave conditions. For that, an underlying wave model (e.g. SWAN, HISWA) of Hydra-NL computes random, short-crested wind-generated waves (Geerse C. , 2009). The normative parameters are those combinations of hydraulic parameters from this large probabilistic set that will form the largest threat to the flood defence.

Some of the most common hydraulic parameters used in dike safety assessment are displayed in figure 7. These are the relevant parameters which will be used in this research. The lake water level (in Dutch: *meerpeil*) is described as the water level relative to NAP (abbreviation of *Normaal Amsterdams Peil*). Wave characteristics, such as significant wave height ($H_s$), peak wave period ($T_p$), and wave steepness ($s_{op}$) are critical for calculations on hydraulic loading. The significant wave height is equal to the average height of the tallest third of the waves over a longer period. Its height is influenced its effective fetch (the length on which waves and water level set-up can develop towards a dike), by wind direction and speed, and local characteristics near the dike toe. The wave period is the time between two successive wave crests, averaged over a larger set of waves. It can be set out in either spectral, peak, average or significant wave periods. For hydraulic loading calculations, the peak wave period ($T_p$) is often consulted. Wave steepness is the ratio between wave height to its length, where a larger steepness relates to a higher wave impact. Often, the steepness remains constant throughout a storm evolution, where water levels, wave lengths and wave heights both increase. In general, for non-plunging waves, the steeper the wave, the larger the wave impact. Typical wave steepness values for waves on lakes range between 0.01 to 0.06 (Smale & Beckers, 2011).

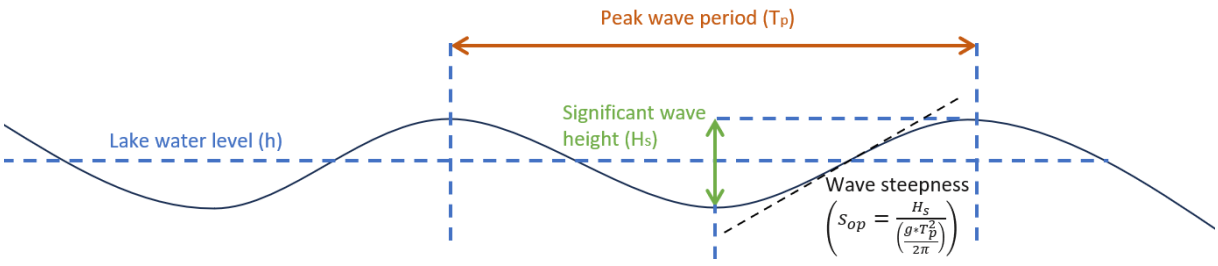


*Figure 7: Hydraulic loadings schematized, with lake water levels, peak period, significant wave height, and wave steepness*

All of the aforementioned parameters are output from probabilistic calculation tools, such as Hydra-NL. Dependent on the norm frequency and to be tested location, water authorities and organizations like Rijkswaterstaat can determine the input for the flood defence safety assessment. This way, the peak values are retrieved. Often, the peak values only are not enough to make an accurate strength assessment. Stationary levels and the way these parameters behave during a storm event are often crucial as well. To see how dike segments behave not only at the peak values but throughout the whole storm event, synthetic storms have been set up.

### 2.1.2. Synthetic storm: evolution and duration

So when assessing a dike on a specific failure mechanism, different combinations of hydraulic parameters are often combined in a schematization. The schematization of hydraulic loading parameters is often described as a synthetic storm. The evolution of the storm and how to use it in dike safety assessments in the BOI are prescribed in the schematisation manuals of Rijkswaterstaat (2022). This schematization can be different per rated failure mechanism. For the IJsselmeer, and applying this to the failure mechanism of outer slope erosion, it is composed of a stationary lake water level, that sees a gradual set-up and decrease with a normative peak high water level, lasting for a certain storm period.

In the WTI-2011, a proposition for a synthetic storm was given by Nieuwenhuijzen et al. (2010), which included a 48-hour storm with a peak duration of 2 hours. Alternatively, Chbab (2012) claimed that a normative storm duration of 40 hours with a peak duration of 2 hours is most adequate to assess the stability of a dike. In the previous dike safety assessment of the WBI-2017, a synthetic storm of 35 hours was used, and this is also recommended for the BOI. When making calculations on block revetments or asphalt cover layers, this storm is recommended to be used (Ministry of I&W, 2007).

The hydraulic conditions play a large role in this assessment and can cause large inaccuracies when not sharply defined. These inaccuracies could lead to unsafe situations, where the dike's strength is underestimated, or lead to unnecessary costly reinforcements when the dike's strength is overestimated. For that reason, a guideline has been set up that describes how to derive lake-level evolution for arbitrary storm events, and related wave characteristics. The locations at which the hydraulic conditions are determined are also fixed and documented in the HRD files, containing for each shoreline location the water levels and specific information on the basic stochastics (i.e. stationary lake water levels, discharges and wind set-up) and the hydraulic loading parameters (i.e. normative wave conditions and extreme lake water levels) (Chbab, 2012).

For fresh water lakes such as the IJsselmeer, a dedicated time-dependent evolution of water levels was constructed by Geo-Delft in collaboration with Rijkswaterstaat (Calle, 2004). This concept is then adopted by Geerse (2007), and improved to a version that is applied nowadays. This evolution follows a certain duration T, during which it increases linearly to a peak water level which is maintained for 4 hours, and then linearly decreases again to the stationary water levels (Geerse C. , 2007). This results in a schematical trapezium shape, see figure 8. The peak water level is probabilistically derived per location, following a computation in Hydra-NL or Riskeer, at the norm frequency. Hydra-NL and RisKeer are two semi-probabilistic tools to derive the hydraulic conditions at a normative location, for different return times. The stationary water level is the normative water level just before a storm event and just after this event.

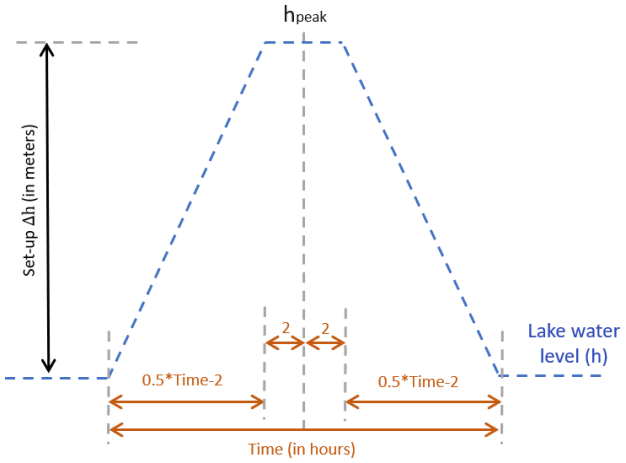


*Figure 8: Standard schematized water level evolution used in Dutch lake dike safety assessment (Ministry of I&W, 2007)*

## 2.2. Dike cover layers

### 2.2.1. Flood defence safety assessment

The stability of flood defence is assessed through failure mechanisms. Examples are cover layer erosion as a result of wave impact, wave overtopping, macro-/micro instability, or piping. Once the failure probability of any mechanism does not meet the legal norm or the so-called 'probability of flooding', the flood defence requires reinforcement. A distinction is made between two probabilities of flooding. The alert safety standard (in Dutch: *signaleringswaarde*) and the lower threshold safety standard (in Dutch: *omgevingswaarde*). The alert safety standard is the probability of flooding where actions need to be planned so that the failure probability will remain below the lower threshold safety standard and is 3 times lower than the lower threshold. The lower threshold is the probability that is not allowed to be exceeded. It can be seen as the design safety standard, on which dikes are constructed (Rijkswaterstaat, 2022).

In the Netherlands, initially, dike trajectories were assessed on probability of exceedance. From 2017 on, the WBI was introduced and with that, dikes were assessed on the probability of flooding. The probability of flooding varies per dike trajectory and is dependent on the consequences of a breach, both related to socio-economic damages and Local Individual Risk (in short: LIR, related to potential loss of life). For Dutch rivers, the norm can be as low as 1/100 years. For areas with larger socio-economic risk related to flooding, due to low-lying hinterland and high economic value behind the flood defences, this norm can be as high as 1/1,000,000 years. For the Ketelmeerdijk, which protects Oostelijk Flevoland, the norm is equal to 1/10,000 years. This norm is dominated by the socio-economic risks related to breach (Ministry of I&W, 2016).

From 2023 on, an improved assessment system will be set up, under the name of BOI. Customized testing (in Dutch: Toets op Maat) is the norm within the system, whereas WBI-2017 only exceptionally promoted to choose own methodologies. A water authority can decide for themselves which method to select, provided that the principles are well funded and the choices are properly motivated. The method should be validated and therefore approved as a tool within BOI.

### 2.2.2. Instability of cover layers

The stability of cover layers is assessed during a safety assessment of the dike. When it shows in this assessment that the cover layer does not contain sufficient stability, reinforcement is planned. Whereas residual strength – hence the strength in the clay cover and sandy core – is not taken into account during the assessment of cover layers, the design is often much stronger than required. In this part of the research, two failure mechanisms are considered. These two mechanisms are treated because they both do not meet the required safety standards for large stretches of the Ketelmeerdijk, looking at the lower threshold safety standard.

**Instability of block revetment (ZST)**

This mechanism relates to the loss of stability in the protective layers of block revetment placed on the outer slope of the dike, resulting from processes such as erosion, settlement, or dislodging of individual blocks. Damage to block revetment always occurs below the water level surface, where steep hydraulic head fronts and wave impact occur in the breaker process (Wolters & Klein Breteler, 2011). In the figures below, two processes are displayed in which the instability of block revetment is visualized. This can be either as a result of a shear plane, which is a direct consequence of the failure mechanism of macro-instability, see figure 9. Another option is the increase of hydrostatic pore pressure below the block revetment, see figure 10. The largest peak pressure often occurs between the water level and half the significant wave height. When a wave hits the slope, first, wave run-up takes place. Then, the water infiltrates between the revetment blocks and is washed back to the water body in the filter layer.

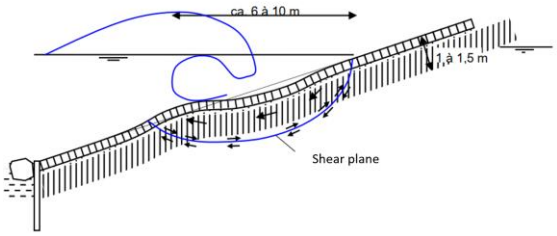


*Figure 9: Schematical resemblance of deformation due to sliding and forming of an S-profile (Klein Breteler, Mourik, & Bosters, 2014)*

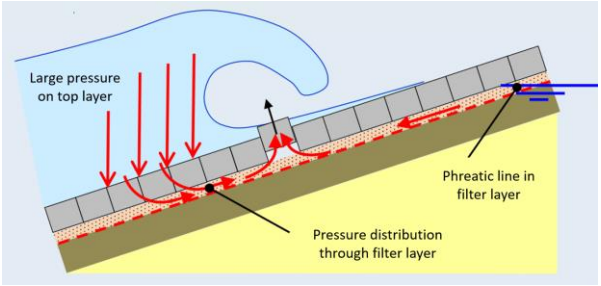


*Figure 10: Schematical resemblance of block revetment failure as a result of a pressure gradient (Klein Breteler M. , 2016)*

**Grass cover failure erosion by wave loading on outer slope (GEBU)**

From wave flume experiments and experiences during past high-water events, it has been found that the density of the root network is a much more important factor in the erosion resistance of grass cover than the erosion resistance of the soil (Rijkswaterstaat, 2012). Failure of grass cover can occur as a result of wave loading caused by wave impact or wave run-up. Grass cover, placed above the wave impact zone, stabilizes the soil and dampens wave impact. When a wave breaks on a slope, it generates both a direct pressure pulse to the grass and an indirect pressure pulse in the soil layer. This pulse could reduce the effective pressure in the soil, potentially leading to deformation. Schematically, the composition of grass cover can be distinguished into two segments. The first segment is exposed to the atmosphere, and is a 20 centimetres thick heavily rooted clay layer with grass placed on top, also called the living turf layer. The second segment is a 30 centimetres thick clay layer which is slightly more compacted than the soil below, making it more erosion resistant. Also, this layer still contains some roots, improving soil resistance.

### 2.2.3. Typical cover layer design on Dutch dikes

In general, most Dutch dikes are constructed with a sandy core, covered with a resistive clay layer and on top of that a cover layer. The type of cover layer is dependent on the water system in which the flood defence is placed, and the related hydraulic loading (i.e. tidal range, discharge fluctuations, effective fetch). Under the definition of revetments are three types distinguished: (1) natural/artificial block revetment, (2) asphalt layer, and (3) grass cover.

Originally, Dutch dikes were covered with natural block revetments, such as basalt rock, Norwegian stone, granite, or Vilvoordse Rock. As a result of scarcity and logistical complexities, a transition took place in which artificial, concrete block revetments have been developed, such as Ronaton, Basalton, Hydroblock, and Hillblock. In practice, these prove to be more resistant to high wave impacts. Block revetment is traditionally placed at the wave impact zone, protecting the dike from the direct wave impact, see figure 11. Below, a filter layer is placed, in which granular material such as coarse gravel or crushed stone is placed. The filter layer traps fine particles and prevents washing out, while allowing free drainage of water, reducing the hydrostatic pressure.

A geotextile fabric separates the filter layer to the clay layer, enhancing the stability of both the revetment (as a result of local settlement) and the clay layer (by reducing peak pressure as a result of wave impact). Below that, the clay layer functions as a water-resistive barrier against seepage and provides overall stability to the structure of a dike. Below the clay cover, a dike core often consisting of sand is placed, which is less susceptible to settlement than clay. Also, it is cheaper, and more easy and predictable to work with than clay soil. Besides that, sand can drain water through its large pores, reducing the risk of water accumulation within the dike body.

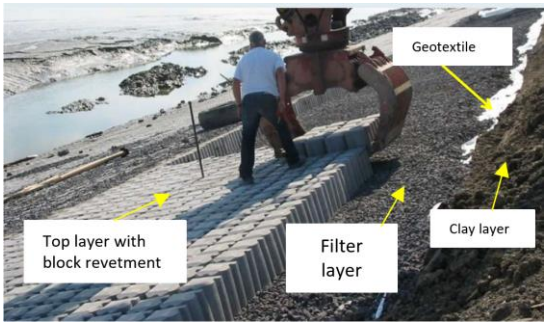


*Figure 11: Construction of artificial Basalton cover layer, with the geotextile, filter layer and clay layer visible*

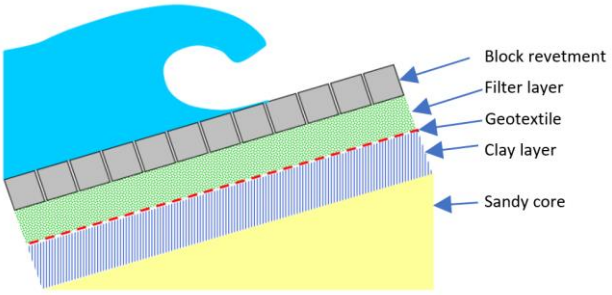


*Figure 12: Composition of the cover layer and the required layers beneath in a schematized overview*

## 2.3. Clay erosion

In dike safety assessment, it is assumed that once the first damage occurs, the full cover layer will not be intact anymore. This is while there are simply no models for (yet). Also, once initial damage occurs, the development of the damage is relatively rapid. Clay erosion is triggered after initial damage has occurred to either grass cover or block revetment.

### 2.3.1. Erosion profile

Typical Dutch dikes have a clay cover layer with a thickness in the range of 0.5 - 2.0 meters (IPLO, 1994). This layer protects the dike against erosion while helping to retain the structural integrity of the dike, and preventing permeability. In figure 13, the erosion pit development is schematically described, for a situation with grass cover on the upper slope, with a hard revetment layer beneath. When no hard revetment would be present, no jump (color indicated with orange) would arise, but the erosion terrace would continue until intersected with the original slope. The erosion pit typically is composed of two planes: the terrace and the cliff. The erosion pit develops as a result of wave impact on the outer slope, above the berm. Here, the asphalt layer on the berm will remain intact, but the grass cover will fail. Grass cover is often placed directly above hard revetment layers (i.e. block revetment, brick, asphalt). Erosion takes place in two phases (Klein Breteler M. , 2022). First, an erosion pit is formed directly behind the transition from hard to soft cover layer, which grows to a certain depth. In the second phase, the erosion pit starts to progress in a horizontal direction. For the first phase, the grass cover quality is an important parameter. For the second phase, the clay cover quality is vital in the progression of the erosion pit.

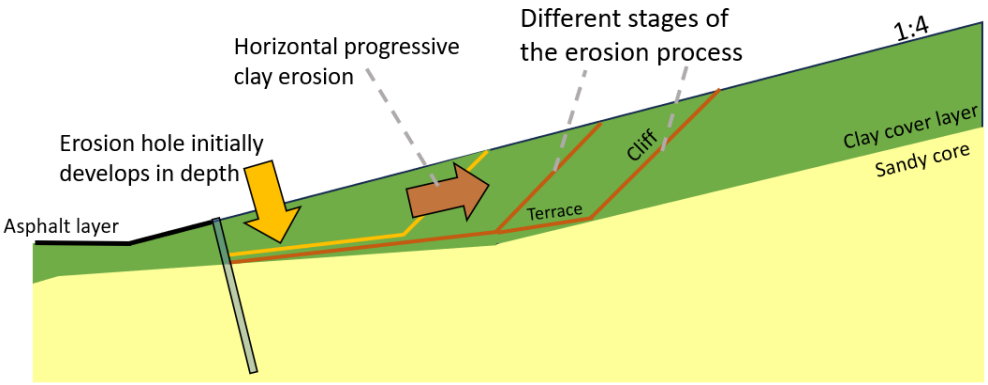


*Figure 13: Schematical representation of the typical erosion process occurring above hard revetment*

Numerous large-scale clay erosion modelling researches have shown that progressive clay erosion often follows the same steps, generating a similar erosion profile. This profile is composed of a gentle submerged slope (also called ‘terrace’), and a steep subsurface slope (also called ‘cliff’), see figure 14. The slope of the terrace often develops from relatively steep (ca. 1:8) to a more gentle slope (ca. 1:10).

The steepness of the terrace is dependent on the moment during the erosion process, but also on the original slope. The steeper the original slope, the steeper the terrace also is. Different findings are available on the cliff, with Mourik (2020) claiming a slope of 1:1 and Klein Breteler (2022) claiming a 2:1 slope. The steepness of the cliff is dependent on the clay properties, where sandy clay will form a gentler slope than lutum-rich clay. The horizontal development of the erosion pit is a result of the erosion cliff eroding more rapidly than the erosion terrace, while the layer of water on top of the terrace has a damping effect. The peak pressures, and resulting high flow velocities occurring during wave impact, are the key drivers behind clay erosion. Besides wave impact, clay erosion can also be initiated or progressed as a result of wave run-up or run-down. However, this research will solely focus on wave impact and the resulting clay erosion.

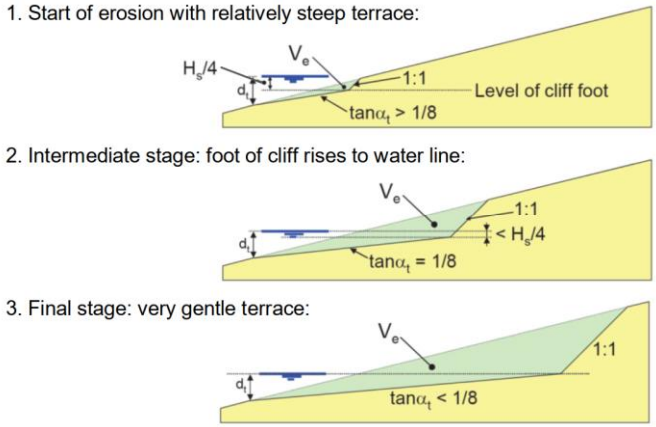


*Figure 14: Schematized development of the erosion profile (Mourik, 2020)*

### 2.3.2. Clay erosion formulas

After one of the cover layers has been compromised, clay erosion will be initiated. Compared to sand erosion, clay erosion is relatively difficult to model. This is due to its heterogeneous composition, its cohesive nature, and complex mechanical behaviour. This means that the clay erosion formulas are mostly empirically based.

The necessity and potential of performing large-scale modelling research to investigate clay erosion when loaded with high hydraulic loading was already recognized and suggested as early as 1992, in an article by Klein Breteler (1992). This was seen as an essential component to improve dike design. Initially, this led to empirical clay erosion formulas that describe a function of maximum resisting time (Van der Meer, 1999; Coeveld et al, 2004; Wolters & Klein Breteler, 2011). This way the residual strength of a dike was expressed as an amount of time before a full breach occurs. Throughout the years, this shifted towards a formula that calculates an erosion volume as a function of time, as shown in studies by Klein Breteler et al. (2012), Mourik (2020) and Klein Breteler (2022). Below, a brief overview of the most prominent studies related to empirical large-scale modelling research concerning clay erosion is placed, with a brief description.

*Table 1: Brief description of preliminary clay erosion models*

| # | Reference | Brief description | Function of … |
|---|---|---|---|
| 1 | (Van der Meer, 1999) | Rudimentary suggestion for an erosion model for dikes. Based on horizontal clay thickness, a coefficient for erosion resistance (quality of clay), a reduction factor for oblique incident waves and a normative significant wave height. | Time (in hours) |
| 2 | (Coeveld, Knoeff, Bizarri, & Klein Breteler, 2004) | Residual strength model for the sandy core of a dike with calculations from a dune erosion model, which is also applicable to clay cover. | Time (in hours) |
| 3 | (Klein Breteler et al. , 2012) | Preliminary erosion formula set up as a result of large-scale modelling research in the Delta Flume. Function of wave characteristics, water level and dike geometry. First publication to come up with an erosion volume over time ($dV_e/dt$), rather than working with residual strength as a function of time. | Volume over time (in $m^3/h/m$) |
| 4 | (Mourik, 2015) and later on: (Mourik, 2020) | Improvement to study of Klein Breteler et al. (2012), with a function based on an erosion volume over time. As of now, this method is often applied when working with clay erosion. It can be applied with significant wave heights larger than 0.4 m. | Volume over time (in $m^3/h/m$) |
| 5 | (Kaste & Klein Breteler, 2015) | Improvement to study of Mourik (2015). Recognized the difficulty for application of this model, when looking at varying water levels, and therefore a working principle is described how to do this. | Volume over time (in $m^3/h/m$) |
| 6 | (Klein Breteler M. , 2022) | Erosion model based on large-scale modelling tests in the Delta Flume, where samples of Wadden Sea dikes have been subjected to various normative hydraulic conditions. Describe two phases of clay erosion. The first phase is for initial clay layer erosion, until a depth of 50 centimetres. The second phase starts from erosion depths deeper than 50 centimetres. | Volume over time (in $m^3/h/m$) |

## 2.4. Case study Ketelmeerdijk

In this report, the concept of residual strength will be applied to the case study of Ketelmeerdijk. This dike did not meet the required safety standard following LBO-1, among others for the failure mechanisms of grass cover (GEBU) and block revetment (ZST). Experts at ZZL doubt whether the dike trajectory still does not meet this norm, once the erosion resistance of the clay and sand layer is also taken into the calculation. Specifically, the Ketelmeerdijk is interesting whereas the dike is characterized by a two-lane roadway on its crest, as well as a wide berm with a bicycle pathway placed on it. The two-lane roadway is on the crest as a result of the reclamation of the northern part of the Flevoland polder and functioned as the only method of transport once pumps started draining the hinterland and created the new land, now called Flevoland. Also, the dike trajectory has a relatively thick clay layer thickness, varying from 0.3 to 1.35 meters (Grontmij b.v., 2000). This makes this trajectory particularly interesting for integrating the principles and prototype modelling methods for residual strength. The question is if the dike trajectory will pass LBO-1, or maybe one of the failure mechanisms (partially) if residual strength is integrated into the calculation.

The Flevopolder is protected from the hydraulic loading of the Ketelmeer with the use of the Ketelmeerdijk, which falls under trajectory 8-4. This dike trajectory has a length of 17.5 kilometres and

stretches from the Ketelbrug in the west to the Reeve sluices near Dronten in the east. The last reinforcements took place in the period 2000-2006, which was necessary according to the standard which was applicable at that moment. This led to a uniform raising of the crest, placement of new block revetment on the outer slope and the predisposition of new drainage on the inner slope (Kaihatu, 2022). Dike drainage was installed below the inner slope to prevent excessive pore water pressure.

The Ketelmeerdijk is over its full length placed on a 1 meter thick sand foundation, with the low-lying weak clay layer acting as a barrier against groundwater flow. Two 1.5 meter high boulder clay dams were placed as anchors, with sand filled between them to achieve the desired crest height, which varies from NAP +3.40 m in the east to NAP +4.92 m in the west. This variation is due to the varying hydraulic loads from the Ketelmeer.

A clay layer was placed on top for stability and impermeability, with a grass cover on the outer slope above the water line and extending to the dike toe at the inner slope. Rubble stones and block revetment were used at the water line. See figure 15 and figure 16 for the latest schematized dike geometry design sketch, and the current state of the outer slope, respectively. This is the cross-sectional profile as designed over the length of HM 13.05 to HM 14.15. The other segments are relatively similar regarding crest height, berm height, and clay layer thickness, all in the order magnitude of at most 0.5 meters difference. To check whether settlement has occurred, a cross-section is taken from AHN4, the latest elevation map. It is checked whether the dike toe, the berm and the crest are all at the same heights are described in the design sketch of figure 15. It showed that all these points were accurate within a range of 2 centimetres. For that reason, it can be concluded that little to no settlement has occurred.

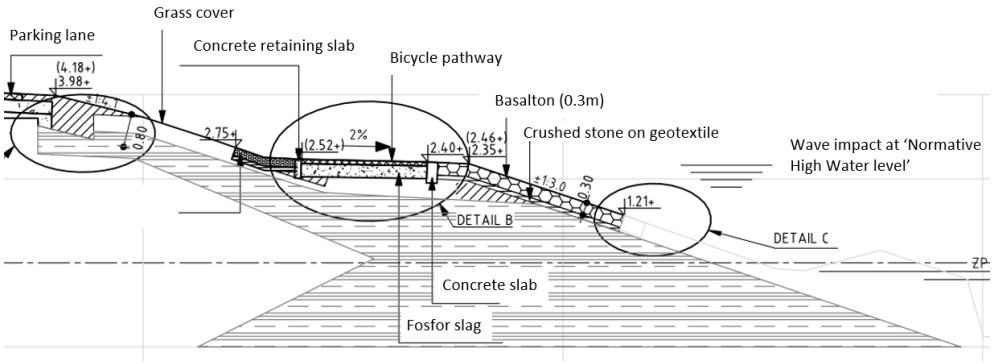


*Figure 15: Cross-sectional profile of dike trajectory of Ketelmeerdijk (HM 13.4)*

*Figure 16: Outer slope of Ketelmeerdijk*

### 2.4.1. Normative cross-section

The case study of the Ketelmeerdijk is applied to one specific normative location, not over the full length of the trajectory. To find a location that is suitable for the application of residual strength, this location has to meet several criteria:

- Not meeting both GEBU and ZST, following LBO-1 (see figure 3);
- The location should see relatively large hydraulic loading;
- Relatively wide crest, and thick clay layer. This is while the attempt is to find a location where residual strength can truly contribute to the strength assessment.
- Should not be reinforced recently as a result of failing either GEBU or ZST.

Based on the criteria posed above, the specific location of HM 13.4 is selected, see the yellow-marked indicator in figure 17. The dike normal orientation is 15.7 degrees.

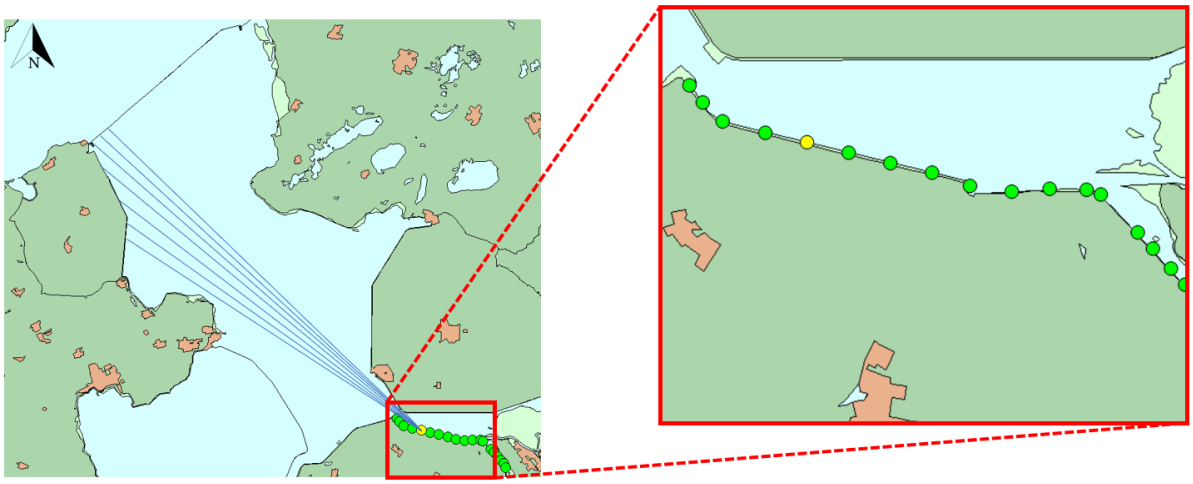

*Figure 17: Normative location with left the effective fetch displayed, on which wind can cause water levels set-up and wave development*

### 2.4.2. Geometric characteristics

At this location along dike trajectory 8-4, natural basalt is placed from 0.14 m+NAP to 0.99 m+NAP. Above the basalt, Basalton, an artificial concrete block revetment, is installed, extending up to the berm at 2.40 m+NAP (see the clear boundary in figure 16). On the 3 meter wide berm, a maintenance road (also utilized as a bicycle pathway) is placed. This maintenance road is constructed with conventional asphalt concrete. Above the road, a planted grass cover starts, at 2.52 m+NAP, and covers the dike over the crest (at 4.18 m+NAP), towards the inner dike toe (at 3 meters below NAP). This grass cover quality is good, and can therefore be called ‘closed’ (Vlaming, 2020). See section 3.2.2 for an explanation of this term. A two-lane asphalt roadway, spanning 11.8 meters in width, has been built on top of the dike’s crest.

### 2.4.3. Clay properties

The cover layer of the Ketelmeerdijk is composed of a combination of clay and boulder clay. In general, boulder clay is known to be as erosion-resistant as, or even more resistant than, regular clay against wave impact (Mourik, 2020). Jet erosion tests have been performed on the IJsselmeerdijk, from which was concluded that the boulder clay indeed carried more erosion resistance (Halter, 2023). This dike trajectory was built in the same period (1950 to 1960), and both clay covers were retrieved from the bottom of the former Zuiderzee, therefore it can be assumed that relatively high certainty is similar for both trajectories 8-3 and 8-4.

Over the full length of the Ketelmeerdijk, the clay quality varies from category 2 to 3, resulting from soil tests performed by Grontmij (2000). Although these soil samples are outdated, and after that reinforcement still has taken place, it still gives an insight into the soil properties, while the cover layer is not replaced. The clay quality is dependent on a range of variables, the most prominent are the homogeneity, the organic content, proctor density and the sand content. The proctor density relates to the moisture content at which the given soil type becomes most dense and is therefore strongest. The sand content becomes important once it shows that the sand content is larger than 70 per cent, whereas the clay has less cohesive properties and with that, is less erosion resistant. For the latest assessment round in the LBO-1, the waterboard calculated with a sand fraction lower than 70 per cent. This is while reports on GEBU describe that it is highly unlikely that clay with a sand fraction larger than 70 per cent has been used to place on top of the sandy layer, and is therefore not realistic to assume (Vlaming, 2020). This is backed up by a report of RHDHV (2021) claiming that the cover layer is suitable for reuse in the

dike reinforcement. For that reason, in this research this assumption is adopted, whereas the results otherwise would not be able to be comparable to the latest LBO-1 results.

# 3. Methodology

This chapter discusses the steps which have been taken to find an answer to the research questions, and the methodological choices which have been made along the process. In figure 5, the dependency between the research questions is documented. First, the hydraulic conditions are gathered, for the case study at a normative location at a cross-sectional level. Once the hydraulic conditions are determined, the cover layer assessment takes place. For that, both the stability of the block revetment is analysed, as well as the grass cover on the upper slope. Then, an inventory of the progressive clay erosion models is made. Together, this will provide the input for the set-up of the progressive erosion model. After making the model, its functionality is tested by performing a time step analysis, multiple univariate sensitivity analyses, and setting up probability curves for the model output.

## 3.1. Hydraulic conditions

The hydraulic conditions form the loading that is necessary to assess a specific failure mechanism, especially for those failure mechanisms that are directly influenced by water levels and/or wave characteristics. For these failure mechanisms of GEBU and ZST, both water levels and wave characteristics during a typical storm event are required input.

### 3.1.1. Hydraulic parameters

To assess the strength of a dike section, it should tested on the peak values that could occur, obviously related to the norm frequency. When looking at the norm frequency of the Ketelmeerdijk, at a relatively high 10,000 years, it is obvious that there is no historical data in which the relevant hydraulic parameters are documented. To obtain valid answers for these high return times, probabilistic tools are consulted.

Within the BOI, two hydraulic models are often used and prescribed, called RisKeer and Hydra-NL (Rijkswaterstaat, 2022). Hydra-NL is a model that calculates the statistics of the hydraulic loads for the assessment of primary dikes and structures. RisKeer can be used to assess primary flood defences according to the latest BOI guidelines while supporting the design process. The target of this research question is to find the statistical hydraulic loading parameters, and therefore, Hydra-NL is selected. The software can run a wide range of scenarios, with a large set of combinations of both wind direction and water levels. For shoreline locations with wave data, there are wave parameters present in the hydraulic conditions database. These wave parameters are then calculated with models that simulate waves nearshore, such as SWAN or HISWA. These models can simulate wave propagation in both space and time while integrating physical processes such as shoaling, refraction due to current and depth, wave growth (due to wind), wave interactions, dissipation and diffraction. This data is input for the Hydra-NL, in which there is placed a probabilistic layer around the calculations. This results in illustrative points, which give a combination of water levels and wave parameters for a wide range of calculations. This wide range of combinations gives a distribution of different combinations of hydraulic conditions from different wind directions arises, see Appendix 1.1. The normative scenario that is used for further calculations are those hydraulic conditions that result from the wind direction with the highest probability of occurrence. This is often related to the effective fetch. The peak values are taken at the design (or lower threshold) safety standard for the Ketelmeerdijk, which has a probability of flooding of 10,000 years.

This way, the peak values of the water level, significant wave height, and peak period are found. The wave steepness is often assumed to be constant throughout a storm event, with the wavelength and wave height increasing in the same order of magnitude.

### 3.1.2. Synthetic storm

While setting up hydraulic loading intended to assess a flood defence on its stability, the hydraulic system in which it is located is leading. In a river system, for instance, long-lasting high water levels can occur. At the IJsselmeer, long-lasting high water levels are unlikely, and therefore other normative hydraulic conditions apply. To schematically derive normative hydraulic conditions, a synthetic storm is set up that describes the evolution of hydraulic parameters of a storm as a function of time. The synthetic storm which is suitable for assessing the Ketelmeerdijk on both GEBU and ZST is a 35 hour storm event, where the water levels linearly increase, as a result of wind set-up (Chbab, 2012). At T = 0 hours, the synthetic storm starts at the maximum target lake water level for winter, which is -0.10 m+NAP. Then, the water levels increase linearly for 15.5 hours, reaching the peak water levels. These peak levels are maintained for 4 hours, after which the water levels linearly decrease again to the winter lake water level.

Hydra-NL makes use of the hydraulic conditions that have been calculated with models behind the software, simulating nearshore waves. Examples of these models are SWAN or HISWA. This way, the normative wave conditions for a wide range of wind directions are determined. The wind direction that

contributes most to the highest wave conditions, is selected as normative. This way, the peak values for both the water levels and wave conditions are derived. The water level set-up is then constant, as a schematical trapezoid, starting at stationary lake water level, linearly increasing to the peak water levels and then linearly decreasing again. Based on this schematization, the wave conditions can be derived. Different methods are known for this derivation. The BOI prescribes a method, called the Q-variant, based on a probability of occurrence. An alternative method is prescribed in a recently published report and model in which two failure mechanisms (GEBU and GEKB: failure of grass cover outer slope, crest and inner slope) are combined. The method describes a new hydraulic conditions conversion (Smale & Klerk, 2023). In this report, it is referred to as 'trapezoidal schematization'.

Below, the two methods are discussed briefly.

1. **Q-variant** (van de Paverd & De Waal, 1999)

The Q-variant is the common methodology for converting schematized water levels to wave conditions, as prescribed in the WBI-2017. It is based on a probability of occurrence and assumes that the storm conditions have an equal probability of occurrence over the whole storm instead of only the peak. This means that wave conditions for lakeside dikes at low water levels are relatively high, and wave conditions near the peak of the storm suddenly drop in size. The Q-variant can therefore overestimate a realistic evolution at low values, and underestimate a realistic evolution at peak values. In figure 23 the method is visualized. Although this is the method prescribed in the latest dike safety assessment, it is rather ambiguous and is physically not rational.

2. **Trapezoidal schematization** (Smale & Klerk, 2023)

As part of a report on combining the failure mechanisms of GEBU and GEKB, Smale & Klerk (2023) propose an alternative for the Q-variant. Here, the peak water levels are linearly interpolated from the maximum target lake water level in winter. Based on this water level evolution, the wave characteristics can be identified, with the use of prescribed relationships. The evolution of the significant wave height follows a similar trapezium form during a storm event, as a superimposition of the lake water level evolution, while these are inflicted through the wind.

The hydraulic peak values are retrieved from Hydra-NL. Per definition, both the wave height and the wave period cannot be equal to zero, whereas in nature there will always be some small amount of wave activity (as a result of disturbances caused by wind, atmospheric pressure variations, or interactions with maritime transport or wildlife). It is not known, however, what the wave height is during stationary conditions for the IJsselmeer. Therefore, the wave height is assumed to start at 0.1 m, to prevent numerical complexities. The peak wave period is a function of the wave height, and will therefore not be equal to zero. For lower values of hydraulic conditions, the computations are not as relevant for safety assessment whereas this will not form a threat to the top layer stability of a dike. According to De Waal & Van Hoven (2015), when calculating damage, waves with a significant wave height lower than 0.4 m do not cause any significant damage with regard to cover layer erosion.

The evolution of normative water levels throughout a storm, based on the target winter lake level, and its normative peak level, is derived from Eq. 1. This formula is applicable for 'time' > 0, which is the moment in time throughout the storm event, hence starting at T=0 hours and ending at 35 hours, with time steps with an interval of dt.

$$h(-0.5T_{base}: dt: +0.5T_{base}) = h_{peak} - \left(\max\begin{pmatrix}|time - 0.5T_{peak}|; \\ 0.5T_{peak}\end{pmatrix}\right)\frac{\partial h}{\partial t}_{flank,\ lake} \qquad \textit{Eq. 1}$$

Here, $h_{base}$ is the winter target lake level (in this research equal to -0.10 m+NAP), $h_{peak}$ is the design peak lake level near the dike toe (in this research retrieved from Hydra-NL per recurrence time), $T_{peak}$ is the peak duration in hours (in this research equal to 4 hours), and $T_{base}$ is the base duration of the trapezoid in hours (in this research equal to 35 hours).

And $dh/dt_{flank,lake}$ gives the gradient of the flanks, calculated as follows:

$$\frac{\partial h}{\partial t}_{flank,lake} = \frac{h_{peak} - h_{base}}{0.5(T_{base} - T_{peak})} \quad \text{Eq. 2}$$

Now the schematization of the water levels as a function of time has been set up. Then, the evolution of significant wave height can be set up as follows:

$$H_s = H_{s,peak} - \left(\max\begin{pmatrix}|time - 0.5T_{peak}| \\ 0.5T_{peak}\end{pmatrix}\right)\frac{\partial H_s}{\partial t}_{flank,\ lake} \quad \text{Eq. 3}$$

Here, $H_{s,peak}$ is the peak significant wave height for large return times. From here on, the time-dependent evolution of the peak wave period can be constructed through the following relation.

$$T_m = \left(H_s \frac{T_{m,peak}^2}{H_{s,peak}}\right)^{0.5} \quad \text{Eq. 4}$$

In this formula the $T_{m,peak}$ is the peak wave period at the design safety norm.

In section 4.1.1, a comparison is set up between the two methods described above. This comparison is set up with realistic, but random parameters from the case study Ketelmeerdijk, with the target to assess their respective functionality.

## 3.2. Failure of dike cover layers

Now, the method of how to set up a synthetic storm for arbitrary return times has been described. This schematization can be used to assess the strength of the dike cover layers that are installed on the outer slope of the Ketelmeerdijk, at HM 13.4. The synthetic storm describes a time series with relevant hydraulic conditions, for 35 hours. The goal of this research question is to identify which part of that time series should be used for clay erosion. To find that, the point along these time series at which initial failure to the revetment layers occurs has to be identified.

The strength of the cover layers is based on hydraulic criteria which have to be met. Below these criteria, the revetment layers provide sufficient resisting strength. Above, the revetment layers are assumed to have fully failed and clay erosion is started. Failure of block revetment is defined as the instability of a singular block from the revetment, at which the failure mechanism of ZST does not meet the safety standard. Failure of grass cover is defined as the development of an exposed hole of minimally 25 centimetres in diameter in the grass cover layer (Rijkswaterstaat, 2022).

Once a block revetment on the lower slope fails, this may cause a decrease in the stability of the blocks placed above (Cirkel, van Dam, & van den Akker, 2015). This is while the stability of the revetment is largest once all blocks are in place. The blocks have the largest stability with the hydrostatic peak pressure occurring at the top, and not at the sides or bottom of the blocks. It will be treated therefore in the hypothetical case, that if failure occurs to one revetment, the other revetment being on the same slope will also subsequently fail. After failure occurs, it is assumed that the clay layer becomes fully bare-lying and wave impact will start to erode the layers beneath that. The strength of the remaining block revetment or grass cover will not be taken into account from that moment on. In practice, the eroded material (either grass cover or blocks) is still in the vicinity and is likely to inflict wave reduction. In this study, however, this is not taken into account for simplicity of calculations.

### 3.2.1. Failure of block revetment

To assess the stability of the block revetment at HM 13.4 of the Ketelmeerdijk, the STEENTOETS software is consulted. Developed by Deltares, STEENTOETS is an Excel-based tool integral in the BOI, designed for evaluating the stability of among others block revetments ('t Hart, 2021). This tool is suitable for implementation in the dike safety assessment of flood defences of inland lakes with the characteristics of the IJsselmeer (Klein Breteler, 't Hart, & van Gent, 2013). As input, the tool requires geometric properties of the flood defence on a cross-sectional level and normative local hydraulic loading, which can be obtained from software like Hydra-NL or RisKeer.

This study focuses on wave impact, and not on wave run-up, as they generate higher peak pressures. Wave impacts occur between the still water level and half the significant wave height below that (van Hoven, 2015). The peak pressure during the erosion process of both revetment layers and the clay layer beneath is dominated by wave impact, rather than wave run-up.

In STEENTOETS, the water levels are kept constant (within the range of each revetment), and only wave conditions are varied. When the trapezoidal schematization would be loaded, it would not be clear at which specific water levels the cover layer would fail for the first time. It would rather give the worst-case scenario. Iteratively, by adjusting the wave conditions, the moment of failure for each of the layers is identified. This point along the time series is found by taking the hydraulic conditions at the point where the failure margin (in Dutch: *dikte overschot*) approaches zero. This is an output parameter of STEENTOETS and gives the remaining strength of the revetment at that particular hydraulic loading. When the hydraulic conditions at near-failure are then translated to the synthetic storm, the point of failure is identified.

It is important to note that the water levels determine whether the wave reaches the revetment, and that the pressure caused by the waves will fail the revetment. The points of failure are determined separately for the block revetments basalt (ranging from 0.138 to 0.99 m+NAP) and Basalton (ranging from 0.99 to 2.40 m+NAP). The revetment layer that fails first during the time series, defines also when the other layer fails. For the two types of block revetment, the iterative process is conducted in STEENTOETS. The results are placed in section 4.2.1 and in this chapter, the hydraulic conditions related to the near-failure of the block revetment are discussed.

### 3.2.2. Failure of grass cover

To assess the grass cover stability, a software called BM Gras Buitentalud is consulted. Again, this software is prescribed in the latest BOI guidelines. Behind the software lie relatively simple formulas, which are methodically documented (de Waal & van Hoven, 2015), and are available for water authorities to be used. This is the reason that there is opted to use these formulas rather than the software of BM Gras Buitentalud itself, which is a relative black-box. The tool can calculate the grass cover strength for both wave run-up and wave impact. Wave impact, which is the sole forcing mechanism treated in this research, is calculated with the parameters a, b, and c, which describe the grass cover quality and soil conditions. The software is split up into two parts: the grass cover, which is 20 centimetres thick and is composed of a living turf layer, and the upper clay layer, which is 30 centimetres thick and slightly compressed, making it stronger than the lower regions of clay. In this sub-question, the formulas behind these two phases are analysed. The target is to find the moment in time at which these two phases fail. For that to happen, first, the water levels should be sufficiently high, for the waves to reach the grass cover. If the water levels are high enough, it is checked whether the wave conditions are sufficient to cause grass cover failure.

In figure 18, the different steps are described which are followed to find the moment in time at which the grass cover fails. Scenario 1 describes the situation in which the cover layer is assumed to be fully composed of clay, and scenario 2 is that of boulder clay. This is while the clay erosion formulas later on described in this study do not cope well with different soil type layers.

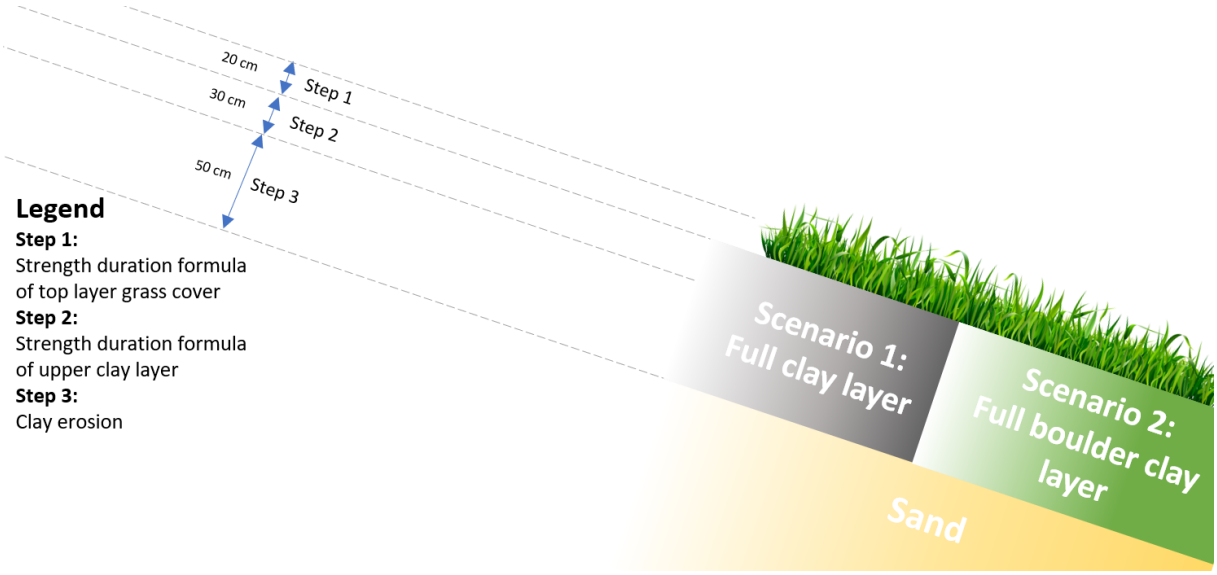


*Figure 18: Different steps in the erosion process and how these are calculated in this research*

**Step 1: Living turf layer (0-20 cm)**

The first phase exists out of 20 centimetres of the so-called living turf layer. For the Ketelmeerdijk, this component is part of the design drawings, and therefore a section of the 1 meter thick clay layer. It can be seen as turf, with clayey properties. The higher the root density of this layer, the more erosion resistant the layer is. The aim is to find at which point in time the grass cover fails. That moment in time is defined as the strength duration ($t_{s,top}$). For the turf layer on the outer slope, a relation between the strength duration and the wave height has been set up (van Hoven, 2015), see Eq. 5. This equation is also used in the software of BM Gras Buitentalud.

$$H_s = a * e^{b*t_{s,top}} + c \qquad \text{Eq. 5}$$

With:

| | | | |
|---|---|---|---|
| a | = | Coefficient related to grass cover quality, $a \geq 0$ | (in meters) |
| b | = | Coefficient related to grass cover quality, $b < 0$ | (per hour) |
| c | = | Coefficient related to sign. wave height and strength duration, $c \geq 0$ | (in meters) |
| | = | default value at 0.25 | |
| $t_{s,top}$ | = | Strength duration: the erosion resisting duration of grass cover | (in hours) |

To determine the actual strength of the grass cover, and to quantify this cover, coefficients have been set up. The grass cover properties are quantified through the coefficients ‘a’, ‘b’ and ‘c’. The grass cover quality is denoted in coefficients ‘a’ and ‘b’. Coefficient ‘c’ is a default value, and is for both open and closed grass cover quality equal to 0.25. When the grass cover quality is poor, the value for ‘a’ becomes lower. Contrary, this means that the value for ‘b’ is higher, which can also be recognized in the exponential function of Eq. 5. For the moment in time at which the living turf layer fails, the value of the strength duration is equal to zero. In other words, the critical hydraulic loading is determined when setting the strength duration equal to zero. This way the critical significant wave height is found for the point at which the grass cover fails, but only just.

For the values of coefficients a, b, and c, the values from the latest LBO-1 assessment round are taken. These describe the grass cover quality. Grass cover quality is categorized as open, fragmentary, or closed grass sod. In table 2 below, the different values for the coefficients of open or closed grass cover are placed. The quality concerns the erosion resistance of the grass cover under wave impact. For this research, it is assumed to be a closed grass cover. The erosion resistance is mainly determined by the density of the root network in the top layer.

*Table 2: Values for closed or open grass cover for each of the quality coefficients*

| Coefficients | Closed grass cover | Open grass cover |
|---|---|---|
| a [m] | 1 | 0.8 |
| b [1/u] | -0.035 | -0.07 |
| c [m] | 0.25 | 0.25 |

The critical significant wave height is the wave height at which the grass cover will fail. The first criterion for the grass cover to fail is that the water levels are sufficiently high, and the second is that the critical wave height is exceeded. Once these two criteria are met, the first point along the time series corresponds to the initial failure of the top layer.

**Step 2: Upper clay layer (20-50 cm)**

After the top layer has failed, the strength of the upper clay layer (with a thickness of 30cm) is calculated with the use of the second part of the equations behind the software of BM Gras Buitentalud. The relation between the strength duration of the upper clay layer and the wave impact (through significant wave height) is described as a function of the grass quality (de Waal & van Hoven, 2015). The general formula is given by:

$$t_{s,sub} = \min\left(\frac{min((d_c; 0.5) - 0.2)}{c_d(tan\,\alpha)^{1.5}\, max\left(f_\beta * H_s - 0.5; 0.001\right)}; t_{s,sub,max}\right) \qquad \textit{Eq. 6}$$

With:

| | | | |
|---|---|---|---|
| $t_{s,sub}$ | = | Strength duration of the upper lay layer (time to failure) | [in hours] |
| $d_c$ | = | Combination of the layer thickness of top layer and upper clay layer | [in meters] |
| $c_d$ | = | constant | [-] |
| | = | $1.1 + max\left(0; 8(F_{sand} - 0.7)\right)$ | |
| $F_{sand}$ | = | sand fraction in the clay | [-] |
| $\alpha$ | = | Angle of the original outer slope in degrees | [in degrees] |
| $f_\beta$ | = | influence factor for angle of wave impact | [-] |

This equation can only be applied once the following conditions apply:

- $a \neq 0$
- $0.2 \leq d_c < 0.5$
- $f_\beta * H_s > 0.5$

To find the moment in time at which the upper clay layer fails, for each time step, the respective contribution to the failure of this layer is calculated. To find that, the strength duration is calculated with the use of Eq. 6. This will give, for each combination of water level and related wave conditions, the duration that the upper clay layer can withstand these conditions. To assess when the upper clay layer has failed, first, the moment of failure of the top layer is determined. From here on, the failure fraction ($FF$) that occurs per timestep is derived, see Eq. 7.

$$FF(t) = \sum_{t_1}^{t_2} \left( FF_{t-1} + \frac{timestep}{t_{s,sub}} \right) \qquad \textit{Eq. 7}$$

Where $t_1$ is the timestep at which the top layer fails, and $t_2$ is the time at which the cumulative failure fraction is equal to 100 per cent. The failure fraction from the previous timestep is added to the failure fraction at that specific timestep and repeated for each timestep. The timestep is initially set at 0.01 hours. By taking the cumulative failure fraction, starting at the point of failure of the top layer, and ending when the cumulative failure fraction is equal to 100 per cent.

To make the calculation less complex, it is assumed that once the upper clay layer has failed somewhere on the upper slope, the entire upper clay layer has failed and clay erosion will be initiated. This takes into account some degree of conservatism, but it aligns with the most recent expert knowledge on the subject (Wolters et al., 2011; Mourik, 2015; Klein Breteler M. , 2022).

## 3.3. Clay erosion

After either the revetment layer or the combination of turf layer and upper clay layer, have eroded fully, clay erosion is initiated. This is targeted to model the clay that remains after initial failure. This sub-question targets to find the formulas and models that can describe the volume that is eroded over time, depending on the normative hydraulic conditions. The goal is to find a specific formula that can be applied to the case study. The motivation behind the eventual choice follows after an inventory of relevant relationships describing clay erosion, and an analysis of their conditions for use and their responsiveness to changes in parameters. Based on the outcome of these analyses, there is opted for a deterministic method, or a bandwidth method, by selecting two methods. The latter will be chosen when it shows that multiple modeling formulations can be useful for our application. The first option will be only chosen if the other modelling methods are proven not to be relevant or cannot be used in this specific application.

### 3.3.1. Inventory clay erosion models

In this chapter, clay erosion formulas are gathered. The models are described in Table 1, as both functions of time as well as functions of eroded volume over time. To make a sound comparison, only models describing erosion volume as a function of time $(dV_e/dt)$ are analysed. For each of the parameters which are water level (and therefore time-) dependent, a 't' is placed between brackets.

**Model 1** (Klein Breteler et al. , 2012)

The first publication that came up with a relationship that described erosion volume over time, as a function of hydraulic loading, was in 2012. Based on four large-scale modelling tests in the Delta Flume spread over more than 2 decades, preliminary empirical formulas describing clay and sand erosion were set up. In Eq. 8 below the clay erosion formula is described. The subscript describes the abbreviation of the author. Sometimes the author is consulted more than once, resulting in an index.

$$V_{e,KB1} = 0.063 \frac{H_s^2(t) \tan(\alpha)}{s_{op}} t \qquad \textit{Eq. 8}$$

With:

| | | | | |
|---|---|---|---|---|
| $V_{e,KB1}$ | = | eroded volume per meter dike over time t | | [$m^3$] |
| $\alpha$ | = | outer slope angle in degrees | [°] | |
| $s_{op}$ | = | offshore wave steepness $\frac{H_s}{(g*T_p^2)/2\pi}$ | | [-] |
| $T_p$ | = | peak period | [s] | |
| $g$ | = | gravitational constant (= 9.81) | [$m/s^2$] | |

The following conditions have to be met, if the formula should be applied:

- Only applicable to the clay of Dutch dikes[1]
- Significant wave height is between 1.0 and 2.0 meters;
- Wave steepness has to be larger than 0.02;
- Clay layer thickness should be smaller than 3 meters;

With the erosion volume ($V_e$) known, the geometric profile can be set up. For that, several reference points have to be obtained. In the report of Klein Breteler et al. (2012), the main reference point is the terrace depth ($d_t$). It is the difference between the normative water level and the point where the original slope intersects the erosion terrace, see figure 19. It can vary, depending on the hydraulic conditions. The value for $d_t$ can be calculated with the use of Eq. 9 below. The value of $c_{m3}$ is equal to the model coefficient. This factor can correct to account for deviations between measured and calculated values.

$$d_t = \min\left(c_{m3}\left(0.4\frac{V_e^{0.25}}{\sqrt{H_s}} + 0.7\right); 2H_s\right) \qquad \textit{Eq. 9}$$

In figure 19, the definition of $d_t$ is visualized, as well as the schematical development of an erosion profile. The slope of the cliff is 1:1. The slope of the terrace varies from 1:7 to 1:15. The earlier in the erosion process, the steeper the erosion cliff.

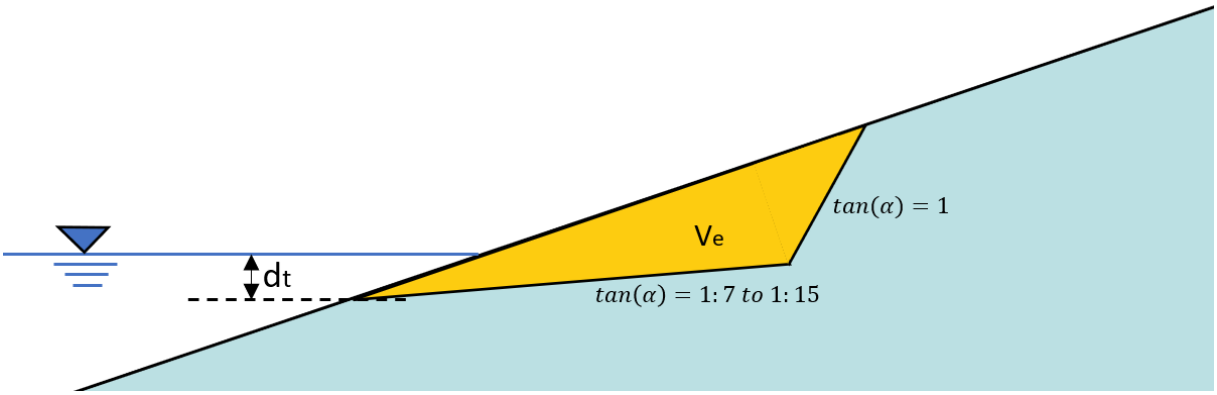


*Figure 19: Definitions of geometry points for erosion formulas of Klein Breteler et al. (2012)*

**Model 2** – (Mourik, 2020)

The formula of Klein Breteler et al. (2012) only roughly estimates the influence of the wave height, wave steepness, and slope angle, because of limited experimental data. In the study by Mourik (2020), a new formula for predicting the erosion velocity of bare clay due to wave impact is developed, based on combining the results of Delta Flume tests with the results of simulations carried out with the numeric wave simulation model ComFlow. These Delta Flume tests were conducted on clay samples that were loaded with block revetment initially, but were bare-lying when tested in the Delta Flume.

At the moment of writing, this model is known to be mostly used in practical applications. The report was first published in 2015, and has seen a revision since then, leading to a republished document in 2020. A formula is set up which predicts the erosion volume variation ($\partial V_e/\partial t$) as a function of $V_e$, $\tan(\alpha)$, $s_{op}$ and $H_s$. In the formula, a distinction is made between clay and boulder clay, with the use of different values for the erosion coefficient $c_e$, see Eq. 10. According to Mourik (2020), no erosion of the clay layer occurs for wave heights smaller than 0.40 meters.

[1] The properties of the clay used in Dutch dikes follow a similar pattern. This involves high sand content, small/medium sand lenses, or clay with high macro-porosity due to poor placement. This is a result of the same treatment of clay before this is placed on a dike, as well as the same soil structure from which the suitable clay is obtained (Wolters & Klein Breteler, 2011).

$$\frac{\partial V_{e,M}}{\partial t} = c_e \left[1.32 - 0.079 \frac{V_{e0}(t)}{H_s^2(t)}\right] [16.4(\tan(\alpha))^2] * \left[\min\left(3.6; \frac{0.0061}{s_{op}^{1.5}}\right)\right] [1.7(H_s(t) - 0.4)^2] \quad \textit{Eq. 10}$$

With:

| | | |
|---|---|---|
| $\frac{\delta V_{e,M}}{\delta t}$ | = | increase of volume of the erosion per meter width per hour ($m^3/m/h$) |
| $c_e$ | = | erosion coefficient (-)<br>clay: mean = 0.55<br>std. dev. = 0.14<br>boulder clay: mean = 0.35<br>std. dev. = 0.09 |
| $V_{e0}$ | = | already present and corrected erosion volume in the loaded zone ($m^3$) |
| $s_{op}$ | = | wave steepness (-) |
| | = | $\frac{H_s}{1.56 * T_p^2}$ |
| $H_s$ | = | significant wave height (in meters) |

This formula can be applied when the circumstances are such that:

- Wave height: $0.9 \leq H_s \leq 1.5\ m$;
- Wave steepness: $0.01 < s_{op} < 0.05$;
- Slope angle: $0.200 < \tan(\alpha) < 0.333$, without berm;
- Clay with a sand content of less than 40 per cent;
- Boulder clay with a sand content of less than 60 per cent;
- Clay and boulder clay with a percentage of organic material of less than 5 per cent.

Setting up the erosion profile follows a somewhat similar methodology to that of Klein Breteler et al. (2012). The terrace consists roughly of a slope of 1:7 to 1:10 and a cliff with a slope of 1:1. The erosion pit grows because the cliff retreats landward due to wave impact. The erosion depth is found for each of the methodologies following the same reasoning of Mourik (2020). In this report, it is claimed that the erosion depth ($d_e$) is a function of the erosion volume ($V_e$), and can be calculated through Eq. 11. The erosion depth is the perpendicular depth of the erosion pit from the original outer slope to the intersection point between the terrace and cliff, see figure 20. To apply this formula, the erosion volume should be larger than 0.75 $m^3/m$. Also, the original outer slope should be in the range of 1:3 to 1:4.

$$d_e = \sqrt{V_e \tan(\alpha)} - 0.14 \quad \textit{Eq. 11}$$

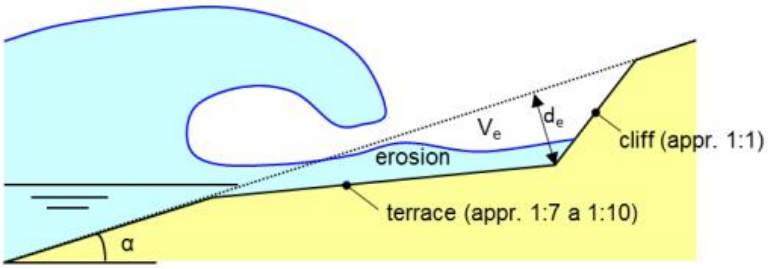


*Figure 20: Geometry erosion profile for erosion formula of Mourik (2020)*

**Model 3 -** (Kaste & Klein Breteler, 2015)

In 2015, a proposition was made on how to work with the model constructed by Mourik (2015) and apply the model to varying water levels (Kaste & Klein Breteler, 2015). A method how to do this was to solve the differential equation prescribed in Eq. 10, which results in Eq. 12:

$$V_{e,KB2} = c_e \left[1.32 - 0.079 \frac{V_{e0}(t)}{H_s^2(t)}\right] [16.4(\tan\alpha)^2] \min\left(3.6; \frac{0.0061}{s_{op}^{1.5}}\right) [1.7(H_s(t) - 0.4)^2] \quad \textit{Eq. 12}$$

The conditions for using Eq. 12 are:

$H_s$ > 0.4 m;
and for $H_s \leq$ 0.4 m: $dV_e/dt = 0$ or V=0

**Model 4 -** (Klein Breteler M. , 2022)

The most recent study published on residual strength incorporated results from the DeltaFlume tests to assess the erosion velocity at large wave impacts, used on undisturbed samples from the Lauwersmeerdijk, protecting against flooding from the Wadden Sea (Klein Breteler M. , 2022). These samples are collected from the upper slope, with a grass cover on top of a clay layer. The tests have been solely performed on the upper slope, above a berm. The other models did not follow such a specific approach and are therefore applicable over a wider range of situations. The tests involved the development of a clay erosion pit as a result of the initial failure of the grass cover. After these tests were completed, two distinct stages were recognized regarding clay erosion after grass cover failure.

*Model 4 - Stage 1: Maximum erosion depth of 50 centimetres*

The first stage describes the development of the erosion pit with regard to depth, reaching an erosion depth $d_e$ (perpendicular to the original angle of the outer slope) of 50 centimetres maximally, and a significant wave height $H_s$ smaller than 0.50 m. The first stage can also be recognized as the clay erosion that is already integrated in the software of BM Gras Buitentalud, or the formulas Eq. 5 and Eq. 6, but then expanded with an influence factor accounting for the berm. In this phase, the erosion is described as an erosion depth, which occurs perpendicular to the original slope, and is shown in figure 21. It should be noted that the significant wave height ($H_s$), is the equivalent significant wave height (in meters) at the dike toe of perpendicular incident waves. The equivalent wave height is therefore corrected for when calculating on oblique incident waves.

$$d_e = m_1 f_{transition} c_d \max(0; H_s - 0.5) (\tan\alpha)^{1.5} t_{loaded} \qquad \textit{Eq. 13}$$

With:

| | | | |
|---|---|---|---|
| $c_d$ | = | coefficient for the first phase of the erosion process | (-) |
| | = | $1.1 + max(0\ ;\ 8 * (F_{sand} - 0.7))$ | |
| $F_{sand}$ | = | sand fraction in the clay | (-) |
| $t_{loaded}$ | = | extent of hydraulic loading | (in hours) |
| $f_{transition}$ | = | factor that incorporates influence of water depth on the erosion velocity in the first phase | (-) |
| | = | $\max\left(0; min\left(1; 0.44\frac{h_{transition}}{H_s} + 0.66\right)\right)$ | |
| $h_{transition}$ | = | the depth below the still water level of the transition point between the hard and soft revetment (see figure 21) | |

In this research, the formulas behind BM Gras Buitentalud account for this stage 1. Therefore, stage 1 can be skipped, and the clay erosion will start at stage 2. The second stage describes the continuation of the erosion, in a progressive horizontal way.

*Model 4 - Stage 2: Minimum erosion depth of 50 centimetres*

For the quantification of stage 2, the results of the Delta Flume experiments have been combined with the numeric wave simulation model OpenFOAM. The basis for this method is the hypothesis of Kruse (Klein Breteler et al. , 2012), in which it is proclaimed that the erosion velocity is determined by the peak pressure of the wave impact against the clay. These peak pressures are measured in the Delta Flume, and the results are calibrated with use of model calculations in OpenFOAM.

This has resulted in Eq. 14. It is applicable for $d_e$ > 0.50 m and $H_s$ > 0.5 m). The model incorporates model uncertainties which can be modelled through the stochastic variable $m_2$. The second phase is applicable for an erosion depth ($d_e$) larger than 0.50 m, and a significant wave height larger than 0.50 m. What can be seen, is that both Eq. 10 and Eq. 14 are differential equations, and therefore difficult to work with. To solve this problem, the differential equations are discretized. See section 4.4.1 how this is done.

$$\frac{\partial V_{e,KB2}}{\partial t} = 0.068 m_2 \frac{(H_s - 0.25)^2}{\sqrt{s_{op}}} \min\left(2.4; max\left(0; 1.2 + 1.6\frac{h_{overgang}(t)}{H_s(t)}\right)\right) * \left(\frac{13}{\frac{B_{berm}}{H_s(t)} \min\left(1; \max\left(0; 2 - \frac{h_{berm}(t)}{H_s(t)}\right)\right) + 8}\right)\left(1.69 - \frac{0.17}{\tan(\alpha)}\right) \quad \textit{Eq. 14}$$

Where:

| | | |
|---|---|---|
| $m_2$ | = | model uncertainty (-) |
| $h_{overgang}$ | = | water level relative to the transition from the hard revetment to the clay cover with grass (in meters) |
| $B_{berm}$ | = | width of the berm (in meters) |
| $h_{berm}$ | = | difference between water level and starting point berm (in meters) |

The relevant clay conditions for which the formula can be applied are described below:

- The sand content in clay should be less than 40 per cent;
- Boulder clay with sand content of less than 60 per cent;
- Clay and boulder clay with less than 5% organic material.

For the model of Klein Breteler (2022), the erosion profile is sketched in figure 21. The erosion terrace slope varies, with 1:8 for original slopes of 1:4 and 1:10 for original slopes of 1:5. The erosion cliff has a slope of 2:1. This varies compared to the erosion profile described by Mourik (2020), which has a slope of 1:1. For this study, there is adhered to the relevant erosion profile per erosion methodology. In the report, the erosion profile can be set up for both stage 1 (for $d_e$ < 0.50m) and for stage 2 (for $d_e$ > 0.50m). For this research, only stage 2 is considered, while stage 1 is already covered in the grass failure module, see section 3.2.2.

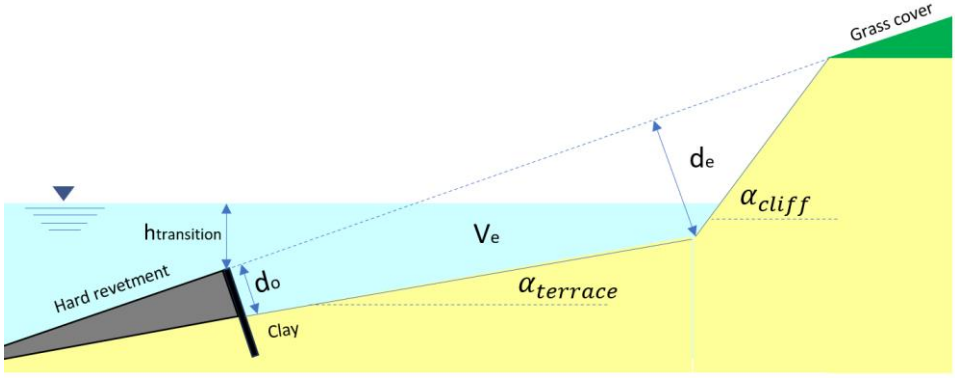


*Figure 21: Schematization of erosion profile with relevant definitions for erosion formula of Klein Breteler (2022)*

The erosion profile is set up with a few geometry points. Once the still water level is higher than the transition point ($h_{transition}$ > 0) the erosion profile will start to develop, provided that the wave impact is large enough. The erosion profile starts directly above the transition with a jump behind the hard

revetment ($d_o$), as sketched in figure 21, and calculated with use of Eq. 15. The jump $d_o$ is the difference between the original slope and the point at which the terrace starts behind the hard revetment.

$$d_o = H_s \max\left(0; \min\left(\frac{h_{overgang}}{H_s} + 1.5; 1\right)\right) * \max\left(0; \min\left(\frac{d_t - h_{overgang}}{H_s \, sin(\alpha)} tan(\alpha - \alpha_{terrace}) ; 0.18\right)\right) \quad \textit{Eq. 15}$$

The perpendicular erosion depth ($d_e$) is calculated with use of Eq. 16.

$$d_e = \sqrt{\frac{2V_e \tan(\alpha - \alpha_{terrace}) + d_o^2}{\left(1 + \frac{\tan(\alpha - \alpha_{terrace})}{\tan(\alpha_{cliff} - \alpha)}\right)}} \quad \textit{Eq. 16}$$

With:

| | | |
|---|---|---|
| $\alpha$ | = | Original slope (in degrees) |
| $\alpha_{terrace}$ | = | Slope of erosion terrace (in degrees) |
| | | if $tan(\alpha)$ = 0.25, then $tan(\alpha_{terrace})$ = 1:8 |
| | | if $tan(\alpha)$ = 0.20, then $tan(\alpha_{terrace})$ = 1:10 |
| $\alpha_{cliff}$ | = | Slope of the erosion cliff (in degrees) |
| | = | $tan(\alpha_{cliff})$ = 2 |

### 3.3.2. Time step selection

The choice of how time intervals are discretized can significantly impact the accuracy and interpretability of differential equations, such as the erosion formulas of Mourik (2020) and Klein Breteler (2022). These formulas could require a certain timestep size, to avoid numerical instability or inaccuracies. Different models can require different timesteps, whereas the detailed models often need a smaller time step. Too small a time step will result however in unnecessarily large computation times. In this section, the time steps are altered and this way, the sensitivity to either enlarged time steps or smaller time steps is analyzed.

### 3.3.3. Sensitivity analyses

To find out the key drivers behind the formulas, as well as to give insight into the uncertainty behind the formulas, a univariate sensitivity analysis is performed. This analysis aims to identify which input parameters have the most significant impact on the output of the model. Understanding (the degree of) these key drivers can help users of the model to give a comprehensive overview of the outcome of the model, its related uncertainties and which input parameters are most valuable to perform research upon. On the other hand, it can quantify the upper and lower limit of the formula, within the boundaries within which it should be used. This is beneficial for the robustness of decisions made with the model, with regard to uncertainty.

In table 3, an overview is given of the range of parameters for which each of the models can be applied. While the models are all empirically based, and validated through model software, the experimental set-up determines the conditions for usage. The more extensive the experimental set-up, the wider the range of applicability is. If the models are used outside these ranges, it does not mean the model cannot be used anymore, but it should be noted that the inaccuracy can be larger. Interpretations of results outside of this range should therefore always be carefully treated. Besides the upper and lower limit of the parameters of the three models, a column is added in which the range of parameters that can be encountered at the Ketelmeerdijk is placed. From these formulas, it can be concluded that those of Mourik (2020) and Klein Breteler (2022) are best applicable. The formula of Klein Breteler et al. (2012) could still be used, but it could only partially cover the erosion process during the normative conditions at the Ketelmeerdijk. For now, however, it will be continued to be used in the calculations.

*Table 3: Overview sensitivity analysis bandwidth parameters*

| **Parameter** | **Symbol** | (Klein Breteler et al. , 2012) | | (Mourik, 2020) | | (Klein Breteler M. , 2022) | | **Case study** |
|---|---|---|---|---|---|---|---|---|
| | | Min | Max | Min | Max | Min | Max | Range |
| Significant wave height | $H_s$ (m) | 1.0 | 2.0 | 0.4 | - | - | 2.8 | 0 to 2.7 |
| Wave steepness | $s_{op}$ (-) | 0.02 | - | 0.01 | 0.05 | 0.02 | 0.055 | 0.05 |
| Slope angle of the original profile | $\alpha$ (-) | 1:4 | 1:3 | 1:5 | 1:3 | 1:6 | 1:2.9 | 1:4 to 1:3 |
| Sand content | $F_{sand}$ (-) | 10% | 50% | For clay: < 40% For boulder clay: <60% | | For clay: < 40% | | Assumption: 40 % |
| Organic material | - | - | | For (boulder) clay: < 5% | | - | | - |
| Other | - | Clay layer thickness < 3 meters | | - | | Berm width: $0 \leq \frac{B_{berm}}{H_s} < 5$ Grass quality: Open or closed grass sod (no fragmentary) | | - |

## 3.4. Progressive clay erosion model

In this section, the procedure for setting up a progressive clay erosion model is described. Based on the model performances from the analyses from the previous section, an adequate choice can be made on which formula is best to use.

### 3.4.1. Model set-up

The formulas of Klein Breteler et al. (2012) and Mourik (2020) apply to all clay erosion processes from the outer slope. The formulas of (Klein Breteler M. , 2022) have only been tested on the upper slope, above a transition with a hard revetment. Both formulas have been constructed after various experiments with a clay sample and a constant water level. For all models it can be said that the experiments have been performed at different water levels, but never a varying water level, which would occur during the synthetic storm which is treated in this report. The model will therefore include, next to the hydraulic conditions and cover layer assessment, first a simple representation of the erosion development where the dike section is tested against the most extreme values. These values are during the 4-hour peak loading. The constant water level during these 4 hours makes the model less complex, and still able to give a substantiated answer to the question of whether residual strength is such a big contributor to the dike's strength.

First, the weakest part of the dike is assessed. Once it shows that that fails, the dike is said to not provide sufficient residual strength, to pass the assessment on GEBU. When it does not fail, there will be looked at ZST and the clay erosion occurring after block revetment failure. Therefore, the 4-hour peak hydraulic conditions (T=15.5 to 19.5 hours) will form the hydraulic input. This way the weakest part of the dike is first tested on the largest hydraulic loading. When it shows that the clay cover will not withstand these conditions, it can be concluded that the clay layer as a component of residual strength is not resistant enough to withstand normative conditions. It remains to be seen, however, in that case, whether the dike core consisting of sand will provide sufficient erosion strength. Secondly, if it shows that the dike does show sufficient residual strength during the 4-hour peak, the full synthetic storm will be tested on the dike's clay layer. At this step, the erosion volume as a function of time is calculated for each of the relevant erosion formulas. These are the models of Mourik (2020) and Klein Breteler (2022), see Eq. 10

and Eq. 14 respectively. The cumulative erosion volume that occurs during this period is then related to the geometric properties. Once it shows that the erosion depth ($d_e$) is larger than the critical depth of the clay cover, at the normative hydraulic conditions, it can be concluded that the dike will not withstand the required normative conditions. The critical depth of the clay cover is 1.0 meter, measured perpendicular from the outer slope, see figure 4.

The model will be set up in the programming software Python. This reduces computational time and increases automation and reproducibility. Especially the latter is important, to find out what occurs when one step in the process is altered. Besides that, it is relatively easy to create visualizations. These advantages make Python a powerful and flexible tool for the computations in this research while providing significant benefits over traditional spreadsheet software like Excel.

The dike erosion model which will be set up, will be initiated after the failure of either the block revetment or the grass cover. Whereas the first focus is placed on step 1, with the 4-hour peak loading, the water levels will reach above the berm and for that reason, the focus is placed on clay erosion after failure of grass cover. The failure mechanism of GEBU will be taken into account by shortening the time series of the normative storm event, based on the results from RQ2. The model is solely focused on delivering results with regard to clay erosion, so it will not integrate the grass cover erosion, nor will the model take into account the strength of the geotextile or sandy core of the dike.

### 3.4.2. Setting up geometric erosion profiles

With the model set up, the erosion volume per time step are calculated. Now these should be related to a cross-section of a dike, to check whether the clay layer is thick enough to withstand the wave impact. For that, it is assumed that revetment failure to the dike has occurred, and erosion of the bare clay layer will start. There will be no influence of residual block revetments which still are in place. This assumption is based on findings from the Delta Flume, which proved that as a block revetment starts to fail, the remaining block revetment usually fails quite rapidly (Mourik, 2020). The slope of the erosion terrace is set at $\tan(\alpha)$= 1:10, and the slope of the cliff at $\tan(\alpha)$=2, which are the erosion profiles following an original slope of 1:3 (Klein Breteler M. , 2022).

Cumulatively this should lead to an erosion pit development. This model will be set up for those methodologies, that prove to stay valid for the case study of Ketelmeerdijk. Either a bandwidth method is selected with multiple methodologies, or a deterministic model in which one erosion volume curve is drawn. Based on the erosion volume curve, combined with the geometric reference points $d_e$, $d_t$ and $d_o$, the geometric profile can be drawn.

For each of the methodologies, there is a different type of linking the volume to a geometric erosion profile. Below, the geometric properties are described which can be calculated:

- Erosion volume ($V_e$)= Cumulative eroded clay, see Eq. 8, Eq. 10 and Eq. 12 (in $m^3/h/m$)
- Erosion depth ($d_e$)= Perpendicular erosion depth, see Eq. 13 and Eq. 16 (in meters)
- Terrace depth ($d_t$)= Depth from still water level to the starting point of the terrace, see Eq. 9 (in meters)
- Erosion jump ($d_o$)= Jump of erosion mostly occurring during phase 1 of the erosion process ($d_e < 0.50m$ & $H_s < 0.50m$), until a stable depth is reached, after which the erosion pit grows horizontally, see Eq. 15 (in meters)

### 3.4.3. Uncertainties

To validate the empirical formulas of Mourik (2020), which resulted from the Delta Flume experiments, a coefficient has been set up. It turned out that the different types of clay had different influences on erosion resistance. Boulder clay was more resistant than normal clay. To cope with this deviation, while maintaining the functionality of the original formula, an erosion coefficient $c_e$ has been set up. It is a correction factor, that can be changed to the desired value to minimize the relative error, caused by fitting the experiment results to the model results of ComFlow. While validating the formula, the coefficient was given a mean for both boulder clay and clay, and a standard deviation for the outliers, see table 4.

*Table 4: Uncertainties related to the type of clay on the dike of Mourik (2020)*

| **Type of cover layer** | **Mean ($\mu$) $c_e$ (-)** | **Variation coefficient (V) of $c_e$** | **Standard deviation ($\sigma = V * \mu$) of $c_e$** |
|---|---|---|---|
| Clay | 0.55 | 0.25 | 0.14 |
| Boulder clay | 0.35 | 0.27 | 0.09 |

Whereas the erosion formulas do not cope very well with two different types of clay, in this research there is opted for a simplification in which it is assumed that the cover layer is fully composed of clay. This means that the calculations carry some degree of uncertainty, but also conservatism. The simplification for the normative location HM 13.4 at the Ketelmeerdijk is placed in figure 4.

Whereas the empirical formulas of Mourik (2020) used the erosion coefficient $c_e$, the formulas of Klein Breteler (2022) use the model coefficients $m_1$ and $m_2$. Only the latter will be given attention, whereas this coefficient describes the model uncertainty of stage 2, which is relevant for this research. The value for $m_2$ is composed of different sources of uncertainty, such as:

- OpenFOAM calculations ($V = \sigma/\mu = 0.1$)
- Relation peak pressure OpenFOAM to measurements ($V = \sigma/\mu = 0.25$)
- Influence of wave and water level parameters ($V = \sigma/\mu = 0.2$)
- Influence of the width and height of the berm, as well as the slope ($V = \sigma/\mu = 0.24$)
- Converting erosion volume to erosion depth ($V = \sigma/\mu = 0.06$)

When all these uncertainties are combined, a cumulative standard deviation of 0.42 is found, see table 5. The largest difference between the model coefficient $c_e$ and $m_2$ is that the formula of Klein Breteler (2022) does not distinguish between multiple types of soils.

*Table 5: Uncertainties related to the type of clay on the dike with the methodology of Klein Breteler (2022)*

| **Type of cover layer** | **Mean ($\mu$) $m_2$ (-)** | **Variation coefficient (V) of $m_2$** | **Standard deviation ($\sigma = V * \mu$) of $m_2$** |
|---|---|---|---|
| Clay | 1.0 | 0.42 | 0.42 |

Besides the known uncertainties in the models, also unknown uncertainties exist. An example of these uncertainties are the parameters related to the soil properties. There are little to no recent drill samples from the case study. To find out the influence of the type of clay, an analysis will be performed in which the model output for different values of the erosion coefficient is calculated, see section 4.4.2. This could be seen as a part of the sensitivity analyses.

## 3.5. Application to case study Ketelmeerdijk

For each of the research questions, a specific conclusion is placed for the normative case study of the Ketelmeerdijk. First, the hydraulic conditions are gathered, for the relevant normative conditions. Then, the moment of failure of each of the revetment layers during these normative conditions is determined, see section 4.1.3. This moment of failure of the revetment layers will be the start of clay erosion beneath these layers, described in section 4.2.3. The process of clay erosion is then documented for the low-lying clay layers, based on the analyses of the different formulas. The results for the normative hydraulic conditions are then gathered in section 4.4.4.

After this assessment has been completed, the probability curves for the erosion volumes, the erosion depths and the failure of the different cover layers are set up, in section 4.4.3. This analysis will show how the system responds to different return times. By selecting the parameters for different failure probabilities, the dike properties will remain constant, and only the model parameters for the hydraulic loading will be varied. This way, the applicability of these formulas for different probabilities also becomes more insightful. This could prove to be valuable when the safety standards are changed, and the analysis has to be performed for a different hydraulic loading. Also, it is insightful in the contribution to the overall probability of failure. When the cover layer would be for instance 1.0 meter thick, the extrapolation of the probability curve for the erosion depth could yield the probability of failure in terms of years.

At last, the contribution of residual strength as a stability component to the failure mechanism of GEBU is calculated. This is done by calculating the probability of failure for first the grass cover layer and then, the upper clay layer. Then, the probability of failure for both the grass cover layer, the upper clay layer and the clay layer beneath that is calculated. Following the latest dike safety assessment, the strength of each failure mechanism track is assigned to seven categories, see table 6.

*Table 6: Categories for the assessment judgment for each section per failure mechanism track (Ministry of I&W, 2019)*

| **Category** | **Denotation category testing judgment per dike trajectory per testing track** | **Limitation of category**<br>$P_{f;dsn}$ Probability of failure per trajectory (1/year)<br>$P_{eis,sig}$ Alert safety standard of the dike trajectory (1/year)<br>$P_{eis;ond}$ Lower threshold safety limit of the dike trajectory (1/year)<br>$P_{eis;sign;dsn}$ Failure probability requirement on cross-sectional level (1/year) |
|---|---|---|
| $I_v$ | Easily satisfies the alert safety standard | $P_{f;dsn} < \frac{1}{30} P_{eis;sign;dsn}$ |
| $II_v$ | Satisfies the alert safety standard | $\frac{1}{30} P_{eis;sign;dsn} < P_{f;dsn} < P_{eis;sign;dsn}$ |
| $III_v$ | Satisfies the lower threshold safety limit and possibly the alert safety standard | $P_{eis;sign;dsn} < P_{f;dsn} < P_{eis;ond;dsn}$ |
| $IV_v$ | Possibly satisfies the lower threshold safety limit or the alert safety standard | $P_{eis;ond;dsn} < P_{f;dsn} < P_{eis;ond}$ |
| $V_v$ | Does not satisfy the lower threshold safety limit | $P_{eis;ond} < P_{f;dsn} < 30 P_{eis;ond}$ |
| $VI_v$ | Is not near the norm of the lower threshold safety limit | $P_{f;dsn} > 30 P_{eis;ond}$ |
| $VII_v$ | No judgment as of now | - |

# 4. Results

In this chapter, the results will be analysed. At first, the selected hydraulic conditions are processed and discussed. The second subchapter discusses the choices that have been made to find the point at which the cover layers fail. Next, this chapter will discuss the various clay erosion models. These models are described, and their bandwidths for usage are documented, and also the sensitivity of the outcome to certain variations in the input parameters is documented. After that, a progressive erosion model is set up, in which the most suitable methodology is applied to the Ketelmeerdijk, at a normative section which fails following the current dike safety standards.

## 4.1. Hydraulic conditions

The Ketelmeerdijk has to withstand relatively large hydraulic loading. The effective fetch, which is the length on which wind can cause water level set-up and wave generation, is relatively large compared to other primary flood defences, see figure 17. Combined with the risk of the socio-economic losses, and the risk for the individuals behind a dike - expressed as Local Individual Risk (or LIR) -, this causes a relatively high safety standard for the dike trajectory 8-4, of which the Ketelmeerdijk is a section, with a failure probability of 1/10,000 years. The upper threshold safety standard is set at 30,000 years. To assess a dike's strength, often the lower safety standard is used, as a sort of design safety standard, which is P = 10,000 years for the Ketelmeerdijk.

### 4.1.1. Hydraulic parameters

In this section, the relevant hydraulic parameters at the design safety standard and their course throughout a normative synthetic storm are documented. Through running the probabilistic tool Hydra-NL, the peak values for both the water levels and wave conditions are derived. The peak water level during a 10,000 year storm event is 2.72 m+NAP. The peak significant wave height is 2.65 m+NAP. The peak wave period is 5.75 seconds.

Where the normative hydraulic conditions above are based on a 10,000-year storm event, different return periods provide different values for hydraulic parameters. The larger the return period, the higher the lake water levels, combined with larger waves. This increase can be identified with the use of a frequency curve, see figure 22. These are the near-shore (so at the dike toe) water levels which have increased as a result of wind set-up. It is important to note that this is the location-specific frequency curve for the observed cross-section of the Ketelmeerdijk, and is therefore not broadly applicable to other points along its trajectory.

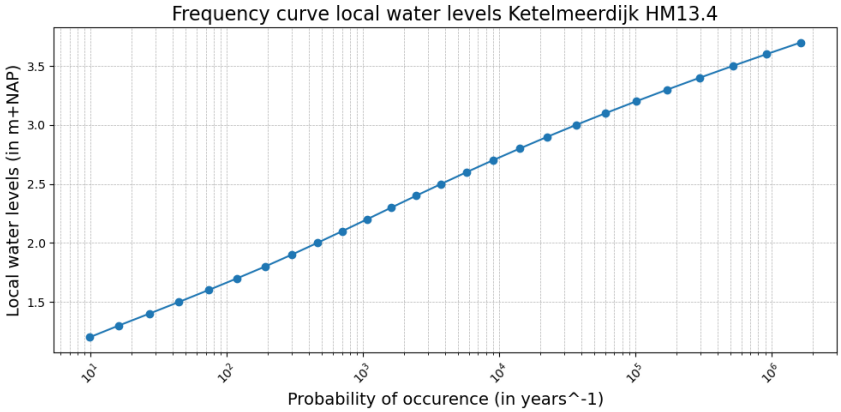


*Figure 22: Frequency curve for HR-location 30 (hm 13.4)*

When stating that the water levels and linked wave characteristics rise equally with the probability of occurrence. However, this logical phrase is not followed in the latest methodology of setting up a synthetic storm, which is the Q-variant. Below, more is described on the working of the Q-variant, and why there is opted for an alternative in this research.

### 4.1.2. Synthetic storm

Now the relevant hydraulic parameters are gathered. From here on, a synthetic storm is set up. This synthetic storm shows schematically how multiple relevant hydraulic parameters vary during a storm event. For setting up a synthetic storm, different options are available. The option which is used mostly right now is the Q-variant. An alternative proposed by Smale & Klerk (2023), is the trapezoidal schematization.

In figure 23 below, the difference between the methods of the Q-variant and the trapezoidal schematization is displayed. This graph is constructed with arbitrary values from the Ketelmeerdijk. The values used are not of importance, the functionality and shape of the graph is. Both methods prescribe how to come up with wave conditions when starting with a trapezoidal graph for the water levels during a storm event. The evolution of water levels is set up in the same manner as the trapezoidal schematization. The upper graph in figure 23 shows small deviations in the respective course between the two methods. The small deviations can be assigned to different step sizes and simplifications within the trapezoidal schematization.

The comparison should be made between the wave conditions, so the significant wave height (bottom left) and the peak wave period (bottom right). The wave conditions (both significant wave height and peak period) show fundamentally different shapes when comparing the two methods. At both the early and end phases of the storm, the Q-variant heavily overestimates the waves relative to the trapezoidal schematization. On the other hand, the peak values of the storm are underestimated. For this research, the part of the storm event where the highest waves occur is the most interesting period. Hence, this research adopts the trapezoidal schematization, and this will be used to determine the values related to a normative synthetic storm.

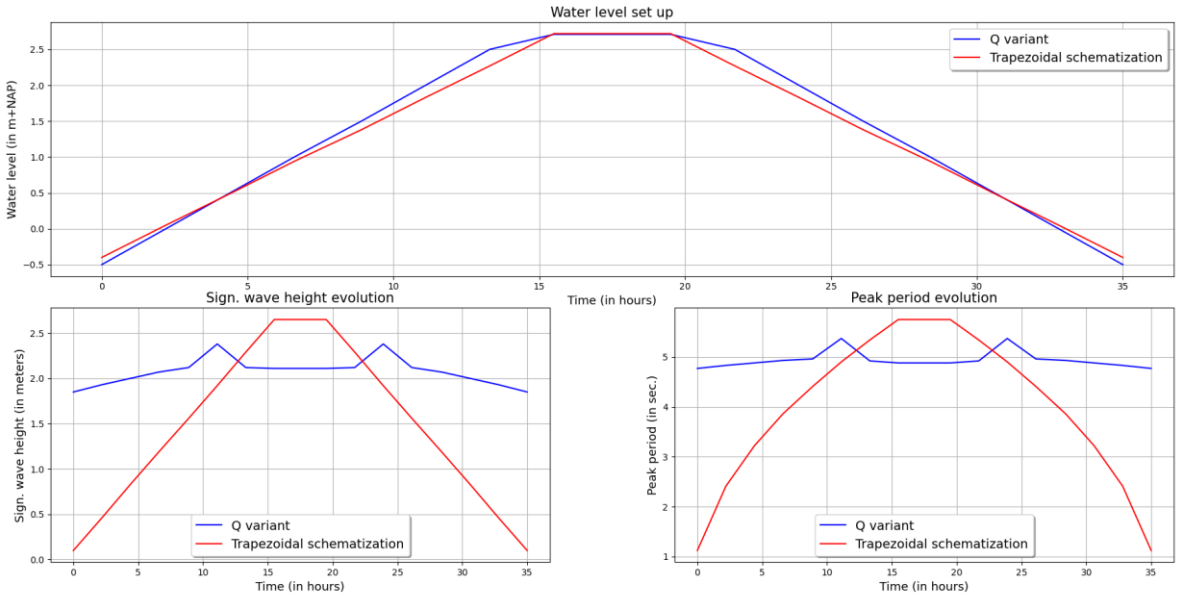


*Figure 23: Difference between the two conversion methods of Q-variant and trapezoidal schematization*

Combining these peak values with the trapezoidal schematization discussed, the storm evolution with all relevant hydraulic conditions is obtained and displayed in figure 24 below. The wave height starts at 0.1 meters, whereas lower values would yield difficulties with regard to numerical processing. The evolution of the spectral wave period is derived based on a constant wave steepness of 0.05. This value was retrieved from various runs in Hydra-NL, which showed to stay relatively constant at different failure probabilities.

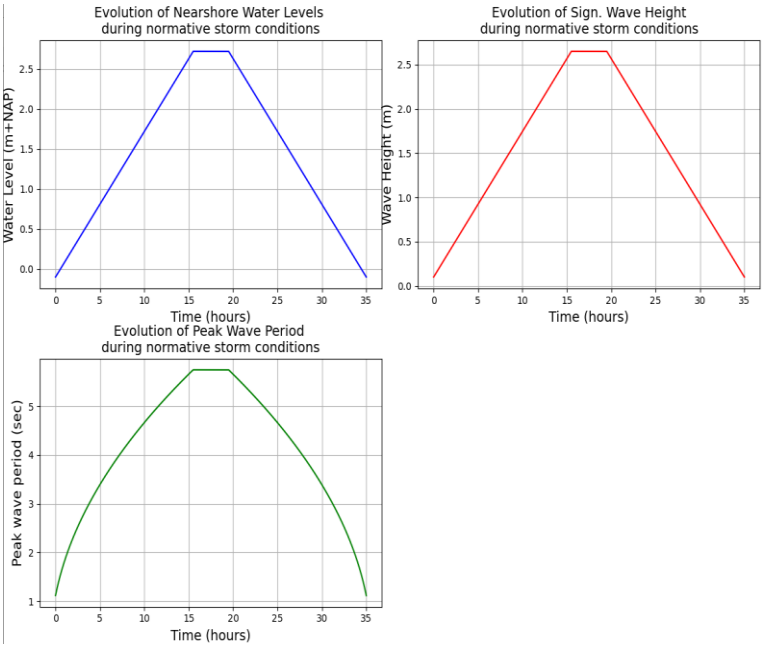


*Figure 24: Storm evolutions of water levels and related wave characteristics for a storm with P = 10,000 years at Ketelmeerdijk HM 13.4*

*Table 7: Values for the storm evolutions for a return time of 10,000 years with the dashed number being the peak values*

| **Time step** | **Water level (in m+NAP)** | **Sign. wave height (in m)** | **Peak wave period (in seconds)** |
|---|---|---|---|
| 0 | -0.10 | 0.10 | 1.12 |
| 1 | 0.08 | 0.26 | 1.82 |
| 2 | 0.26 | 0.43 | 2.31 |
| 3 | 0.45 | 0.59 | 2.72 |
| … | … | … | … |
| 15.5 | *2.72* | *2.65* | *5.75* |
| … | *2.72* | *2.65* | *5.75* |
| 19.5 | *2.72* | *2.65* | *5.75* |
| … | … | … | … |
| 33 | 0.26 | 0.59 | 2.72 |
| 34 | 0.08 | 0.43 | 2.31 |
| 35 | -0.10 | 0.10 | 1.12 |

### 4.1.3. Conclusion for the case study Ketelmeerdijk

To set up wave conditions, based on an initial trapezoidal water level evolution, in this research there is opted for the trapezoidal schematization. This option is chosen as the preferred option over the standard option 'Q-variant', whereas it shows physically more realistic results during a storm set-up. Especially at the extreme conditions, which is most interesting in this study, the Q-variant tends to underestimate the peak values.

This means that, for a 10,000 year storm, the synthetic storm rises from -0.10 to 2.72 m+NAP linearly within a timeframe of 15.5 hours. After a 4-hour period constant at this maximum water level, the water levels drop again to the winter target level, at -0.10 m+NAP. The evolution of significant wave height follows a similar set-up, from waves ranging from 0.10 to 2.65 meters. The peak wave period ranges from 1.18 sec at the start to 5.75 sec at the peak of the storm. The wave steepness is kept constant at 0.05 throughout the time series.

## 4.2. Failure of dike cover layers

Now the hydraulic conditions have been selected, this can be used as input for the assessments of both the block revetment and the grass cover of the current state of the Ketelmeerdijk, at location HM 13.4. This is the location at which the dike fails for both ZST and GEBU, following the latest dike safety assessment round (LBO-1). The goal of this question is to find the moment in time during the storm event, at which the revetments fail and clay erosion will be initiated.

### 4.2.1. Instability of block revetment

This section describes the moment of initial failure for block revetment, specifically for the Ketelmeerdijk trajectory (HM 13.4). Through iteratively running STEENTOETS, while loaded with the relevant hydraulic conditions and the block revetment properties at this specific location, a strength analysis is made. See Appendix 1 and 2 for an overview of both the relevant hydraulic conditions and block revetment properties. From each iteration, it can be seen how much strength is left in the revetment, or that is required, through the variable called failure margin (in Dutch: *dikte overschot*). This gives the extra required thickness, necessary to withstand the normative hydraulic conditions, indicating a negative sign for extra required strength, and a positive sign for remaining strength left in the revetment.

To find the point at which the revetment fails, iteratively the hydraulic conditions are varied over the range in water depths within which the specific revetment type is placed, with varying wave conditions.

The Ketelmeerdijk at the normative cross-section, is covered with both basalt and Basalton. The average diameter of the typical basalt rock at the Ketelmeerdijk is 0.25 meters, and that of Basalton is 0.30 meters (Wegman, Mom, & Fetlaar, 2020). In this question, it is identified at which hydraulic conditions either cover layer fails, and this will be linked to a moment in time during the storm event. This moment will be the moment on initiation of clay erosion. The results are posed in table 8 below. Here, for both the basalt and Basalton layer, the hydraulic conditions are given for which failure occurs.

*Table 8: Conditions for near-failure for the block revetment layers*

| **Type cover layer** | **Basalt** | **Basalton** | **Unit** |
|---|---|---|---|
| Bottom height | 0.14 | 0.99 | m+NAP |
| Top height | 0.99 | 2.45 | m+NAP |
| Water level (h) | 0.96 | 1.75 | m+NAP |
| Significant wave height ($H_s$) | 1.38 | 1.85 | meters |
| Peak period ($T_p$) | 4.14 | 4.81 | seconds |
| $H_s/\Delta D$ | 3.02 | 4.6 | - |
| Failure margin (or *dikte overschot*) | -0.01 | 0.01 | meters |

Now the hydraulic conditions at which the failure occurs are identified, and the link can be made back to the synthetic storm. This will result in figure 25 below, with for each of the three revetment layers a subplot. Here, the evolution of the storm regarding the water levels is described. For each of the layers of basalt, Basalton and the remaining clay layer below, the graph is color-indicated. The full and original water level evolution is described in blue. In the graph, it is shown at which point during the storm event, the different revetment types are first loaded (indicated with orange), then fail at a certain point (indicated with yellow dot), and conclude with clay erosion beneath this layer. Once one of the revetments fails, the other will also be considered to have failed. The instability of one revetment will cause the other revetment to slide, and become unstable. The figure shows how the revetment first should be loaded by a certain water level, and after that, requires a significant wave height to fail. For the grass cover, however, this will fail directly once water levels reach the grass cover above the berm.

The type of revetment that will first fail, will be the block revetment. The basalt layer fails at T = 7.8 hours and at a water level of 1.46 m+NAP. The Basalton layer will fail at T = 10.6 hours, at a water level of 1.72 m+NAP. Whereas the Basalton layer will start to slide already once the basalt has failed, it can be said that the point of failure for the full block revetment is at T=7.78 hours. From this moment on clay erosion on the lower slope will start.

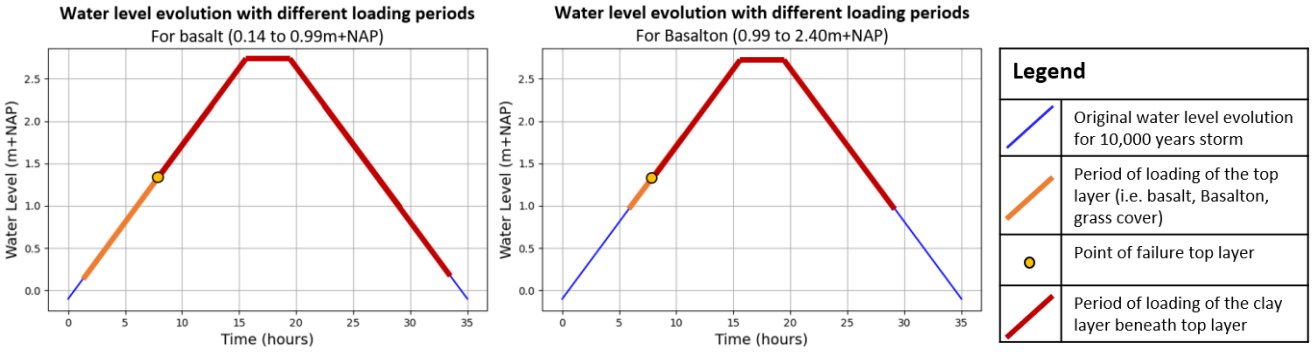


*Figure 25: Graph with hydraulic loading for first basalt, then Basalton, and the time series which remains after block revetment failure*

### 4.2.2. Erosion of grass cover

Similar to the previous section, now again the point of failure for the grass cover has to be determined. The software used for the failure assessment of the grass cover is BM Gras Buitentalud. This is a relatively simple computational software and for that reason, there is opted for the use of the simple formulas behind the software. The formulas are described in section 3.2.2, for first the top layer of 20 cm in Eq. 5 and the upper clay layer (20-30 cm below ground level) in Eq. 6.

See Appendix 2 for a full overview of the relevant parameters which have been selected, and the motivation behind the choices and assumptions.

**Phase 1: Living turf layer (0-20 cm)**

First, the strength duration of the top layer is analysed. It is a 20-centimetre turf layer with grass cover placed on top. Eq. 5 is used to find the point at which this grass cover layer fails, but only just. This point is the failure criterion, which has to be met to make the grass cover fail. It is a property of the grass cover and is constant for the full dike trajectory, provided that the properties are constant. In the formula, the grass cover properties are described through the constants a, b, and c. The values for these constants are defined by the density and quality of the grass cover. The erosion resistance is mainly defined by the density of the roots in the top layer. For the Ketelmeerdijk, the grass cover is good, and therefore 'closed'. This means that the values from table 2 are used for the closed grass cover. This gives for a, b, and c respectively the values 1, -0.035 and 0.25, and the value of $t_{s,sub}$ is set equal to zero, yielding our failure criterion $H_{s,critical}$.

Now the failure criterion is found at $H_{s,critical}$ = 1.25 meters, the moment of failure has to be defined. The moment of failure is the point at which both the water levels are sufficiently high to load the grass cover, but also the failure criterion ($H_{s,critical}$ > 1.25m) should be met. During the storm event, this failure criterion is met after 6.9 hours. At this point, however, the water level is still too low, to load the grass cover. This is reached once the water levels become higher than 2.52 m+NAP, which is the boundary between the hard revetment on the berm and the grass cover. Looking at the storm event, the water level reaches for the first time above this point after 14.38 hours, causing the wave to impact not only the lower slopes but also the upper slope and therefore the grass cover. This cover will fail as soon as the water levels reach above the berm, while the wave height is already well above the failure criterion.

**Phase 2: Upper clay layer (20-50 cm)**

The moment in time where the closed grass cover fails is at T=14.38 hours during the storm. From this moment on, it is assumed that the full top layer fails. From this moment on, erosion to the second layer starts: the upper clay layer of the clay cover. The upper clay layer is the layer of clay below the top layer, composed of 30 centimetres of moderately packed and rooted clay. It, therefore, is stronger than the layer of clay beneath and treated differently compared to the clay layer below. This upper clay layer is from 20 to 50 centimetres below the ground level. The strength layer of this layer can also be calculated with the use of a formula that functions behind the software of BM Gras Buitentalud, see Eq. 6.

Now the graph showing the relation between the strength duration of the upper clay layer and the hydraulic loading is plotted, see figure 26. Looking physically at the formula, the strength duration is a function of $H_s$. The larger the significant wave height, the smaller the strength duration (and the shorter the time before failure of the upper clay layer occurs).

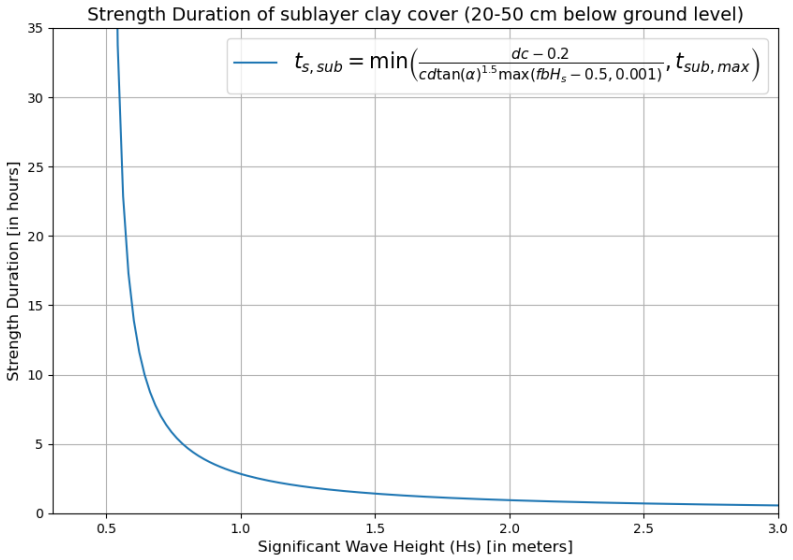


*Figure 26: Strength duration graph for upper clay layer showing the time before failure occurs*

To find the point at which the upper clay layer fails, the cumulative failure fraction of the upper clay layer is calculated, by using Eq. 7. First, for each time step the strength duration is calculated. Then, the respective failure fraction for the particular timestep is calculated, by dividing the time step (which is constant) over the calculated strength duration. This gives the contribution of this time step to the strength duration. Therefore, for each time step, a failure fraction is added to the cumulative failure of the upper clay layer. Then this fraction becomes equal to 1.0 (or when calculating with percentages: 100%), the upper clay layer has fully failed. The cumulative failure fraction must start at the moment of failure for the top layer. This means that the erosion of the upper clay layer does not start sooner than T=14.38 hours. The results are posted in table 9 below. From the table, it can be concluded that the erosion of the upper clay layer occurs in a timeframe of 0.7 hours (or 42 minutes). This means that both the turf layer and upper clay layer are fully eroded before the start of the peak.

*Table 9: Calculation to acquire cumulative erosion of the upper clay layer*

| **Time (hours)** | **Sign. wave height ($H_s$) in meters** | **$T_{s,sub}$ (in hours)** *With use of* Eq. 6 | **Cumulative erosion of the upper clay layer** $Erosion\ sublayer\ (\%) = \frac{Timestep}{T_{s,sub}}$ |
|---|---|---|---|
| 14.38 | 2.469 | 0.721 | 0% |
| 14.39 | 2.471 | 0.720 | 2.47% |
| 14.40 | 2.473 | 0.720 | 3.71% |
| 14.41 | 2.474 | 0.719 | 4.94% |
| … | .. | … | … |
| 15.05 | 2.578 | 0.683 | 96.78% |
| 15.06 | 2.580 | 0.682 | 98.09% |
| 15.07 | 2.581 | 0.682 | 99.41% |
| 15.08 | 2.583 | 0.681 | 100.72% |

Now, the moment in time for which the top layer of grass cover fails is known, as well as the moment in time for which the upper clay layer fails. This means that the erosion of the clay layer beneath the upper clay layer started at T=14.38 + 0.7 = 15.08 hours. This means that the storm evolution (following the T=10,000 years storm event) is almost at its peak, which is at T = 15.5 hours. Whereas the assessed erosion formulas are solely tested on constant water levels, this will also be the starting point for calculating the erosion profile of the clay cover.

### 4.2.3. Conclusion for the case study Ketelmeerdijk

The full block revetment will fail as soon as either basalt or Basalton fails, following the computations in STEENTOETS. For the Ketelmeerdijk specifically, at HM 13.4, during a normative storm event of 10,000 years, the basalt layer will fail at T = 7.8 hours. The Basalton layer, placed higher up the slope, will fail at 10.4 hours. After that, clay erosion will start to occur, all while the water level increases along the slope.

The grass cover, on the other hand, will fail as soon as the water levels reach above the berm. This occurs for the first time at T = 14.38 hours. This is the point at which the grass cover (top layer of 20 centimetres) will fail. Then, the upper clay layer (30 centimetres below) will fail after 0.7 hours. This means that the clay erosion at the upper slope will start at T = 15.08 hours. This is near the constant peak water levels at T = 15.5 hours.

The clay layer below the berm and thus, beneath the block revetment is at least 2 meters thick, which means that the horizontal clay width is over 7 meters. On the other hand, the clay erosion on the upper slope, beneath the grass cover is relatively thin, with 1 meter thick and a horizontal clay width is less than 2 meters at its weakest spot. This means that initially, the strength of the clay layer above the berm is analysed. Besides that, the complications of calculating with varying water levels and set-up a time-dependent erosion level are significant, are not taken into account while setting up the erosion formulas, and will therefore be neglected in this research.

## 4.3. Clay erosion

Now that the moment of failure for both the block revetment and grass cover layers has been obtained, the focus can be shifted to clay erosion. The moment of failure for block revetment is at 7.8 hours. The moment of failure for the grass cover is at 14.38 hours. Although the block revetment will first fail, this research is set up such that first the peak values are assessed on the weaker upper slope. Once it shows that the clay cover will fail for the 4-hour peak period, this gives us an answer on the residual strength of the clay cover. Once it shows that that dike possesses sufficient clay cover to withstand such a period, there will be looked at the impact of a varying water level on the erosion profile.

In this section, three clay erosion methodologies will be applied, see section 3.3.1 for their description.

1. (Klein Breteler et al. , 2012)
2. (Mourik, 2020)
3. (Klein Breteler M. , 2022)

For these, the respective erosion volumes are plotted over time. Also, their model performance will be analysed through univariate sensitivity analyses. Then, the modelling choice regarding the time step size will be described. Based on the outcome of these steps, the most suitable clay erosion formulas will be selected, and a model will be developed which can be applied to the case study of the Ketelmeerdijk. The goal of this upper clay question is to find the most suitable clay erosion model for this specific case study.

### 4.3.1. Timestep selection

In the three figures below, the results of a timestep analysis are placed. There is a degree of convergence for the smaller timestep sizes. The timestep size of 1 hour gives relatively the largest deviation and is for that reason expected to yield inaccurate answers. The gap between a timestep of 1 hour and 0.1 hour is relatively large.

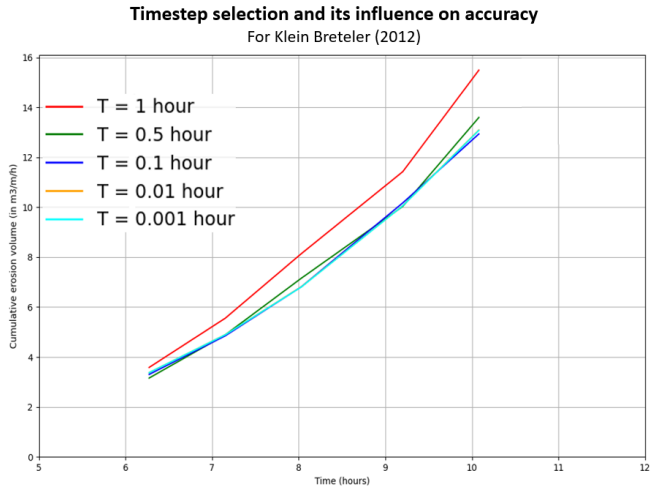


*Figure 27: Time step size analysis for application of Klein Breteler et al. (2012) computation*

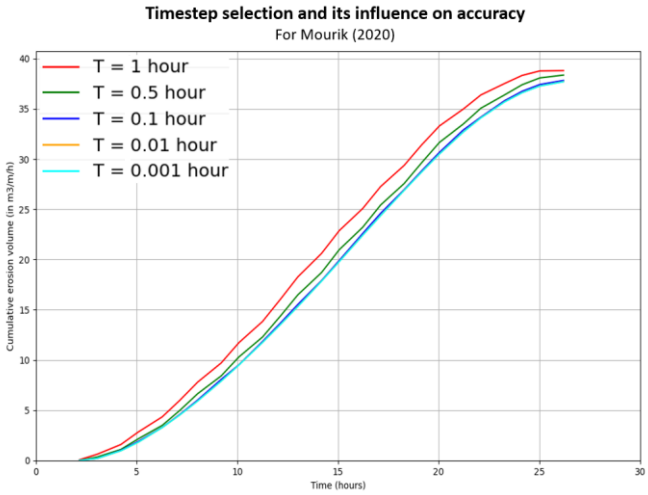


*Figure 28: Time step size analysis for application of Mourik (2020) showing the impact of using different time steps in a computation*

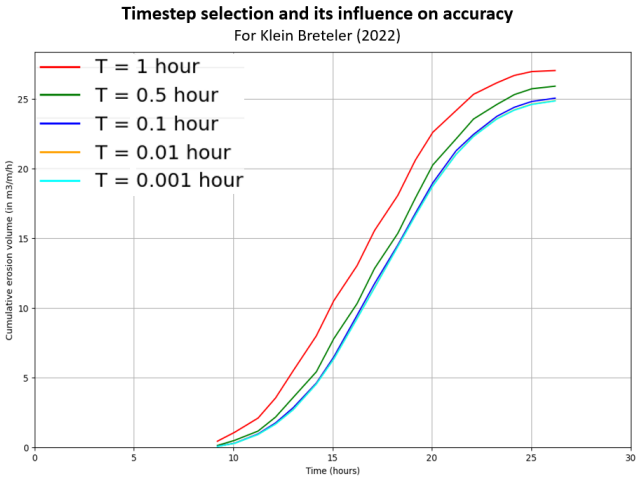


*Figure 29: Time step size analysis for application of Klein Breteler (2022) showing the impact of using different time steps in a computation*

To quantify the difference between two time measures, and see the difference between the formulas, an indicator has been set up. For the 4-hour peak duration, the cumulative erosion volume is gathered, see table 10. The values of both Mourik (2020) and Klein Breteler (2022) are comparable, whereas these are both applicable to large hydraulic conditions. The values for Klein Breteler are selected for the period T = 5 to 8 hours, and can therefore not be compared with the other models, but it shows clearly the convergence. Behind the calculated erosion volumes, the percentual difference is indicated between brackets, relative to the erosion volume at the smallest time step. Based on this outcome, it can be concluded that for both models a time step size of 0.1 hours is sufficient to retrieve reliable results. A larger time step becomes unreliable. A smaller time step is more accurate but could result in longer computational times. The selected time step size is therefore 0.1 hours for all methodologies.

*Table 10: Erosion volume calculated for varying time step size*

| **Timestep (in hours)** | **Erosion volume ($m^3/m$) for Klein Breteler et al.** (2012) | **Erosion volume ($m^3/m$) for Mourik** (2020) | **Erosion volume ($m^3/m$) for Klein Breteler** (2022) |
|---|---|---|---|
| 2 | 4.9 (37.3%) | 12.81 (52.8%) | 10.08 (44.3%) |
| 1.5 | 6.0 (12.2%) | 19.52 (0.3%) | 15.12 (3.9%) |
| 1 | 6.81 (1.0%) | 18.97 (3.2%) | 14.58 (0.2%) |
| 0.1 | 6.74 (0.1%) | 19.52 (0.3%) | 14.60 (0.3%) |
| 0.01 | 6.73 (0.0%) | 19.57 (0.0%) | 14.56 (0.1%) |
| 0.001 | 6.73 | 19.57 | 14.55 |

### 4.3.2. Overview clay erosion models

In figure 30 the different cumulative erosion volumes as a function of time are described for the case study of the Ketelmeerdijk. Here, there is not accounted for the resistive behaviour of the cover layers. This means that the graphs show the clay erosion formulas for their application within the bandwidths of usage, and not at the start of clay erosion. Hence, during the synthetic storm, once it shows that for instance, the significant wave height is lower or higher than the intended range of applicability, the results are not taken into account. This is while, in this step, there is purely focussed on the functionality of the different models. The results of a full 35-hour event storm event are modelled, but the graph is capped at the values where the cumulative erosion volume does not increase any further. See Appendix 3.1 for the input parameters used for this erosion volume graph.

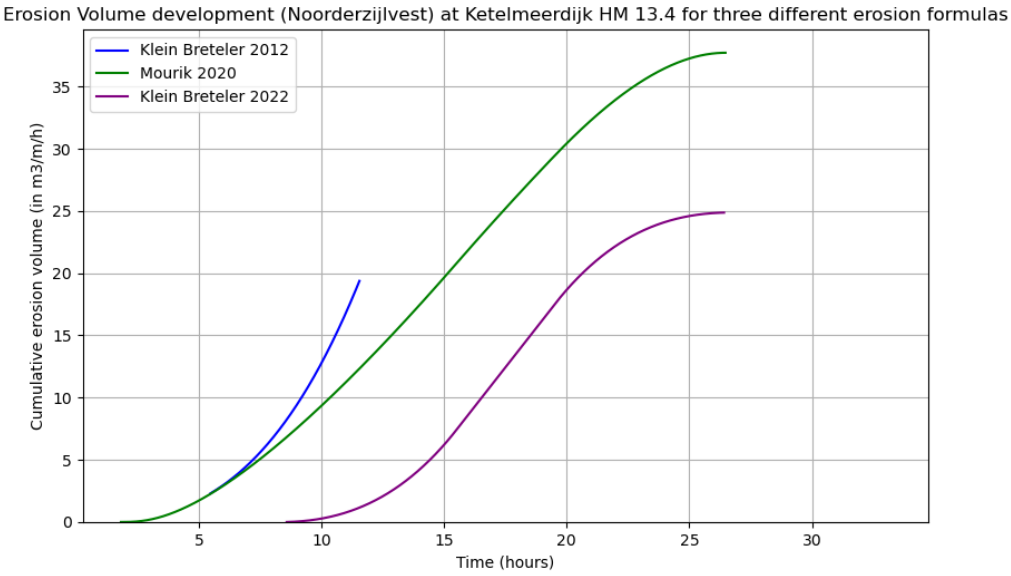


*Figure 30: Calculated erosion volume for the Ketelmeerdijk with normative hydraulic conditions, using different relevant clay erosion methodologies*

At first sight, a few aspects stand out very clearly. At first, the formula of Klein Breteler et al. (2012) is only applicable within a small bandwidth (for $1 < H_s < 2$ m). Besides that, the values are relatively high, and could therefore be conservative. This conservatism is also recognized by Mourik (2020), which was the reason a new methodology was developed to model erosion volumes as a result of wave impact. This means that the methodology proposed by Klein Breteler et al. (2012) is not very suitable for the case study, whereas the interest of this research is particularly focused on the high water levels and related wave conditions. The range in which the experiments have been conducted for Mourik (2020) is also relatively narrow, with a significant wave height between 0.9 and 1.5 meters. The difference between

the two methods is however, that Mourik has used ComFlow during its study, to first calibrate and validate the formula on the model results and then use these results to use the formula outside of this experimental range, so at higher and lower wave heights than described.

Secondly, the two models of Mourik (2020) and Klein Breteler (2022) (stage 2; with $d_e > 0.50$ m and $H_s > 0.50$ m) show similar behaviour. A gradual increase in erosion volume, which leads over time to a steeper incline in erosion volume. Near the end of the erosion profile development, the graph gradually flattens again, until a maximum erosion volume is reached. At this point, a constant erosion volume is obtained and the development of the erosion pit is stopped. An important difference between these two models is the moment at which the erosion starts, with Klein Breteler (2022) starting significantly later than Mourik (2020). This is a result of the modelling of stage 2, so after an erosion depth ($d_e$) of 0.50 meters has developed and the wave heights ($H_s$) are larger than 0.50 meters.

### 4.3.3. Sensitivity analysis

To find out the key drivers behind the formulas, as well as to give some insight into the uncertainty behind the formulas, a sensitivity analysis is performed. It helps to identify which input parameters have the most significant impact on the output of the model. Understanding (the extent of) these key drivers can help users of the model to give a comprehensive overview of the outcome of the model, its related uncertainties, and which input parameters are most valuable to perform research upon. On the other hand, it can quantify the upper and lower limit of the formula, within the boundaries within which it should be used. This is beneficial for the robustness of decisions made with the model, with regard to uncertainty.

The results of the univariate sensitivity analysis are displayed in *figure 31* to *figure 33* below. By comparing the different models in the graph, a lot can be said about the responsiveness of the model to situational changes, hence the application to other flood defences. In the table below, the relative change is described. Here, the change per time step and change of the full range are described. For that, the middle value of the range is taken as the norm (being equal to 1.0). Above the graphs, the default values for the model are depicted. The analysis is performed at a specific time step, at T = 6 hours during the storm event. Where the erosion volume becomes higher than zero, the time series is started. This is done to accommodate for Klein Breteler (2022), while stage 2 is modelled.

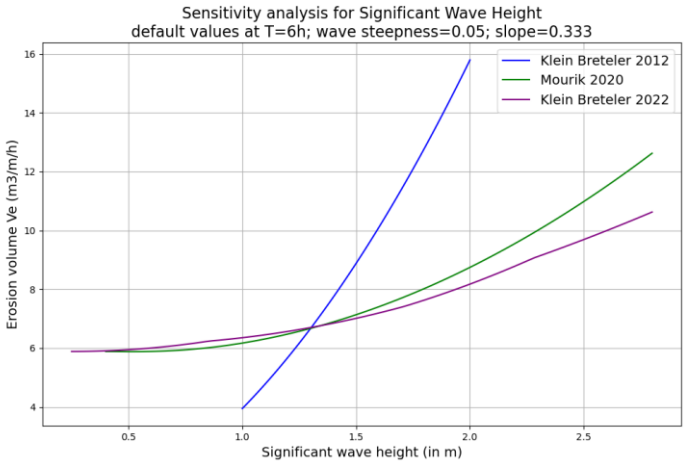


*Figure 31: Sensitivity analysis for significant wave height*

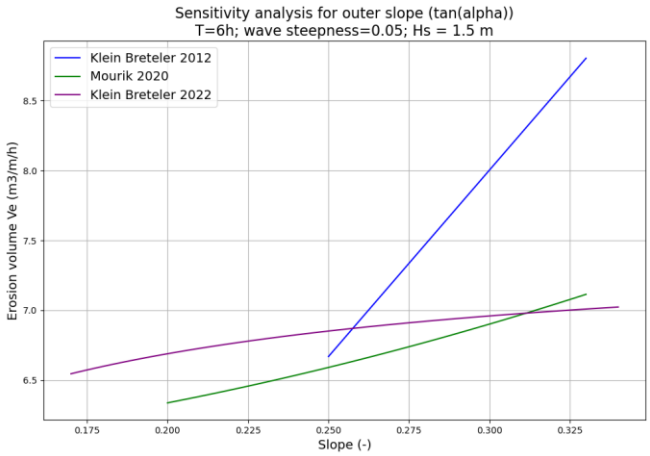


*Figure 32: Sensitivity analysis for slope steepness tan(α)*

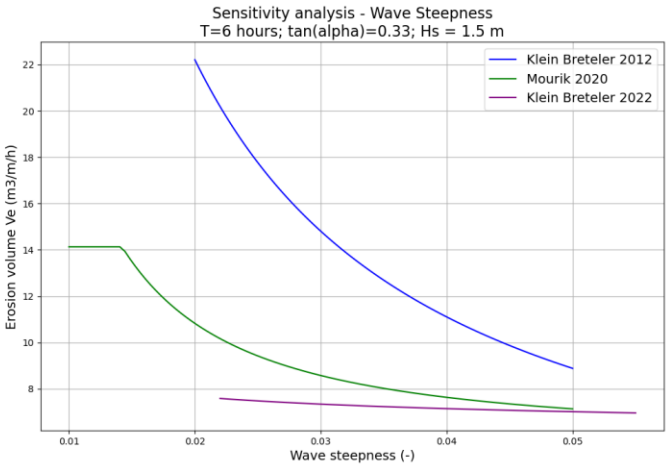


*Figure 33: Sensitivity analysis for wave steepness*

To find the amplitude of response, an overview is provided in table 11 in which the deviation for both the full range and deviation per step size is given. The latter is necessary for normalization purposes and to be able to properly compare the different models. For each of the model, the time step size is similar in size. The formula of Klein Breteler et al. (2012) shows to be most responsive to changes in significant wave height. The formula of Mourik (2020) is more responsive to a change in wave steepness. The formula by Klein Breteler (2022) is most sensitive to changes in the significant wave height. This conclusion amplifies the importance of a justly selected hydraulic conditions, which show to have a large impact when changed slightly.

The difference between clay types is given by Mourik (2020) solely, through the erosion coefficient $c_e$. It can be found that the variation in clay erosion for different clay types is relatively large. When looking at the standard deviation of clay ($\mu$=0.55; $\sigma = 0.14$) or boulder clay ($\mu = 0.35;\ \sigma = 0.09$), a relatively large uncertainty is related to the clay type.

*Table 11: Results of univariate sensitivity analysis with percentual changes per parameter and model option*

| **Parameter** | **Indicator** | **Klein Breteler et al.** (2012) | | **Mourik** (2020) | | **Klein Breteler** (2022) | |
|---|---|---|---|---|---|---|---|
| | | Min | Max | Min | Max | Min | Max |
| Sign. wave height *Step size = 0.5 m* | Relative change per time step (%) | -223% | +177% | -18.7% | +21.7% | -14.6% | +17.2% |
| | Relative change over full range (%) | -223% | +177% | -27.1% | +68% | -19.5% | +50.3% |
| Slope *Step size = 0.025 (-)* | Relative change per time step | -9.6% | +8.4% | -2.8% | +1.9% | -1.0% | +0.9% |
| | Relative change over full range | -16.0% | +13.7% | -6.0% | +5.8% | -4.9% | +2.5% |
| Wave steepness *Step size = 0.01 (-)* | Relative change per time step | -40.2% | +27.7% | -35.1% | +5.5% | -1.9% | +2.6% |
| | Relative change over full range | -77.0% | +41.6% | -76.9% | +11.4% | -5.6% | +3.8% |
| Erosion coefficient *Step size = 0.1 (-)* | Relative change per time step | - | - | **2015** -17.1% **2020** -15.2% | +17.1% +15% | - | - |
| | Relative change over full range | - | - | **2015** -218% **2020** -213% | +218% +213% | - | - |

| | | | | | | | |
|---|---|---|---|---|---|---|---|
| Model coefficient m2 *Step size = 0.05 (-)* | Relative change per time step | - | - | - | - | -0.88% | +0.88% |
| | Relative change over full range | - | - | - | - | - 2.55% | + 2.55% |

From this table, it can be seen that the model of Klein Breteler (2012) is very responsive to changes in wave height, and slope, but also wave steepness. This means the model is not very suitable to apply to our specific case study, while it will be calculated with varying water levels and higher wave heights than the model can cope with. For that reason, this methodology will not be used for the case study.

### 4.3.4. Conclusion for the case study Ketelmeerdijk

Based on the sensitivity analysis, it is concluded that Mourik (2020) and Klein Breteler (2022) are the most adequate models. With these two models selected, there is opted for a bandwidth method. This means that there are two best estimates, and the answer is likely to lie somewhere in the vicinity. Nonetheless, there is a chance that the answer is still outside this window. For now, however, this methodology is the best way to get as close to the truth as possible. These two options show to perform best in a situation similar to the Ketelmeerdijk at a norm frequency of 10,000 years. This does not imply, however, that this is a guarantee for the best option to use for other dikes with comparable characteristics or located near the Ketelmeerdijk.

When using both formulas, it should be noted that the wave steepness and significant wave height are important parameters. It is therefore recommended to spend extra attention on obtaining the right values for these two parameters when setting up a dike safety assessment. These two parameters can have a decisive role in determining whether a dike trajectory should see reinforcement or not.

## 4.4. Progressive clay erosion model

Now the model input has been obtained. For that, first, the values for the hydraulic conditions are derived, then the moments in time for near-failure of both the revetment layer and the grass cover have been identified, and a selection is made for the two most adequate clay erosion models. In this section, the model will be constructed, and designed in such a way that it can calculate the erosion development during an arbitrary return time at the Ketelmeerdijk.

### 4.4.1. Clay erosion during peak at constant water level

First, the erosion process above the berm is described, during a 4-hour peak loading on the grass cover. To check whether the clay layer will withstand the earlier derived normative 10,000 year storm, it is loaded with the hydraulic conditions described in section 4.1. The initiation point of clay erosion will be at T = 15.5 hours, where the water levels become constant for the first time. In practice, the grass cover would already fail at T = 15.2 hours. However, first, it is checked how the constant hydraulic conditions at the peak of the storm would inflict damage to the clay cover.

While the formulas both are differential functions, they are not easy to use in practice. To cope with differential formulas during a calculation, these formulas can be discretized. Below, the discretization step is explained for the formula of Mourik (2020). For Klein Breteler (2022), the same principles are followed.

$$\frac{\partial V_{e,M}}{\partial t} = c_e \left[1.32 - 0.079 \frac{V_{e0}(t)}{H_s^2(t)}\right] \left[16.4(tan\alpha)^2\right] \left[\min\left(3.6; \frac{0.0061}{s_{op}^{1.5}}\right)\right] \left[1.7(H_s(t) - 0.4)^2\right] \qquad \textit{Eq. 17}$$

Above the differential equation of Mourik is described. First, the function is rewritten as follows, where the function F(t) describes the formula on the right hand side of the denominator.

$$\frac{\partial V_{e,M}}{\partial t} = F(t) \qquad \textit{Eq. 18}$$

Now, rewritten this equation will give the following, knowing that $\partial V_{e,M} = V_{e,t}(t) - V_{e,t-1}(t)$

$$\partial V_{e,M} = F(t)\partial t \qquad \textit{Eq. 19}$$

$$V_{e,t}(t) = V_{e,t-1}(t) + F(t)\partial t \qquad \textit{Eq. 20}$$

Now this will result in the following formula, which will be used to calculate for each time step the erosion formula, dependent the previous timestep.

$$V_{e,t}(t) = V_{e,t-1}(t) + c_e \left[1.32 - 0.079 \frac{V_{e0}(t)}{H_s^2(t)}\right] [16.4(tan\alpha)^2] * \left[\min\left(3.6; \frac{0.0061}{s_{op}^{1.5}}\right)\right] [1.7(H_s(t) - 0.4)^2] \partial t \qquad \textit{Eq. 21}$$

The formula above, as well as the formula for Klein Breteler (2022), are both coded in Python[2]. In the footnote, a link to GitHub is placed, in which the two models are both described. This programming tool makes it easy to rapidly work with (changes in) the formula. Also, it gives a great overview of a complex dataset, through structured ordening in variable datasets. Besides the formula behind the clay erosion, also the erosion depths are described in the models.

With the use of these models, it is checked whether or not the dike section will withstand the peak hydraulic loading. The clay layer thickness is the narrowest above the berm. By checking the 4-hour peak duration, and its resulting erosion pit development, a simple stress test is performed.

This section will look at the grass cover and not the block revetment, whereas there is looked at the peak loading during a high return time. This means that the water levels reach above the berm. The consequences of block revetment failure is neglected in this stage. The failure of the grass cover is covered in section 4.2.2 and showed to be for the first top layer T=14.38 hours, for wave impacts with significant wave heights of nearly 2.5 meters high. For the upper clay layer, it showed to be T=0.7 hours. This means that clay erosion is initiated at 15.1 hours, just before the peak of the storm has been reached. Now for the clay cover, the erosion formulas of both Mourik (2020) and Klein Breteler (2022) will be applied. For each of these two models, first, the cumulative erosion volume is calculated. Then, these are linked to an erosion depth, with the use of Eq. 11. This erosion depth describes the deepest point of the erosion pit, seen from the original upper slope, or the intersection between the cliff and terrace. This depth can therefore also be used to see when the critical clay layer thickness is reached, and therefore the clay layer will fail. The critical clay layer thickness of this study is 0.50 meters, whereas the first 0.50 metres are described by the formulas used for the grass cover failure module.

### *Methodology of Mourik (2020)*

For an overview of the relevant hydraulic parameters that are used to compute the methodology of Mourik, see Appendix 1.1. Then, the initial point of erosion volume development occurs at T = 15.1 hours, so after both the top layer and upper clay layer have failed. This resulted in the erosion volume development, as described in figure 34. Here, the cumulative erosion volume is capped, as soon as the value remained constant, which occurred after T=26.3 hours. The cumulative erosion volume at the peak of the storm – meaning from T=15.5 to 19.5 hours – is equal to 8.64 $m^3/m$ over 4 hours of peak loading.

[2] *https://github.com/jildertdejong/master-thesis-residual-strength*

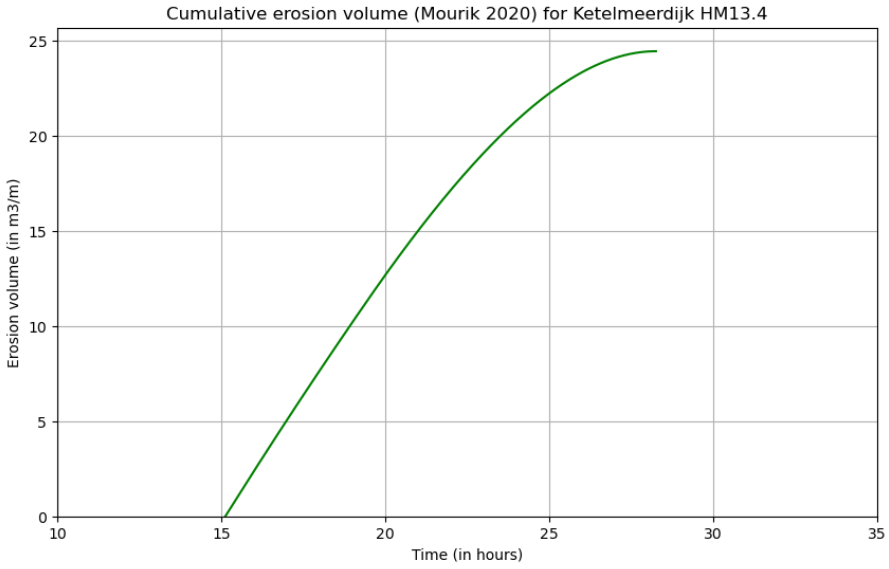


*Figure 34: Cumulative erosion volume following the approach of Mourik (2020)*

Now the erosion volume is obtained, the erosion depth (perpendicular to the original slope) can be determined. This means that there is still 50 cm of clay layer available to erode before the sandy core is reached. The erosion depth is derived with the use of Eq. 16, and is equal to 0.51 meters. Combined with the depth which has already been developed through the grass cover failure, this leads to a depth of 1.01 meters. With a 1.0-meter clay layer, this means the sandy core is just reached before the storm event will start to slowly drop down. The resulting erosion profile is shown in figure 35. Here, the three steps of clay erosion after grass cover failure are displayed. First, the living turf layer, which will fail after 14.38 hours, is indicated with green. Then the upper clay layer which fails after 15.08 hours, is indicated with yellow. After that, the 4-hour peak causes wave impact on the remaining 50 centimetres of the clay cover, and the resulting erosion profile is indicated with red.

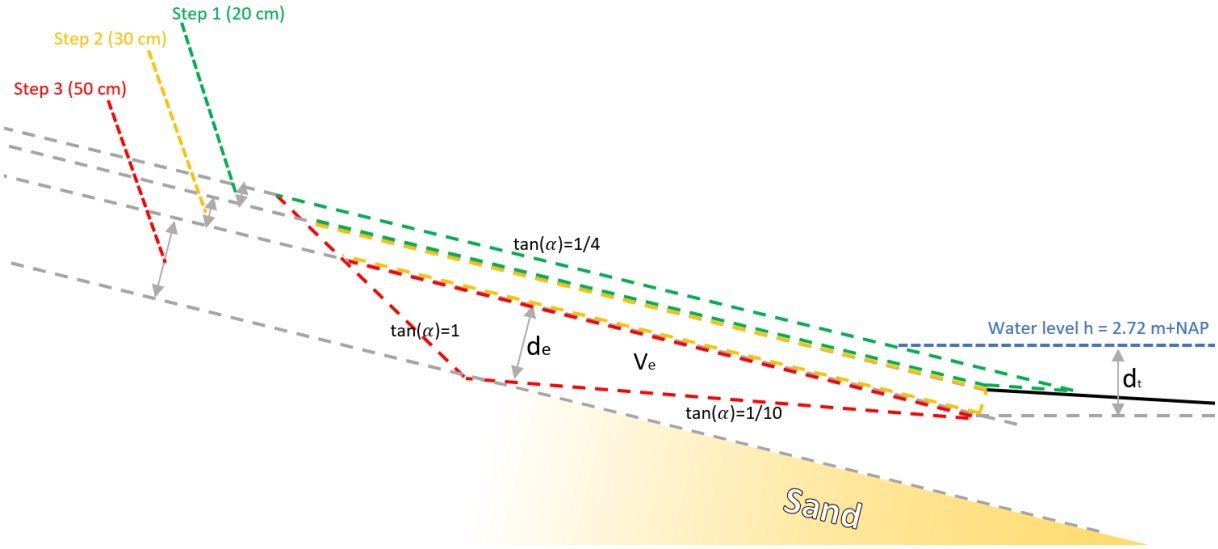


*Figure 35: Erosion profile during peak of the storm (from T=15.5 to 19.5 hours) following approach of Mourik (2020)*

### *Methodology of Klein Breteler (2022)*

For Mourik, it can be said that the upper slope will not withstand the normative hydraulic conditions. Now, the same analysis is performed for Klein Breteler (2022). It should be noted that the methodology of stage 2 of Klein Breteler (2022) is only applied, whereas stage 1 encompasses the same erosion as described for the grass cover failure (for an erosion depth $d_e$<0.50 m). In figure 36 the cumulative erosion volume is plotted, for the normative conditions at the Ketelmeerdijk HM13.4, starting at T=15.1 hours.

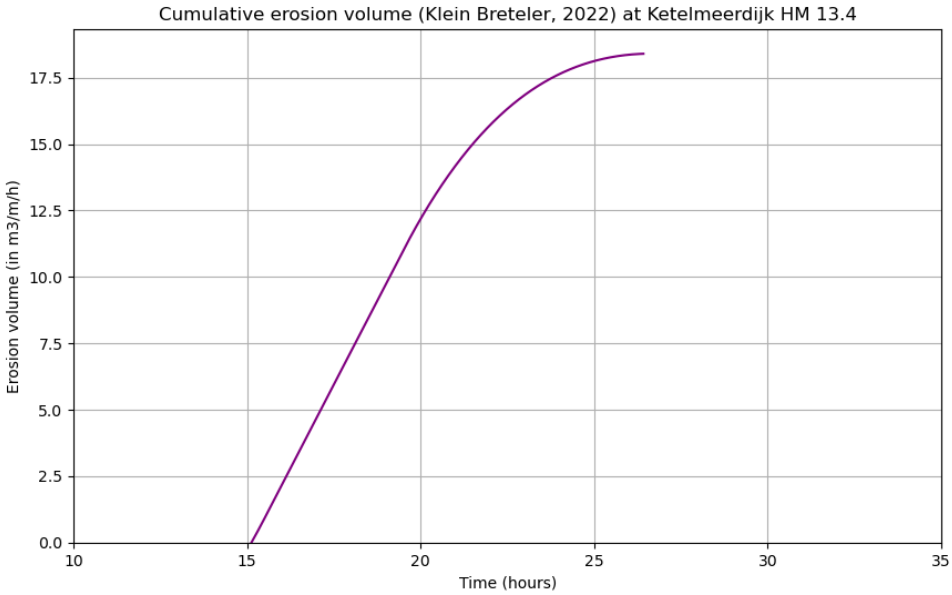


*Figure 36: Illustration of erosion volume development at Ketelmeerdijk for Klein Breteler (2022)*

The cumulative erosion volume at the peak of the storm, taking a constant water level of h=2.72 meters, is equal to 10.08 $m^3$/m. When relating this to a geometry (using Eq. 11), this results in an erosion depth ($d_e$) of 0.86 m. Combined with the erosion that has occurred in the grass cover failure modules, this results in an overall erosion depth of 1.36 meters. For the method of Klein Breteler (2022), which has to be applied on a grass cover on the upper slope, so above the berm, this results in the erosion profile shown in figure 37. To locate the geometric reference points, the value for $d_0$ has to be determined, with the use of Eq. 15, which is the jump directly after the hard revetment. After the 4-hour peak load, the value for $d_0$ is equal to 0.477 meters, which has become constant at this value, leading only to horizontal progressive erosion from here on.

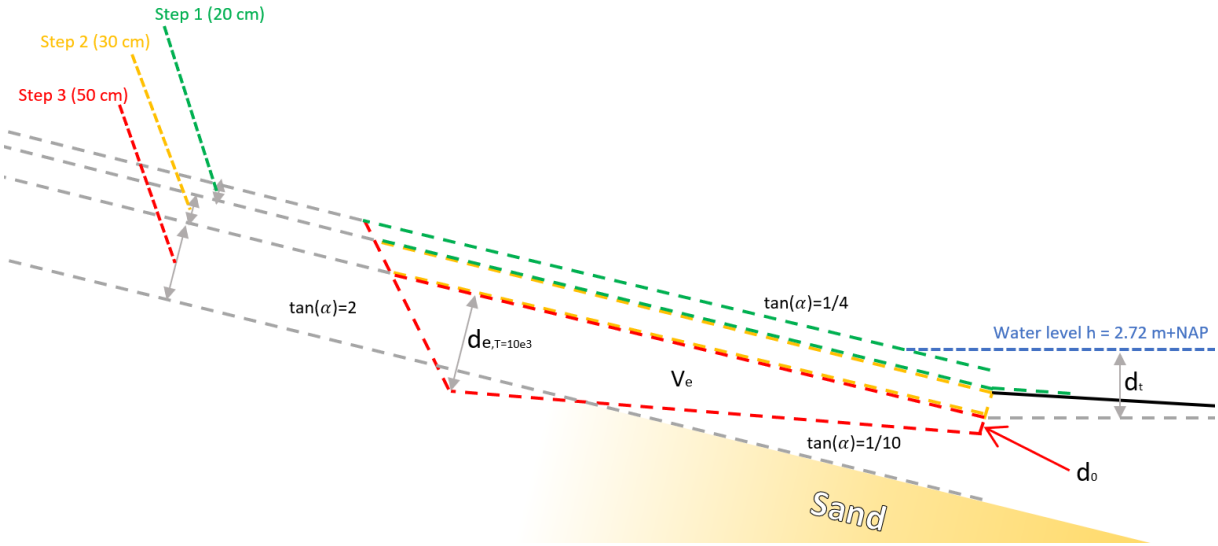


*Figure 37: Erosion profile during peak of the storm (from T=15.5 to 19.5 hours) following approach of Klein Breteler (2022)*

Whereas both formulas show different results, the answer is likely to lie somewhere in between these values. However, due to related uncertainties, the answer could also lie out of this range. In either case, this research assumes the worst case scenario and with that, the model of Klein Breteler (2022) gives the decisive factor. This shows that during the 4-hour peak loading, the clay layer will fail and sand erosion will start.

### 4.4.2. Influence of clay type on erosion

For both methodologies, it is not possible to calculate with the use of two different types of soil. For the Ketelmeerdijk however, two types of cover layers are placed, which are both clay (top 40 cm) and boulder clay (bottom 60 cm). These two types of soil have different strength properties. Boulder clay is said to carry more erosion resistance. This report has presumed, to give a conservative but safe answer, that the cover layer is fully composed of clay. In this section, however, the influence of selecting the soil type is analysed. What would happen if field measurements showed that the assumption for a full clay is unfounded, and actually, it is a full boulder clay layer? To find an answer to that question, this analysis tries to quantify the difference between a full clay layer and a full boulder clay layer.

In the erosion formulas of Mourik (2020), the influence of the type of clay is placed in the erosion coefficient $c_e$. The erosion coefficient is intended to make a distinction between clay and boulder clay. For clay, the mean is 0.55, with a standard deviation of 0.14. For boulder clay, the mean is 0.35 with a standard deviation of 0.09. These values are obtained by testing Eq. 10 which has been developed against historical tests in the DeltaFlume. The results of applying the formula of Mourik (2020) to the different values of erosion coefficients are described in table 12. Here, the erosion volume ($V_e$) and the erosion depth ($d_e$) are both calculated for clay and boulder clay, with their respective standard deviations, see figure 35. These results show that the type of clay is of significant importance. When the clay cover is assumed to be fully composed of boulder clay, this would imply that the dike does carry sufficient residual strength to withstand the normative storm. However, while this is not known (yet), the most conservative value has to be taken, which is the assumption that the cover layer is fully composed of clay with the least erosion resistant properties.

*Table 12: Results of erosion volumes and erosion depth for formula of Mourik for different values for the erosion coefficient*

| **Erosion coefficient** | **Erosion volume $V_e$ (in $m^3/h/m$)** With Eq. 17 | **Erosion depth $d_e$ (in meters)** With Eq. 11 |
|---|---|---|
| Clay | | |
| 0.41 ($\mu - \sigma$) | 6.84 | 0.46 |
| 0.55 ($\mu$) | 8.64 | 0.51 |
| 0.69 ($\mu + \sigma$) | 10.26 | 0.55 |
| Boulder clay | | |
| 0.26 ($\mu - \sigma$) | 4.62 | 0.38 |
| 0.35 ($\mu$) | 5.99 | 0.43 |
| 0.44 ($\mu + \sigma$) | 7.24 | 0.47 |

For the formula of Klein Breteler (2022), there is no such distinction parameter that can differentiate between clay and boulder clay. This is while the tests which were analysed were solely focused on clay from the Wadden Sea dikes, where no boulder clay at such was used.

### 4.4.3. The erosion process for different failure probabilities

For this research, the safety norm lies at the lower threshold safety standard (in Dutch: *omgevingswaarde*), which is equal to a 10,000 year storm event. The values of these safety standards are defined by the Government and can see changes over a dike's lifetime. Also, the model constructed is intended for dikes such as the Ketelmeerdijk, so it could also be applied to other cases.

### *Erosion volume development*

This makes it interesting to take a look at the effect of different probabilities of occurrence on erosion volume development. For that reason, a probability curve is drawn, for the erosion model made with the formulas from Mourik (2020), for both the erosion volume as well as the erosion depth. This gives the curves displayed in figure 38 and figure 39. In these figures, a distinction is made, to show the difference in both full clay cover layer and full boulder clay cover layer. For Klein Breteler (2022), the probability curve is not as relevant for this research, whereas this methodology also incorporates run-up. This part is not included in this research, and therefore only a deterministic erosion volume is calculated.

In figure 39, the probability curve of the erosion depth is displayed. The extrapolation of the probability curve could yield different clay thickness (regarding the erosion depth curve), and the contribution of residual strength to the overall probability of failure. Below, the erosion depth probability curve is seen. It can be seen that the erosion depth does not vary a lot over the different return times. This is while it is a root function of the erosion volume, as described in Eq. 11. It should be noted that this probability curve for erosion depth gives great potential for possible advice on the required thickness of the clay layer. However, it is based on a few assumptions. These values are based on the 4-hour peak loading and should be modelled for the full storm duration. If the full storm duration however would be modelled, then the water levels would drop below the berm and the block revetment would be loaded. Its principles, however, give a neat overview of the potential use of the probability curve for erosion depth on the future dike (re)design.

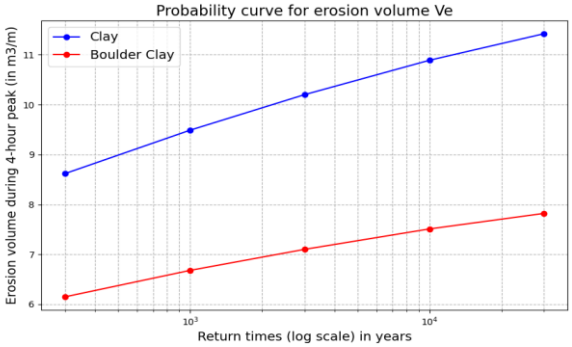


*Figure 38: Probability curve for erosion volume with use of the erosion formulas of Mourik (2020)*

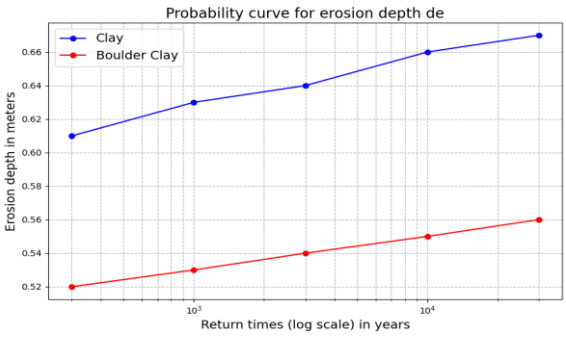


*Figure 39: Probability curve for the erosion depth with the erosion formulas of Mourik (2020)*

### *Probabilities of failure – the strength component of clay*

The strength of the clay cover can be determined by comparing its probability of failure with the situation in which the clay cover is not taken into account. This is the standard at the moment of writing for the dike safety assessment as it was performed in LBO-1. Here, only the probability of failure is determined for the grass cover and upper clay layer, as derived from the formulas of BM Gras Buitentalud. In this research, the failure probability for the component of clay erosion is derived. First, for both models of Mourik (2020) and Klein Breteler (2022), the point of failure is determined. First, iteratively the respective score of the dike trajectory on the failure mechanism of GEBU incorporating clay erosion is assessed. This is calculated by assessing the dike section on different storm evolutions, which are based on the principles of the trapezoidal schematization, see figure 40. In this figure, the respective moments in time for the failure of the respective layers are depicted.

The probability of failure for the failure mechanism of GEBU is determined by looking at the return times at which the water levels do exceed the berm, and impact the grass cover, and at the return time at which the water does not exceed the berm, causing the grass cover to remain intact. The probability of occurrence for GEBU will then lie in between. This resulted in a probability of failure for the Ketelmeerdijk, at HM13.4, which is equal to once per 2,710 years, category Vv. Now, the strength component of clay cover erosion is derived by looking at the storm frequency at which the clay cover theoretically will hold, and at which frequency it will fail.

The probability of failure lies between these two frequencies. This resulted in a probability of failure for residual strength is equal to once in the 6,110 years, category IVv. It should be noted that this number is accompanied by uncertainties, which result in the disclaimer that the actual probability of failure in practice is different. However, this value is for the most conservative situation (assuming a full clay layer), which means it can be said with a fair amount of certainty that the actual number lies higher than that.

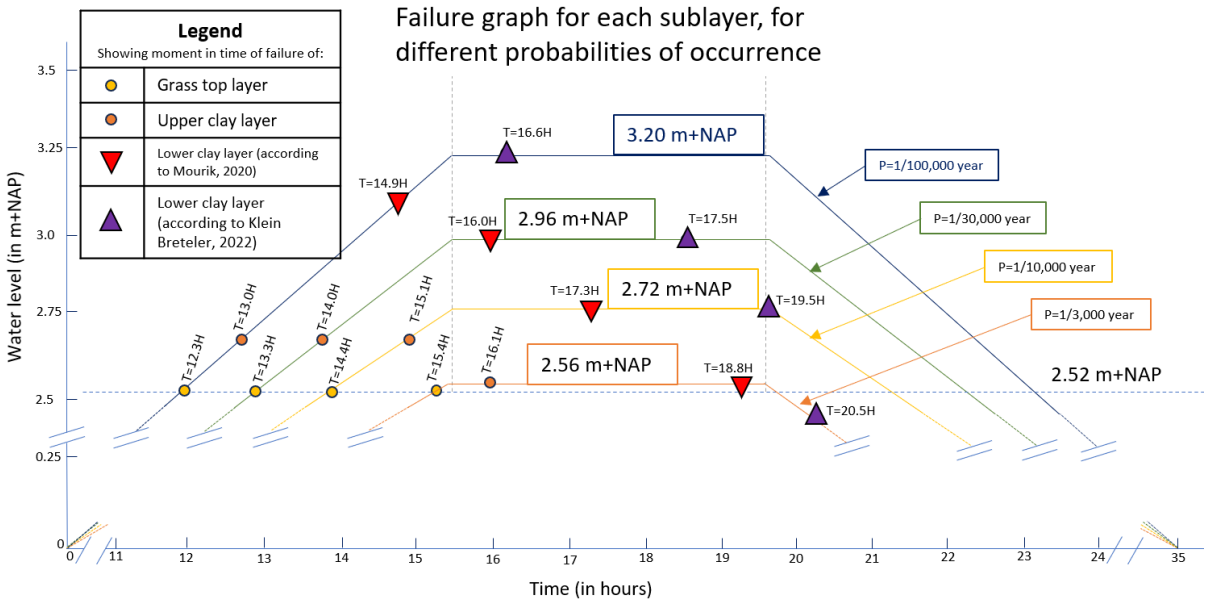


*Figure 40: Water level evolutions with different probabilities of occurrence, indicating points of failure for top layer (yellow), upper clay layer (orange), clay erosion with Mourik (2020) (red) and Klein Breteler (2022) (purple)*

When looking at the difference between the two probabilities of failure, this makes that the clay cover provides at least 125 per cent of extra strength when taking into account the clay cover. Although the calculations have shown that the Ketelmeerdijk would still require reinforcement regarding block revetment and grass cover, when loaded with the normative wave loading of T=10,000 years, the incorporation of clay cover erosion proves to be a substantial factor in the stability assessment of the dike. When comparing these values to the results of the LBO-1 or other assessment rounds, it should be noted that this value is only based on wave impact, and not on wave run-up. In practice, however, this mechanism is also predominant for assessing the probability of failure. The results of the probability curves of the strength duration are plotted in figure 41. It is important to note that this curve is cumulative, and specific for the upper slope of the Ketelmeerdijk. First, the top layer fails (as a result of high water levels), then the upper clay layer fails within 1 hour after that, and then the clay layer fails, for the two methodologies of Mourik and Klein Breteler.

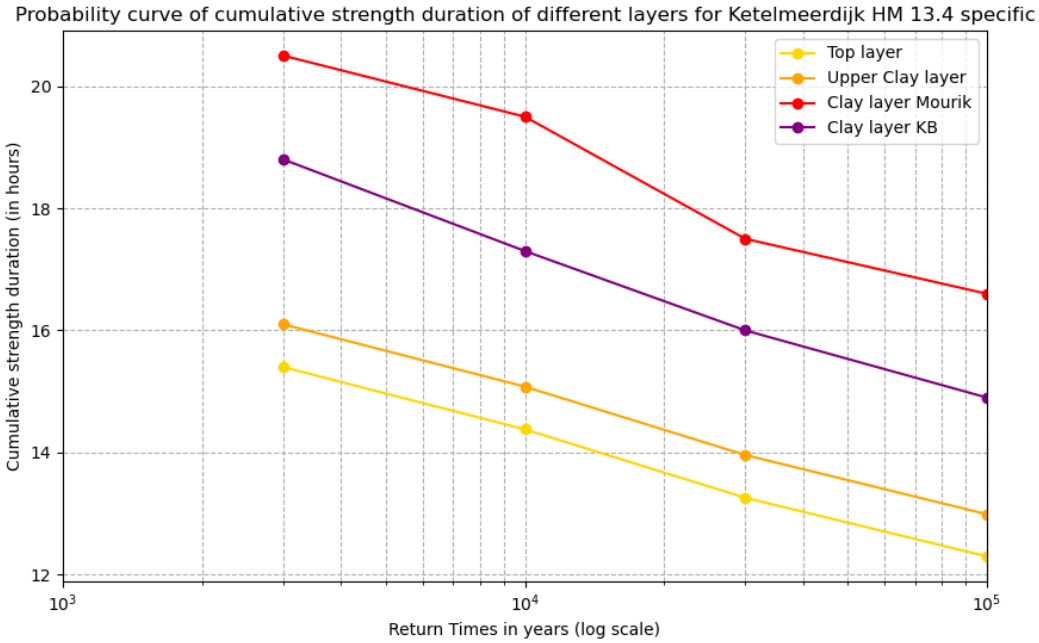


*Figure 41: Probability curve for strength duration of different sublayers*

### 4.4.4. Conclusions for the case study Ketelmeerdijk

When assessing the stability of the Ketelmeerdijk based on the normative conditions at T=10,000 years, it shows that the clay erosion is not sufficient for the dike to pass the latest dike safety assessment on GEBU at the specific dike cross-section at HM 13.4. In practice, once it would show that the clay cover would be larger than 1.3 meters, it would pass the safety assessment on GEBU.

This research shows that taking into account the clay cover is a large improvement towards justly phrasing the actual dike strength. The probability of failure improved, with 2,710 years for solely the grass cover, and 6,110 years for the grass cover including the clay layer beneath that. Therefore, it can be said that clay cover strength can contribute to its overall strength by more than 125 per cent.

# 5. Discussion

In this chapter, the results from the previous chapter are discussed as well as the progressive clay erosion model performance. The validity of the research is discussed, after which the limitations of this research are described. Based on among others these limitations, recommendations are set up.

## 5.1. Validity of research

The research which has been conducted is based on the results from large-scale modelling research from the Delta Flume. These results are internally validated with the use of the models ComFlow and OpenFOAM. The attempt is to develop a framework that possibly could be applied to other fields of study, even though it is still recommended to be careful in using these methodologies for application in the field. However, before application even can occur, the case study of the Ketelmeerdijk requires thorough fieldwork. If this is not done, the conclusions drawn in this research should be interpreted with great care, and proper validation of the input parameters is highly advised. These input parameters relate to properties of the dike, such as the clay characteristics. The conclusions are therefore difficult to generalize. In this research, the calculations are made with the latest available information on the clay cover properties. Even though these sources (for instance, LBO-1) are reliable and relatively recently published, the claims are often assumption-based. Also, the current categorization of clay quality used by Klein Breteler (2022) does not make a good differentiation for the erodibility of clay as a material. For Mourik (2020), this was possible to do so through the erosion coefficient $c_e$. Important elements that should be considered are the distribution of sand lenses and pockets throughout the clay layer (could be tested with arbitrary drill samples along trajectory), organic content, proctor density, lutum content, sand fraction, and the structure of the clay.

## 5.2. Discussing results

With the results from the research, it can be concluded that incorporating clay erosion in the dike safety assessment can significantly sharpen the latest knowledge. With that, it can result in preventing unnecessary dike reinforcements. A main question which still remains however, after this research, is how the sandy core would impact the final probability of failure.

The results showed that the incorporation of the clay cover could inflict more than 125 percent of strength addition to the failure mechanism of GEBU. This was however, calculated with the assumption that the clay cover existed fully out of clay, and not boulder clay. Whereas boulder clay in general is more erosion resistant, this makes this claim conservative and could therefore lead to an even larger strength addition when the soil composition would properly be estimated. When the clay cover is assumed to be fully composed of boulder clay, this would imply that the dike does carry sufficient residual strength to withstand the normative storm. However, while this is not known (yet), the most conservative value has to be taken, which is the assumption that the cover layer is fully composed of clay with the least erosion resistant properties.

## 5.3. Limitations

This study encompasses some limitations. The schematization of the 35-hour storm, resulting wind set-up, and wave characteristics is one of the limitations. This theoretical schematization is an overly simplified and conservative attempt to describe a complex storm event. In practice, this storm event could see a lot more variations. So is the wind direction highly unlikely to constantly come from one direction, as derived from the software of Hydra-NL. Besides that, there is opted for the more realistic trapezoidal schematization rather than the Q-variant, to provide a more realistic schematization. In order to create a cleaner frame of reference however, and to be able to properly compare a flood defense with or without residual strength, arguably the Q-variant is more suitable. Still the Q-variant is not ideal to use as a synthetic storm, while it shows that the peak values are underestimated and lower values are heavily overestimated.

Another limitation of this study is the fact that the Ketelmeerdijk top layer is composed of both clay and boulder clay. In this research, it is assumed that this is one type: either clay or boulder clay. This is while the formulas of both Klein Breteler, Mourik (2020) and Klein Breteler (2022) cannot work with differences in types of clay. This means that the most conservative (in other words: least resistive) soil type will be selected. Besides this assumption, another aspect that could be present in the soil is sand pockets or other inhomogeneities, which are proven to significantly weaken the soil erosion resistance (Klein Breteler M. , 2022). Besides that, the variability of the erosion coefficient is also rather large, which makes the formula highly dependent on the type of clay. For that reason, to achieve a reliable residual strength calculation, it is very important to know the exact clay properties of the clay cover of the dike.

The model of Klein Breteler (2022) was explicitly not advised by Rijkswaterstaat-WVL to be used yet (before further validation) outside the intended relevant area, which is the Wadden Sea dikes. Although the hydraulic system is different (e.g. tidal range, salinity), the types of dikes show similar properties (e.g. outer slope, geometry, soil types) and comparable hydraulic conditions (e.g. range of testing the hydraulic conditions, and comparable lower threshold safety standard). Nonetheless, the hydraulic conditions at the IJsselmeer do not include tides and constant wave loading, which could occur at the Wadden Sea. Therefore, proper validation should be done to see whether these methodologies are applicable as well for the clay cover that lies on the Ketelmeerdijk slope, rather than the clay on the Lauwersmeerdijk slope.

Besides that, the angle under which the waves enter the regime is not taken into consideration in this study. Waves entering the dike trajectory at this angle rather than perpendicular are called oblique incident waves. Interactions of waves with coastal structures and bathymetrical variations lead to phenomena like refraction and diffraction, which change the general direction of the waves, all while significantly impacting the wave height, peak period and water levels. The erosion models described in section 3.3.1 are set up by taking the results of erosion tests on slopes with perpendicular incident waves. This is therefore also treated that way in this research. Neglecting the effect of oblique waves could, however, lead to an overestimation of the wave impact, and considering the component could result in a decrease in the hydraulic loading. Besides, the lateral movement of the wave impact could massively influence the erosion process. Also, alongshore currents could influence sediment transport. Even though the influence of oblique incident waves is not taken into account in this study, a preliminary calculation is made on the effect of these waves, see Appendix 1.2. This calculation shows a decrease of 12.7 per cent of the significant wave height as a result of shoaling and refraction. This could imply that the clay cover would contain sufficient residual strength following the methodology of Mourik to approve the dike section on GEBU.

Also, this study does not incorporate wave run-up, but only wave impact. Even though wave impact is the dominant mechanism causing high peak pressure, wave run-up is a supplementary component which could also cause erosion, and washing away of eroded material.

At last, this study is not able to encompass the entire erosion process of erosion from the start of the schematized storm event to the end. The varying water levels made it difficult to model the erosion process during the flanks of water level set-up and set-down. When assessing the stability of the outer slope, it shows that the lower threshold safety limit is not met yet when taking into account the clay erosion. When looking at lower return times, however, clay erosion could likely mean the difference between meeting and not meeting the required safety standard. In that case, the erosion volume development at varying water levels does become important. It is therefore one of the largest recommendations for future studies. This aspect could also imply that the methodology described in this research, could be applied to other dike trajectories, and possibly even in other hydraulic systems.

## 5.4. Implications of research

This study could improve the dike safety assessment trajectory. Even though the study has quite some limitations and recommended improvements, it still gives some very clear conclusions. One of these is that the contribution of the clay cover to the overall dike strength can be quantified. Also, the method applied could provide a minimally required clay thickness, would could prove valuable in dike design or reinforcement.

The focus of the case study was solely the Ketelmeerdijk, at one specific normative cross-section. A dike ring is as strong as its weakest link. For that reason, the full dike ring should be assessed on the component of residual strength. For that, extensive research regarding the hydraulic conditions for each cross-sectional location, combined with an analysis of the dike ring on its clay thickness. For this specific research, this would also involve the IJsselmeerdijk, Vossemeerdijk, Drontermeerdijk and possibly the Knardijk.

## 5.5. Follow-up studies

Based on this study, and especially its limitations, some suggestions for follow-up studies have been set up. This research has focused purely on the erosion that occurs on the upper slope of a dike. For the normative location that was tested, this proved to be sufficient to answer the research question. For another location, however, with different geometric properties and other hydraulic conditions, it could become interesting to see the impact of the hydraulic conditions at varying water levels during the beginning or end of a storm event. It would be a study targeted at setting up a geometric profile, in trying to integrate the varying water levels in the model, so that the set-up and set-down can be taken into account. This could prove crucial when assessing dike trajectories, with lower norm frequencies. This study could be extended with a model (such as OpenFOAM), to visually display the erosion pit development.

Another follow-up study is to convert this semi-probabilistic study into a fully probabilistic study. This can be performed by running for instance a Monte Carlo simulation, in which the water levels and related wave conditions are varied, resulting in a probability distribution for the erosion volume development.

The last follow-up study recommended is to integrate the aspect of sand erosion. What would happen regarding sand erosion in the case that the clay cover would withstand the 4-hour constant water level? The normative location at the Ketelmeerdijk could be selected while it has a remarkably large width below the clay cover. A range of options is available for this type of erosion, and it is the main question that remains after concluding that the clay layer is not sufficiently strong for the normative hydraulic conditions. Preliminary calculations with the formula of Klein Breteler (2012) show that once the clay cover fails halfway during the peak of the storm, the rest of the storm causes the erosion pit to grow further to a perpendicular erosion depth of 5.8 meters. This gives an insight into the erosion velocity of wave impact on sand, rather than clay erosion. See Appendix 4 for the preliminary calculations.

# 6. Conclusion

This research investigated the bridge between the latest knowledge available on clay erosion and its application in practice. To knowledge gap was attempted to bridge with the use of the case study of the Ketelmeerdijk. A computational model has been developed, in which the erosion development during an extreme storm can be analysed, on a cross-sectional level. This research had the main goal:

*"To evaluate the possibilities and the influence of integrating residual strength, subsequent to the failure of the revetment on the outer slope, in a dike safety assessment"*

To achieve this goal, it was attempted to set up a progressive erosion model, which involved hydraulic loading, failure of the cover layer and then initiating calculations regarding clay erosion. To make it comprehensible, four sub-questions were set up, of which the first was:

1. *How can the evolution of a storm event at the IJsselmeer be schematized, and how does this result in the normative hydraulic loading for Ketelmeerdijk?*

The schematization of normative hydraulic conditions was retrieved from Hydra-NL, where the peak values are calculated for different return times. During a storm event, the water levels follow a trapezoidal shape, starting at the target lake water levels in winter to a 4-hour at peak water levels, and dropping again to the target lake water levels. This provided a synthetic storm of 35 hours, where the water levels and wave characteristics are time-dependent variables. Based on the trapezoidal schematization method, the wave conditions (significant wave height, peak wave period) were obtained, specifically for the Ketelmeerdijk at HM 13.4 during its norm frequency of 10,000 years, which is the normative location. In this research, there was opted for the alternative Trapezoidal schematization, rather than the normal schematization of the Q-variant, whereas this showed to give a more realistic storm evolution. This formed, per time step, the hydraulic loading resulting in wave impact on the outer slope of the dike.

Then, the following research question would give us insight into the moment of failure of the cover layers:

2. *In what way are the hydraulic conditions determined for the failure of the grass cover and block revetment, based on the latest dike safety assessment methods, during a normative storm event at Ketelmeerdijk?*

To find the moment in time at which the revetment or grass cover fails, the critical hydraulic conditions were determined. This is the loading at which the water levels are sufficiently high, such that the waves can load the revetment. When the wave is large enough, the revetment layer and grass cover can then fail. To derive the hydraulic conditions at which the revetment fails, the latest BOI software was used. To find the hydraulic conditions for the block revetment, STEENTOETS was used. This software requires an iterative approach in which the hydraulic conditions are varied, to find the moment at which the failure margin of the revetment layer fails (so approaching zero). When this was linked to the time series constructed in RQ1, the moment in time for failure of both revetments was obtained. In this research, it was found for a normative storm event that had a return time of 10,000 years, the revetment below the berm failed after 7.8 hours.

The critical hydraulic conditions for the grass cover were obtained by analysing the formulas behind BM Gras Buitentalud. The first of these formulas was suitable for finding the critical significant wave height at which the living turf layer (20 cm below slope) just fails, and was defined at normative conditions at 14.38 hours. Here, the water levels reach for the first time during the time series above the berm and the relatively large wave impact causes the grass cover to directly fail. The second formula was used for finding the strength duration for the upper clay layer (20-50 cm below slope) and was defined at normative conditions at 42 minutes.

Clay erosion to the lower slope occurs after 7.8 hours and clay erosion to the upper slope occurs after 15.2 hours. After this moment, clay erosion is initiated and for that, empirical formulas were necessary to find the relation between hydraulic loading and progressive clay erosion. To assess the weakest spot of the dike, the upper slope will first be analysed.

3. *Which methods for modelling clay erosion are most suitable for the Ketelmeerdijk, for application in a progressive erosion model?*

An extensive inventory of the latest expertise on clay erosion models has resulted in the selection of three suitable methods for modelling clay erosion, and could be applied to the Ketelmeerdijk:

1. Klein Breteler et al. (2012)
2. Mourik (2020)
3. Klein Breteler (2022)

After the models had been set up in Python, first a univariate sensitivity analysis was set up. The first methodology of Klein Breteler et al. (2012), showed in this analysis that the model's conditions caused it not to be applicable at relatively large return times. The other models showed to be adequate to be applied for the Ketelmeerdijk and were for that reason selected as the two models to create a bandwidth method. Both models 2 and 3 showed to be most responsive to the hydraulic parameters, in the form of wave steepness and significant wave height. It is therefore recommended to select the right hydraulic parameters, according to the latest expertise. There will always be some uncertainties related to these parameters while working with extremely high return times, but it is important to define these hydraulic conditions as close to full accuracy as possible.

4. *How can a progressive erosion model be set up for the Ketelmeerdijk, and how can this model be validated?*

To evaluate the strength of the clay layer beneath the cover layers, a computational model was set up, to determine the erosion volume and related erosion profile loaded with normative hydraulic conditions, on a cross-sectional level. The model requires input such as hydraulic loading conditions (water levels and wave conditions) and dike properties (geometry, soil characteristics, and current condition). These input variables are processed through the model to simulate clay erosion development over time.

This resulted that on the upper slope, a normative storm that occurs once in 10,000 years, caused the top layer (living turf layer of 20 centimetres) to be eroded after 14.38 hours during a 35-hour storm with a trapezium shaped set-up. The upper clay layer (clay layer of 30 centimetres) was eroded after 0.7 hours, which resulted in a bare clay layer that starts to erode after 15.08 hours. Based on the assumption that the thickness of the clay layer is consistently 1.0 meters (which is in line with the construction drawings), it showed that the dike has almost enough sufficient residual strength when calculated with Mourik (2020) (erosion volume of 8.64 $m^3/m$ and erosion depth of 1.01 m), but when calculated with Klein Breteler (2022) it showed clearly not enough sufficient strength(erosion volume of 13.2 $m^3/m$ and erosion depth of 1.38 m).

Integrating clay erosion as a strength component in dike safety assessment can prove to be particularly valuable for a sharp stability assessment. Applying it to the Ketelmeerdijk however showed that a normative 10,000 year storm event will cause the clay cover erode, and not prevent dike reinforcements to be made. The results indicate that incorporating the clay cover as a residual strength component in determining the probability of failure due to outer slope dike erosion could lead to a 125% improvement in strength. This comparison is made between the current standard of grass cover strength and the combined strength of grass and clay covers.

# 7. Recommendations

As this research is concluded, several key recommendations emerge that are essential when adopting the latest residual strength expertise and trying to perform tests on practical cases:

The hydraulic conditions database is crucial to properly estimate the erosion volume, whereas the erosion volume showed to be heavily sensitive to slight changes in the wave steepness and wave height. It is therefore important to truly reconsider the Q-variant and look at the Trapezoidal schematization instead. Also, the values of Hydra-NL should be as accurate as possible. For the Ketelmeerdijk, these should not only include the influence of the IJsselmeer, but also high discharges from the Vecht- IJsseldelta, which is not taken into consideration as of now.

As discussed in this research, it is of crucial importance to gain insight into the soil properties of the dike. Important clay parameters are sand content, proctor density, lutum and organic content, and the degree of sand lenses present in the dike. Important sand parameters are the grain size and porosity. Also, it is interesting to know where the phreatic line is in the dike. When this phreatic line is high enough, it could inflict higher pore water pressure, reducing the effective stress and with that also reducing the overall strength of the soil. Wet clay is the strongest. Too wet clay however is less strong. Clay which is too dry is also less strong. This means that the environmental influences are also of great importance. The dike should drain properly, at the inner slope, which would cause high precipitation amounts to cause no excessive high pore water pressures. However, during summer times, with prolonged periods of extreme heat, the clay layer could crack open, which would instantaneously become the weakest spot of the dike section. For all these components, it is highly recommended to carry out fieldwork by placing CPTs and making drill samples.

Another small recommendation is to perform a feasibility study into the clay erosion model described by Klein Breteler (2022). This could be done by placing the model results from the Wadden Sea dikes next to the model results of those studies regarding lakeside dikes. This could be the erosion rate experiments done on the Wieringermeerdijk for instance.

The basis for the erosion rate formulas looks good, with the extensive research done by Mourik (2020) and Klein Breteler (2022). However, when applying the formulas a lot of simplications and assumptions have to be made, to generate a workable answer, within the given timeframe, with limited resources. Surrounding the use of the model coefficient and erosion coefficient, a lot of uncertainties are related which could be reduced when the model results are validated with some type of model such as OpenFOAM. Besides that, when the input parameter is known, but only within a range, often the most conservative value is taken. And whereas this research's sole purpose is to reduce conservatism in dike safety assessment – by taking into account the component of residual strength – this is not the most desirable working method.

Also, the component of sand erosion has not been taken into account in the assessment. A large recommendation of this study is to find out what the soil properties of the sandy core are, and then perform estimations on how much residual strength the sandy core still has after clay layer failure.

# 8. General advice

**In this section, advice will be formulated specifically for the WBZZL.**

Specifically for the Ketelmeerdijk, taking into consideration the clay layer as part of the failure mechanism related to outer slope erosion proves to be rather significant. For the relatively large return time of 10,000 years, the Ketelmeerdijk shows to carry almost sufficient erosion resistance, based on calculations on the upper slope. Particularly, the strength of the clay layer below the berm, which is almost twice as thick as the clay cover above the berm, carries a large erosion resistance which should be taken into account in future dike safety assessments.

Therefore the board is advised to take into account residual strength in their dike safety assessment. For the Ketelmeerdijk however, this is too short of a notice. The calculations made are often based on assumptions. Also, no information is yet available on the sand erosion velocity. The assumptions could be removed by performing extensive drill samples over the full length of a dike. These samples would provide more accuracy on the clay and sand properties, such as organic matter content, sand fraction, grain size distributions. The investment in the expenses of data acquisition could prove to be worth it when some dike sections could be taken out of the reinforcement assignment.

**Specifically for the research institution of the University of Twente.**

The subject of residual strength is very relevant in trying to make our Dutch dike design more efficient. It is rather ambiguous that we do not take into account the residual strength of our clay cover, which is the most erosion-resistant component of a dike, in the safety calculation of erosion to the outer slope. Whereas the concept is promising, it is, however, still based on a range of assumptions. Limited tests have been performed, creating limited research and that research which has been performed, making it difficult to apply to other fields of study. For that reason, more research should be done. This could be either small scale (looking at the erosion rate of different types of clay), but especially large scale (to see the physical erosion process when loaded with extreme waves). This is advised to be conducted for both sea dikes, lake dikes, and river dikes. Besides that, close collaboration between Deltares and the UT is necessary so that innovations can be shared.

# 9. References


Botterhuis, T., Waterman, R., & Geerse, C. (2017). *Gebruikershandleiding Waterstandsverloop.* HKV lijn in water. Rijkswaterstaat WVL.

Calle, E. (2004). *Waterstandsverloop Markermeer: Hydraulische randvoorwaarden t.b.v. grondmechanische toetsing van dijken.* Rijkswaterstaat.

Chbab, H. (2012). *Waterstandsverlopen Meren.* Deltares.

Cirkel, J., van Dam, C., & van den Akker, E. (2015). *Handreiking Dijkbekledingen.* Deltares.

Coeveld, E., Knoeff, J., Bizarri, A., & Klein Breteler, M. (2004). Residual strength of dike after failure of cover layer. *Proceedings ICCE 2004 conference.* Lisbon, Portugal.

de Waal, J., & van Hoven, A. (2015). *Failure Mechanism Module Grass Wave Impact Zone - Requirements and Functional Design.* Deltares.

Geerse, C. (2007). *Methode bepalen waterstandsverlopen Vecht- en IJsseldelta.* Lelystad: HKV Lijn in Water.

Geerse, C. (2009). *Overzichtsdocument probabilistische modellen zoete wateren - Hydra-VIJ, Hydra-B en Hydra-NL.* HKV lijn in water.

Grontmij b.v. (2000). *Toetsing 8-4.*

Halter, W. (2023). *Jet Erosion Tests on samples from Lelystad.* Fugro.

IPLO. (1994). *Kruinbreedte - Bijlage 3.* Technische Adviescommissie voor de Waterkeringen, Grondmechanica Delft Afdeling Grondconstructies.

Kaihatu, J. (2022). *Het verhaal van de kering traject 8-4.* Waterschap Zuiderzeeland, Waterveiligheid, Lelystad.

Kaste, D., & Klein Breteler, M. (2015). *Rekenmodel voor kleierosie bij variërende waterstand.*

Klein Breteler et al. , M. (2012). *Erosie van een dijk na bezwijken van de steenzetting door golven.* Deltares.

Klein Breteler, M. (1992). *Taludbekledingen van gezette steen.* Waterloopkundig Laboratorium, Grondmechanica Delft.

Klein Breteler, M. (2016, November 2). *Theorie beoordeling steenzettingen.* Retrieved from edepot.wur.nl: https://edepot.wur.nl/406295

Klein Breteler, M. (2022). *Erosie van kleibekleding met gras op boventalud van Waddenzeedijken.*

Klein Breteler, M., Kaste, D., & Mourik, G. (2020). *Documentatie Steentoets.* Deltares.

Klein Breteler, M., Mourik, G., & Bosters, M. (2014). *Stabiliteit van steenzettingen bij golfaanval.* Deltares.

Klein Breteler, M., 't Hart, R., & van Gent, M. (2013). *Documentatie Steentoets2010: Excel-programma voor het berekenen van de stabiliteit van steenzettingen.* Deltares.

KNMI. (2023). *KNMI'23 Klimaatscenario's.*

Ministry I&W. (2017). *Regeling veiligheid primaire waterkeringen 2017: Bijlage ii voorschriften bepaling hydraulische belasting primaire waterkeringen.* The Hague: Rijkswaterstaat.

Ministry of I&W. (2007). *Hydraulische Randvoorwaarden primaire waterkeringen.*

Ministry of I&W. (2016). *Factsheets normering primaire waterkeringen.*

Ministry of I&W. (2019). *Regeling veiligheid primaire waterkeringen 2017 - Bijlage III Sterkte en Veiligheid.* Rijkswaterstaat.

Mourik, G. (2015). *Predication of the erosion velocity of a slope of clay due to wave attack.* Deltares.

Mourik, G. (2020). *Prediction of the erosion velocity of a slope of clay due to wave attack.* Deltares.

Nieuwenhuijzen, L., Geerse, C., & Bosters, M. (2010). *Aansluiting Hydra's op VTV-tools voor bekledingen in WTI2011.* Royal Haskoning en HKV lijn in water.

Remmerswaal, G., Hicks, M., & Vardon, P. (2019). Influence of Residual Dyke Strength on Dyke Reliability Using the Random Material Point Method. *Proceedings of the 7th International Symposium on Geotechnical Safety and Risk.* doi:10.3850/978-981-11-2725-0 IS4-4-cd

RHDHV. (2021). *Resultaten laboratoriumonderzoek keileem en toepassingsmogelijkheden hergebruik.*

Rijkswaterstaat. (2012). *Handreiking Toetsen Grasbekledingen op Dijken t.b.v. het opstellen van het beheerdersoordeel (BO) in de verlengde derde toetsronde.*

Rijkswaterstaat. (2018). *Peilbesluit IJsselmeergebied.* Retrieved from Helpdesk water: https://www.rijkswaterstaat.nl/water/projectenoverzicht/ijsselmeer-zoetwatervoorraad-op-peil

Rijkswaterstaat. (2021). *Schematiseringshandleiding steenzetting.*

Rijkswaterstaat. (2022). *Schematiseringshandleiding grasbekleding.*

Rongen, G. (2020). *A probabilistic load model for dike revetments.* Retrieved from https://edepot.wur.nl/551612

Ros, B., & Vlaming, J. (2021). *Wettelijke Beoordeling Primaire Waterkering dijktraject 8-4.*

Smale, A., & Beckers, J. (2011). *Aangepaste Q-variant binnen Hydra-K.* Deltares.

Smale, A., & Klerk, W. (2023). *Probablistisch beoordelen en ontwerpen grasbekleding.*

't Hart, R. (2021). *Schematiseringshandleiding steenzettting.* Rijkswaterstaat.

van de Paverd, M., & De Waal, J. (1999). *Randvoorwaarden voor het toetsen van bekledingen langs het IJsselmeer en Markermeer.*

Van der Meer, J. (1999). *Rudimentaire opzet erosiemodel dijken.* Infram.

van Hoven, A. (2015). *Erosie van grasbekleding in golfoploopzone.* Deltares.

van Hoven, A. (2015). *Memo Grass erosion model in wave impact zone.* Deltares.

Vlaming, J. (2020). *Logboek GEBU voor traject 8-4: Grasbekleding erosie buitentalud.* Lelystad: Waterschap Zuiderzeeland.

Waterschap Zuiderzeeland. (2017). *Legger Ketelmeerdijk.* Lelystad.

Wegman, R., Mom, R., & Fetlaar, B. (2020). *Logboek ZST voor traject 8-4 stabiliteit steenzetting.* Waterschap Zuiderzeeland.

Wolters, G., & Klein Breteler, M. (2011). *Reststerkte van een dijk met steenzetting op een kleilaag.* Deltares.

# Appendix 1 – Hydraulic conditions

## Appendix 1.1 - Hydra-NL output

```
Hydra-NL            Versienummer: 2.8.2                mei 2021              Berekeningsresultaten
Naam gebruiker                                          = jilde
Gebruikersmodus                                         = Beoordelen
Datum berekening                                        = 14-02-2024 11:34:51

Invoerdatabase                                          = WBI2017_IJsselmeer_8-4_v02.sqlite
Locatie                                                 = KM_2_8-4_dk_00030
  X-coördinaat                                          =  175551 (m)
  Y-coördinaat                                          =  511654 (m)


Berekeningstype                                         = Waterstand

De berekening is uitgevoerd conform de WBI2017

Berekening met statistische onzekerheid.
Berekening met onzekerheid in de waterstand.
De parameterwaarden van de modelonzekerheid zijn uit de database afkomstig.
  Verwachtingswaarde onzekerheid waterstand             =         0.00 (m)
  Standaarddeviatie onzekerheid waterstand              =         0.35 (m)
  Aantal gebruikte waarden onzekerheid waterstand       =            7


Berekeningsresultaten
    Frequentie:          Waterstand:
     1/     10           1.204 (m+NAP)                  Illustratiepunten   Percentielen
     1/     30           1.422 (m+NAP)                  Illustratiepunten   Percentielen
     1/    100           1.664 (m+NAP)                  Illustratiepunten   Percentielen
     1/    300           1.900 (m+NAP)                  Illustratiepunten   Percentielen
     1/   1000           2.184 (m+NAP)                  Illustratiepunten   Percentielen
     1/   3000           2.447 (m+NAP)                  Illustratiepunten   Percentielen
     1/  10000           2.724 (m+NAP)                  Illustratiepunten   Percentielen
     1/  30000           2.958 (m+NAP)                  Illustratiepunten   Percentielen
     1/ 100000           3.197 (m+NAP)                  Illustratiepunten   Percentielen
     1/ 300000           3.401 (m+NAP)                  Illustratiepunten   Percentielen
     1/1000000           3.614 (m+NAP)                  Illustratiepunten   Percentielen


Illustratiepunten bij waterstand  2.72 (m+NAP) en terugkeertijd 10000 (jaar)

Locatie                         = KM_2_8-4_dk_00030 (175551,511654)
Berekeningstype                 = Waterstand
Waterstand                      =     2.72 (m+NAP)
Terugkeertijd                   =    10000 (jaar)
Overschrijdingsfrequentie       = 1.00E-04 (per jaar)

  r       | meerp.   |      -- |      -- | windsn.  | waterst.| ov. freq    | ov. freq
          | m+NAP    |      -- |      -- | m/s      | m+NAP   | *0.001/whj  | %
----------+----------+---------+---------+----------+---------+-------------+---------
  NNO     |     1.93 |      -- |      -- |      7.2 |    2.72 |       0.000 |      0.0
  NO      |     1.97 |      -- |      -- |      7.0 |    2.72 |       0.000 |      0.0
  ONO     |     1.96 |      -- |      -- |      8.4 |    2.72 |       0.000 |      0.0
  O       |     1.72 |      -- |      -- |      6.4 |    2.72 |       0.000 |      0.0
  OZO     |     1.74 |      -- |      -- |      5.1 |    2.72 |       0.000 |      0.0
  ZO      |     1.72 |      -- |      -- |      6.4 |    2.72 |       0.000 |      0.0
  ZZO     |     1.99 |      -- |      -- |      7.0 |    2.72 |       0.000 |      0.0
  Z       |     1.99 |      -- |      -- |      7.0 |    2.72 |       0.000 |      0.0
  ZZW     |     1.93 |      -- |      -- |      9.8 |    2.72 |       0.000 |      0.0
  ZW      |     1.88 |      -- |      -- |     11.2 |    2.72 |       0.000 |      0.1
  WZW     |     1.83 |      -- |      -- |     11.8 |    2.72 |       0.000 |      0.1
  W       |    -0.13 |      -- |      -- |     35.4 |    2.72 |       0.008 |      8.2
  WNW     |    -0.19 |      -- |      -- |     32.0 |    2.72 |       0.038 |     37.8
  NW      |    -0.19 |      -- |      -- |     30.7 |    2.72 |       0.042 |     41.7
  NNW     |    -0.19 |      -- |      -- |     31.2 |    2.72 |       0.012 |     11.6
  N       |    -0.13 |      -- |      -- |     33.3 |    2.72 |       0.000 |      0.4
----------+-----------------------------------------------------+-------------+---------
  som     |                                                     |       0.100 |    100.0
```

Hydra-NL Versienummer: 2.8.2 mei 2021 Berekeningsresultaten
Naam gebruiker = jilde
Gebruikersmodus = Beoordelen
Datum berekening = 13-03-2024 16:21:20

Invoerdatabase = WBI2017_IJsselmeer_8-4_v02.sqlite
Locatie = KM_2_8-4_dk_00030
X-coördinaat = 175551 (m)
Y-coördinaat = 511654 (m)

De golfparameters uit de database zijn in de berekening gebruikt.

Berekeningstype = Piekperiode

De berekening is uitgevoerd conform de WBI2017

Berekening met statistische onzekerheid.
Berekening met onzekerheid in de golfperioden.
De parameterwaarden van de modelonzekerheid zijn uit de database afkomstig.
Verwachtingswaarde onzekerheid spectrale golfperiode = 0.96 (-)
Standaarddeviatie onzekerheid spectrale golfperiode = 0.11 (-)
Verwachtingswaarde voor onzekerheid piekperiode = 0.96 (-)
Standaarddeviatie voor onzekerheid piekperiode = 0.11 (-)
Aantal gebruikte waarden onzekerheden golfperioden = 5

Berekeningsresultaten

| Frequentie: | Piekperiode: | | |
|---|---|---|---|
| 1/ 10 | 4.132 (s) | Illustratiepunten | Percentielen |
| 1/ 30 | 4.402 (s) | Illustratiepunten | Percentielen |
| 1/ 100 | 4.691 (s) | Illustratiepunten | Percentielen |
| 1/ 300 | 4.954 (s) | Illustratiepunten | Percentielen |
| 1/ 1000 | 5.236 (s) | Illustratiepunten | Percentielen |
| 1/ 3000 | 5.495 (s) | Illustratiepunten | Percentielen |
| 1/ 10000 | 5.750 (s) | Illustratiepunten | Percentielen |
| 1/ 30000 | 5.983 (s) | Illustratiepunten | Percentielen |
| 1/ 100000 | 6.192 (s) | Illustratiepunten | Percentielen |
| 1/ 300000 | 6.360 (s) | Illustratiepunten | Percentielen |
| 1/1000000 | 6.566 (s) | Illustratiepunten | Percentielen |

Illustratiepunten bij piekperiode 5.75 (s) en terugkeertijd 10000 (jaar)

Locatie = KM_2_8-4_dk_00030 (175551,511654)
Berekeningstype = Piekperiode
Piekperiode = 5.75 (s)
Terugkeertijd = 10000 (jaar)
Overschrijdingsfrequentie = 1.00E-04 (per jaar)

| r | meerp. m+NAP | -- | -- | windsn. m/s | waterst. m+NAP | Tp s | ov. freq *0.001/whj | ov. freq % |
|---|---|---|---|---|---|---|---|---|
| NNO | -0.25 | -- | -- | 38.9 | 1.67 | 5.75 | 0.000 | 0.0 |
| NO | -0.25 | -- | -- | 35.1 | 0.06 | 5.75 | 0.000 | 0.0 |
| ONO | -0.10 | -- | -- | 34.8 | -0.08 | 5.75 | 0.000 | 0.0 |
| O | -- | -- | -- | -- | -- | -- | 0.000 | 0.0 |
| OZO | -- | -- | -- | -- | -- | -- | 0.000 | 0.0 |
| ZO | -- | -- | -- | -- | -- | -- | 0.000 | 0.0 |
| ZZO | -- | -- | -- | -- | -- | -- | 0.000 | 0.0 |
| Z | -- | -- | -- | -- | -- | -- | 0.000 | 0.0 |
| ZZW | -- | -- | -- | -- | -- | -- | 0.000 | 0.0 |
| ZW | -- | -- | -- | -- | -- | -- | 0.000 | 0.0 |
| WZW | -0.25 | -- | -- | 39.3 | 1.53 | 5.75 | 0.000 | 0.1 |
| W | -0.25 | -- | -- | 32.6 | 1.71 | 5.75 | 0.013 | 13.0 |
| WNW | -0.25 | -- | -- | 29.1 | 1.67 | 5.75 | 0.049 | 49.1 |
| NW | -0.25 | -- | -- | 28.5 | 1.74 | 5.75 | 0.034 | 33.8 |
| NNW | -0.25 | -- | -- | 30.7 | 2.00 | 5.75 | 0.004 | 4.0 |
| N | -0.25 | -- | -- | 39.7 | 3.00 | 5.75 | 0.000 | 0.0 |
| som | | | | | | | 0.100 | 100.0 |

Hydra-NL Versienummer: 2.8.2 mei 2021 Berekeningsresultaten

Naam gebruiker = jilde
Gebruikersmodus = Beoordelen
Datum berekening = 15-02-2024 13:19:45

Invoerdatabase = WBI2017_IJsselmeer_8-4_v02.sqlite
Locatie = KM_2_8-4_dk_00030
  X-coördinaat = 175551 (m)
  Y-coördinaat = 511654 (m)

De golfparameters uit de database zijn in de berekening gebruikt.

Berekeningstype = Significante golfhoogte

De berekening is uitgevoerd conform de WBI2017

Berekening met statistische onzekerheid.
Berekening met onzekerheid in de golfhoogte.
De parameterwaarden van de modelonzekerheid zijn uit de database afkomstig.
  Verwachtingswaarde voor onzekerheid golfhoogte = 0.99 (-)
  Standaarddeviatie voor onzekerheid golfhoogte = 0.19 (-)
  Aantal gebruikte waarden onzekerheid golfhoogte = 5

Berekeningsresultaten

| Frequentie: | Significante golfhoogte: | | |
|---|---|---|---|
| 1/ 10 | 1.317 (m) | Illustratiepunten | Percentielen |
| 1/ 30 | 1.512 (m) | Illustratiepunten | Percentielen |
| 1/ 100 | 1.736 (m) | Illustratiepunten | Percentielen |
| 1/ 300 | 1.950 (m) | Illustratiepunten | Percentielen |
| 1/ 1000 | 2.190 (m) | Illustratiepunten | Percentielen |
| 1/ 3000 | 2.413 (m) | Illustratiepunten | Percentielen |
| 1/ 10000 | 2.652 (m) | Illustratiepunten | Percentielen |
| 1/ 30000 | 2.864 (m) | Illustratiepunten | Percentielen |
| 1/ 100000 | 3.088 (m) | Illustratiepunten | Percentielen |
| 1/ 300000 | 3.282 (m) | Illustratiepunten | Percentielen |
| 1/1000000 | 3.490 (m) | Illustratiepunten | Percentielen |

Illustratiepunten bij significante golfhoogte 2.65 (m) en terugkeertijd 10000 (jaar)

Locatie = KM_2_8-4_dk_00030 (175551,511654)
Berekeningstype = Significante golfhoogte
Significante golfhoogte = 2.65 (m)
Terugkeertijd = 10000 (jaar)
Overschrijdingsfrequentie = 1.00E-04 (per jaar)

| r | meerp. m+NAP | -- | -- | windsn. m/s | waterst. m+NAP | Hm0 m | ov. freq *0.001/whj | ov. freq % |
|---|---|---|---|---|---|---|---|---|
| NNO | -0.25 | -- | -- | 34.4 | 1.21 | 2.65 | 0.000 | 0.0 |
| NO | -0.10 | -- | -- | 35.7 | 0.23 | 2.65 | 0.000 | 0.0 |
| ONO | -- | -- | -- | -- | -- | -- | 0.000 | 0.0 |
| O | -- | -- | -- | -- | -- | -- | 0.000 | 0.0 |
| OZO | -- | -- | -- | -- | -- | -- | 0.000 | 0.0 |
| ZO | -- | -- | -- | -- | -- | -- | 0.000 | 0.0 |
| ZZO | -- | -- | -- | -- | -- | -- | 0.000 | 0.0 |
| Z | -- | -- | -- | -- | -- | -- | 0.000 | 0.0 |
| ZZW | -- | -- | -- | -- | -- | -- | 0.000 | 0.0 |
| ZW | -- | -- | -- | -- | -- | -- | 0.000 | 0.0 |
| WZW | -0.25 | -- | -- | 39.8 | 1.58 | 2.65 | 0.000 | 0.1 |
| W | -0.22 | -- | -- | 33.7 | 1.86 | 2.65 | 0.008 | 7.7 |
| WNW | -0.25 | -- | -- | 30.0 | 1.80 | 2.65 | 0.040 | 40.2 |
| NW | -0.25 | -- | -- | 28.8 | 1.79 | 2.65 | 0.042 | 41.7 |
| NNW | -0.25 | -- | -- | 29.5 | 1.83 | 2.65 | 0.010 | 10.1 |
| N | -0.25 | -- | -- | 32.5 | 1.93 | 2.65 | 0.000 | 0.2 |
| som | | | | | | | 0.100 | 100.0 |

# Appendix 1.2 – Angle of incidence

Wave refraction affects the wave angle and loses energy as a result. It is a consequence of a wave propagating from deep to shallow water. The key formula to describe wave refraction is Snell's law, see Eq. 22.

$$\frac{\sin(\theta_i)}{c_i} = \frac{\sin(\theta_f)}{c_f} \qquad \textit{Eq. 22}$$

With:

| | | | |
|---|---|---|---|
| $\theta_i$ | = | initial wave angle at deep water | [°] |
| $\theta_f$ | = | wave angle at shallow water | [°] |
| $c_i$ | = | initial wave speed at deep water | [m/s] |
| | = | $\sqrt{gh_i}$ | |
| g | = | gravitational constant = 9.81 | [m/s$^2$] |
| h | = | water depth at deep water ($h_i$) or shallow water ($h_f$) | [m] |
| $c_f$ | = | wave speed at deep water | [m/s] |

The refraction coefficient ($K_r$) is then calculated through Eq. 23 below. This coefficient corrects for the wave height which changes due to refraction.

$$K_r = \sqrt{\frac{\cos(\theta_i)}{\cos(\theta_f)}} \qquad \textit{Eq. 23}$$

The refracted wave height ($H_f$) can then be calculated with the use of Eq. 24, with the initial wave height ($H_i$) multiplied by the refraction coefficient.

$$H_f = K_r * H_i \qquad \textit{Eq. 24}$$

**Case study Ketelmeerdijk**

The highest waves are resultants of the largest effective fetch. This makes that Hydra-NL gives the largest waves for a west-north-west storm, which is relatively to the pole an angle of 292.5 degrees. The dike trajectory is angled at 13.5 degrees. This makes that the wave are arriving at an angle of 9 degrees relative alongshore to the dike trajectory, see figure 42.

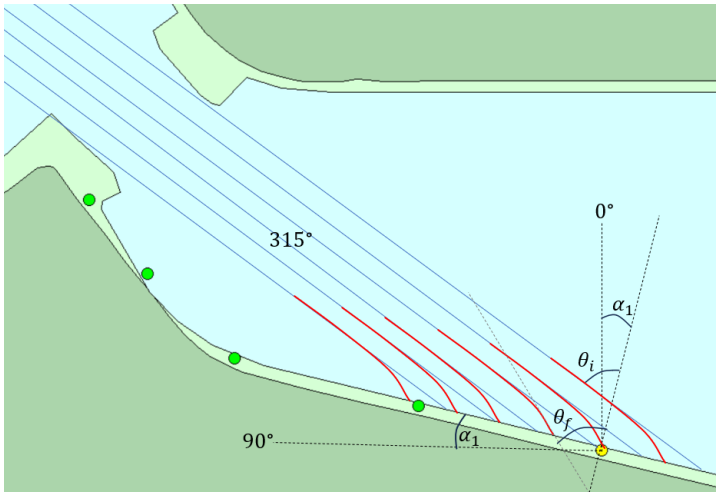


*Figure 42: Refraction of waves near the Ketelmeerdijk*

First, the wave speed is calculated. At deep water, the Ketelmeerdijk is 4.6 meters deep, measured from the winter target level. At shallow water, so near the dike toe, the water depth is 3.35 meters, based on the latest dike drawings (Waterschap Zuiderzeeland, 2017). This makes that the wave speed are 6.72 m/s and 5.73 m/s, respectively for deep and shallow water, following Eq. 22. This makes that – with a incident wave angle of $\theta_i$ = 58.5° - the refracted wave angle $\theta_f$ is equal to 46.7°. Eventually, this gives a refraction factor (Kr) of 0.87. This gives the results posed in table 13 below, describing the decrease in significant wave height. This makes that the waves will decrease overall with 12.73 per cent.

*Table 13: Incorporating refraction for the relevant sign. wave heights at Ketelmeerdijk HM 13.4*

| **Probability of occurrence (years$^{-1}$)** | **Initial sign. wave height ($H_i$)** | **Refracted sign. wave height ($H_f$)** |
|---|---|---|
| 10 | 1.204 | 1.051 |
| 30 | 1.422 | 1.241 |
| 100 | 1.664 | 1.452 |
| 300 | 1.9 | 1.658 |
| 1000 | 2.184 | 1.906 |
| 3000 | 2.447 | 2.136 |
| 10000 | 2.724 | 2.377 |
| 30000 | 2.958 | 2.582 |
| 100000 | 3.197 | 2.790 |

# Appendix 2 - Cover layers

## Appendix 2.1 - STEENTOETS input

Below, the relevant parameters are filled in, see Table 14. The table gives each layer with separate and specific revetment or soil characteristics an own column: ZBC134-1, …, ZBC134-8. In each column, the respective properties of this layer is indicated, with dike geometry, block revetment properties, both upper and lower geotextile properties, filter layer description, clay and sand properties. All cells that have been filled in are specifically for the Ketelmeerdijk, at location HM 13.4. All cells that are blank, are automatically filled in through the software of STEENTOETS. For that, a wide range of default values is available, through documentation of Klein Breteler, et al. (2020) and Rijkswaterstaat (2021).

*Table 14: STEENTOETS input for the Ketelmeerdijk at location HM 13.4, following the latest LBO-1 assessment round*

| | | **ZBC134-1** | **ZBC134-2** | **ZBC134-3** | **ZBC134-4** | **ZBC134-5** | **ZBC134-6** | **ZBC134-7** | **ZBC134-8** |
|---|---|---|---|---|---|---|---|---|---|
| | | | | | | | | | |
| Dike geometry | Dike normal (degrees) | 13.57 | 13.57 | 13.57 | 13.57 | 13.57 | 13.57 | 13.57 | 13.57 |
| | Lower boundary level (m NAP) | 0.14 | 0.99 | 2.45 | 2.55 | 4.48 | 4.24 | -2.62 | -3.81 |
| | Upper boundary level (m NAP) | 0.99 | 2.45 | 2.55 | 4.48 | 4.48 | 4.48 | 4.24 | -2.62 |
| | Slope ($\tan(\alpha)$) | 0.43 | 0.36 | 0.03 | 0.25 | 0.00 | -0.04 | -0.34 | -0.06 |
| | Segment width (for tan a=0) | 0.0 | 0.0 | 3.5 | 0.0 | 4.8 | 5.5 | 0.0 | 18.5 |
| | Top layer | 26.1 | 27.1 | 1 | 20 | 20 | 20 | 20 | 20 |
| | Sub layers (filters, geotextile, clay, etc. | pu kl | st ge kl | | | | | | |
| Block revetment properties | D (m) | 0.25 | 0.3 | | | | | | |
| | B (m) | | | | | | | | |
| | L (m) | | | | | | | | |
| | Gap width (mm) | | | | | | | | |
| | Open surface area (%) | 12 | 13 | | | | | | |
| | Holes in stone? (yes/no) | No | No | | | | | | |
| | Characteristic opening (mm) | 60 | 70 | | | | | | |
| | Specific gravity (kg/m3) | 2900 | 2400 | | | | | | |
| | Filled with wash material (yes/no) | yes | Yes | | | | | | |
| | D15 wash material (mm) | 16 | 16 | | | | | | |

| | | | | | | | | | |
|---|---|---|---|---|---|---|---|---|---|
| | Well clamped? (yes/no) | yes | Yes | | | | | | |
| Geotextile between top layer and filter layer | Thickness | | | | | | | | |
| | Permeability – discharge (l/s/m2) | | | | | | | | |
| | Permeability – decay/decline (mm) | | | | | | | | |
| Upper filter layer | b (m) | 0.15 | 0.1 | | | | | | |
| | D15 (mm) | 30 | 22 | | | | | | |
| | D50 (mm) | | | | | | | | |
| | Porosity (-) | 0.4 | 0.4 | | | | | | |
| | Second filter layer? (yes/no) | No | | | | | | | |
| Geotextile | O90 (mm) | | 0.05 | | | | | | |
| | Thickness (mm) | | | | | | | | |
| | Permeability - discharge (l/s/m2) | | | | | | | | |
| | Permeability - decay/decline (mm) | | | | | | | | |
| Clay | Dike construction (gk/kl/kk/zs) | Kl | Kk | | | | | | |
| | b_clay | 2.5 | 3 | | | | | | |
| | Quality (c1/c2/c3) | c1 | c1 | | | | | | |
| | D50 (mm) | | | | | | | | |
| | D90 (mm) | | | | | | | | |
| Sand | D15 (mm) | | | | | | | | |
| | D50 (mm) | | | | | | | | |
| | D90 (mm) | | | | | | | | |
| | Type of transition construction (a0 … c1) | a0 | b0 | | | | | | |
| | Dike width on water level at norm (m) | | | | | | | | |

# Appendix 3 – Model set-up

## Appendix 3.1 - Input case study

**Revetment and grass cover properties**

- Thickness of the block revetment:
  Basalt: D50 of 25 centimetres
  Basalton: D50 of 30 centimetres
- Open surfaces of 12 per cent between the revetment
- Filter layer with a D15 of 30 mm, and a porosity of 0.4.
- No geotextile present between top layer and filter layer
- Values for (closed) grass cover quality coefficients:
  a = 1.0
  b = -0.035
  c = 0.25

**Clay properties**

- Clay cover of 40 centimetres, with a 60 centimeter boulder clay layer, below that a sandy core
- D50 of the sandy core is 0.13 mm
- Percentage of sand in the clay: 40 %
- Clay quality (c1, c2, c3): c1 -> good

**Geometry of the dike**

- Location in coordinates of HM13.4: x=175,551; y=511,654
- 3.0 meter wide berm, angled at 2%, with an asphalt maintenance road on phosphorus slacks
- Slope of 1:3 below the berm, and 1:4.1 above the berm
- Crest at 4.18 m+NAP

# Appendix 4 – Sand erosion

In this section, the preliminary results of the erosion of the sandy core are described. The formula that is used follows from the study of Klein Breteler (2012), see Eq. 25. This formula is also based on similar large scale modelling tests in the Delta Flume, and requires the same input parameters.

$$\frac{\partial V}{\partial t} = \frac{H_s^2}{T_p}\left(\frac{0.15}{s_{op}^{1.3}}\tan(\alpha)^{0.8} * (135 - 1500 s_{op}) * exp\left(-0.0091\left(\frac{B_t}{H_s}\right)^2\right)\right) \quad \textit{Eq. 25}$$

The formula is applicable if the following conditions hold:

- $0.7 < H_s < 3.0\ meters$
- $0.22 < tan(\alpha) <= 0.5$
- $0.015 < s_{op} < 0.06$
- $0.18 < D_{50} < 0.22\ mm$

For simplicity, there is assumed that the berm is not present, which would further complicate these calculations. The formula is applied from the halfway mark of the peak of the storm. It is then continued until the water levels drop again below the berm. Using the normative parameters as described in Appendix 3.1, this results in an overall erosion depth of 5.8 meters. Based on geometrical calculations, this shows that the point where the erosion cliff intersects the erosion terrace is more than 18 metres from the initial terrace foot. With a cliff angled at 2:1, this would result in the lowering of the crest. Therefore, it result in breach, already at the peak of the storm. For that reason, little trust can be placed in sand erosion.

This calculation is made with the large disclaimer that it is a preliminary calculation, and intented to show the erosion rate of the sandy core. No value can be placed on the numbers given. Further calculations should be still made, while including the berm, and more accurate soil properties.